FABRICATION AND CHARACTERISATION OF DYE DOPED POLYMER OPTICAL FIBRES WITH DIFFERENT REFRACTIVE INDEX PROFILES FOR PHOTONIC APPLICATIONS

Thesis submitted to the

Cochin University of Science and Technology

in partial fulfilment of the requirements

for the award of the degree of

Doctor of Philosophy

by

M. Kailasnath

INTERNATIONAL SCHOOL OF PHOTONICS

COHIN UNIVERSITY OF SCIENCE AND TECHNOLOGY

COCHIN -682022, KERALA, INDIA

April 2010

FABRICATION AND CHARACTERISATION OF DYE DOPED POLYMER OPTICAL FIBRES WITH DIFFERENT REFRACTIVE INDEX PROFILES FOR PHOTONIC APPLICATIONS

Ph.D Thesis in the field of Photonics

Author :

M. Kailasnath
International School of Photonics
Cohin University of Science and Technology
Cochin -682022, Kerala, India
Email: mkailasnath@gmail.com

Supervisor:

Dr. P. Radhakrishnan
Professor
International School of Photonics
Cochin University of Science and Technology
Cochin -682022, Kerala, India

April 2010

International School of Photonics
Cochin University of Science and Technology,
Kochi, India.

Dr. P. Radhakrishnan
(Supervising guide)
Professor
International School of Photonics
Cochin University of Science and Technology

Date:.....

Certificate

This is to certify that this thesis entitled "**FABRICATION AND CHARACTERISATION OF DYE DOPED POLYMER OPTICAL FIBRES WITH DIFFERENT REFRACTIVE INDEX PROFILES FOR PHOTONIC APPLICATIONS**" is a bonafide record of the research work carried out by Mr. M. Kailasnath under my supervision at International School of Photonics, Cochin University of Science and Technology. The results embodied in this thesis or parts of it have not been presented for any other degree.

Dr. P. Radhakrishnan

എന്റെ മാതാപിതാക്കൾക്ക് സമർപ്പണം.....

Declaration

I hereby declare that this thesis entitled "**FABRICATION AND CHARACTERISATION OF DYE DOPED POLYMER OPTICAL FIBRES WITH DIFFERENT REFRACTIVE INDEX PROFILES FOR PHOTONIC APPLICATIONS**" is a bonafide record of research work done by me under the guidance and supervision of Prof.(Dr.) P. Radhakrishnan, International School of Photonics, Cochin University of Science and Technology during the course of research and no part of the work reported in this thesis has been presented for the award of any degree of any other institution.

Cochin -22 **M.Kailasnath**
Date:

Acknowledgement

As my teacher puts it "Research is not inventing or discovering anything, it is the process of patient learning of how to solve a problem successfully". This process cannot be completed without the help and cooperation of many people.

Firstly I would like to express my sincere gratitude to my supervising guide Prof.P.Radhakrishnan firstly for offering me a research position and for the guidance, support and blessings. His alchemy of teaching and research had a great impact on my research career. In addition to science I could learn many valuable know how on other important fields of life.

I am grateful to Prof. V.P.N.Nampoori, my co-guide and Director, International School of Photonics, for his constant encouragement and concern, and for extending the enormous facilities of the Department for my research. His easily approachable character and his remarkable skill of solving problems was greatly helpful during my research.

My sincere thanks to Dr. C.P.Girijavallabhan former Director, International School Photonics, Cochin University of Science and Technology. It was his vision that gave birth to such a wonderful establishment with international facilities.

I am grateful to Prof. V.M.Nandakumaran, former Director, International School Photonics, Cochin University of Science and Technology, for his well-timed care in my research, valuable suggestions and constant encouragement to improve my work.

My special and sincere acknowledgement goes to the researchers at ISP, Dr. Ritty.J.Nedumpara, Dr. Litty Mathew Irimpan, Lyjo.K.Joseph, B.Nithyaja, Sudheesh, Linesh, Jinesh, Thomas, Soney , Mathew and project students of CELOS for their whole hearted support, constant encouragement and valuable suggestions.

I would also like to thank Mr.Muraleedharan and Mr. Joshy of Instrumentation department for their technical support through out my work.

I whole heartedly thank Mr. G.Santhoshkumar Faculty, Department of Computer Science , Dr.V.Sivanandan Achari Faculty, School of Environmental Studies and Dr.D.Rajeev Faculty, School of Legal Studies, for their encouragement and blessings that helped me tide over my difficulties.

My sincere thanks to all non teaching staff of International School of Photonics, for their amicable relation, sincere cooperation and valuable helps.

I wish to place on record my gratitude to my teachers, mentors and my friends at all stages of my education.

I am deeply indebted to my wife Saritha.K.V and other family members for their continuous encouragement, understanding and support.

Above all there is the god almighty whose blessings and kindness helped me a lot to tide over.

M. Kailasnath

PREFACE

In the last few years, interest in polymer optical fibers (POFs) has increased significantly because of its ease of handling, flexibility and potential low cost. Although the loss of POF is still much higher than that of silica optical fiber, recent progress has led to poly (methyl methacrylate) based POF with a loss less than 100 dB/km, low enough for many short length applications. A recent study forecast the market for POF will grow at a compound annual rate of 20% . These intensified activities point to the fact that POF may be a serious competitor to silica optic fiber in short distance data and signal links where cost effectiveness is more relevant to the ease of handling and implementation rather than the optical attenuation. One of the important advantages of transparent polymers compared to the traditional optical materials is that it is possible to introduce organic dyes or other compounds that can play the role of active components into the polymers, which appreciably changes the characteristics of the polymer matrix. The proposed thesis presented in eight chapters deals with the work carried out on dye doped poly (methyl methacrylate) (PMMA) based optical fibres with different refractive index profiles which can be employed for development of different photonic devices.

Chapter1 gives a general introduction to polymer optical fibre**s (**POF) and a glimpse of the potential of the doped optical fibres in modern optical communication network. The chemical structure of PMMA and that of the dyes used for doping the POF is discussed. The importance of the use of dye mixtures for doping the POF is explained using a rate equation based theory of energy transfer among dyes. The techniques used in the present investigation for the fabrication and characterization of the dye doped polymer optical fibres with different refractive index profiles have been explained.

Chapter 2 explains the study conducted to identify the concentration dependence of the operating wavelengths and the relative intensities in which a dye mixture doped polymer optical fibre can operate. A comparative study of the radiative and Forster type energy transfer processes in Coumarin 540:Rhodamine 6G, Coumarin 540: Rhodamine B and Rhodamine 6G: RhodamineB in methyl

methacrylate (MMA) and poly (methyl methacrylate) (PMMA) was done by fabricating a series of dye mixture doped polymer rods which exhibited two emission peaks with varying relative intensities. These rods can be used as preforms for the fabrication of polymer optical fibre amplifiers operating in the multi wavelength regime. The energy transfer rate constants and transfer efficiencies were calculated and their dependence on the acceptor concentration was analysed.

Chapter 3 deals with the details of the investigations conducted to find the dependence of energy transfer parameters on excitation wavelength in poly (methyl methacrylate)(PMMA) optical fibre preforms doped with Coumarin 540:Rh.B dye mixture. This investigation was carried out by studying the fluorescence intensity and the lifetime variations with a fixed donor concentration and varying the acceptor concentrations. The fluorescence emission from the polymer rods was studied at four specific excitation wavelengths viz; 445nm, 465nm, 488nm and 532 nm.

Chapter 4 gives the details of the preparation of dye doped graded index poly (methyl methacrylate)(PMMA) rods by interfacial gel polymerization method carried out using PMMA tubes. The refractive index profiles of the rods were measured by interferometric technique and the index exponents were estimated. Dye doped polymer tubes were also fabricated that can be used to prepare hollow polymer optical fibre.

In the second part of this chapter, the fabrication and characterization of a compact low cost polymer optical fibre drawing machine is discussed. The temperature profile inside the furnace was evaluated at different applied furnace voltages.. The transmission loss measurement on the GI fibres fabricated using this fibre drawing machine was carried out and was compared with that of the step index fibres. The output beam profiles of the fibres were also measured by injecting a Gaussian mode into the fibres using a DataRay Beam R2 scanning type beam profiler and analyzing the output using the software DR Ver 6.0.

Chapter 5 details the observation of multimode laser operation at wavelengths corresponding to whispering-gallery modes (WGM) from a free

standing micro ring cavity based on Rhodamine B dye doped PMMA hollow optical fibre. Cylindrical microcavities with diameters 155μm, 340μm and 615μm were fabricated from a dye doped hollow polymer optical fibre preform. Transverse illumination using a cylindrical lens from the side along the length of the fibre using a 532 nm frequency doubled Nd:YAG laser resulted in multimode laser emission.

Chapter 6 explains the results obtained from the investigation of fluorescence emission from a Rhodamine 6G doped hollow polymer optical fibre filled with a solution of the dye Sodium Fluorescein. At first, Rhodamine 6G doped hollow polymer optical fibre has been fabricated and characterized. The technique of side illumination fluorescence was used for the characterization of the fibre. A diode pumped solid state laser emitting at 532nm and 488nm line of an Argon ion laser were used as the pump sources.

Chapter 7 deals with the enhanced spectral narrowing and laser emission observed from a graded index Rhodamine6G: Rhodamine B mixture doped polymer optical fibre. A comparison with the dye doped step index polymer fibre showed that the effect of amplified spontaneous emission and line narrowing was more prominent in graded index optical fibres . The graded index profile of the fibre and the use of dye mixture as the gain medium leads to lower thresholds and better tunability.

Summary and conclusions of the work carried out are given in **chapter 8.** Future prospects are also discussed in this chapter. Some of the results have been published in standard international journals and in the proceedings of various national as well as international conferences, the details of which are given below.

……ൠ……

List of Publications

International Journal

[1] **M.Kailasnath**, T.S.Sreejaya, Rajeshkumar, P.Radhakrishnan, VPN.Nampoori and CPG .Vallabhan. *Fabrication and fluorescence characterization of dye doped graded index polymer optical fibre preform.* **Journal of Optics and Laser Technology 40, 687, 2008.** doi: 10.1016/j.optlastec.2007.10.015.

[2] **M.Kailasnath**, P.R.John, P.Radhakrishnan, VPN.Nampoori and CPG .Vallabhan. *A comparative study of energy transfer in monomer and polymer matrices under pulsed laser excitation.* **Journal of Photochemistry and Photobiology A 195, 135, 2008.** doi: 10.1016/jphotochem.2007.09.015.

[3] **M.Kailasnath**, Nishant Kumar, P.Radhakrishnan, VPN.Nampoori and CPG .Vallabhan. *Excitation wavelength dependence of energy transfer in dye mixture doped polymer optical fibre preforms.* **Journal of Photochemistry and Photobiology A 199, 236, 2008.** doi: 10.1016/j.jphotochem.2008.05.026.

[4] Bikas ranjan, **M.Kailasnath**, Nishant Kumar, P.Radhakrishnan, V. Sivanandan Achari and VPN.Nampoori "*Influence of solvent on the size and properties of ZnO nanoparticles"* **American Institute of Physics, Conf. Proc. 1147, 287, 2009.** doi: 10.1063/1.3183446.

[5] **M.Kailasnath**, P.Radhakrishnan, VPN.Nampoori, C.P.G.Vallabhan "*Wide range tunability from a dye solution filled dye doped hollow polymer optical fibre"* **Chem.Phys.Lett.** (Communicated)

[6] **M.Kailasnath**, P.Radhakrishnan, VPN.Nampoori,C.P.G.Vallbhan *"A free standing microcavity laser using a dye doped hollow polymer optical fibre"* **Appl.Phys.Lett.** (Communicated)

[7] **M.Kailasnath**, P.Radhakrishnan, VPN.Nampoori,C.P.G.Vallbhan *"Light amplification in a dye doped graded index polymer optical fibre"* **Optics.Lett.** (Communicated)

International Conference

[1] **M.Kailasnath**, Ravikumar, Krishna Murari, P.Radhakrishnan, VPN.Nampoori "*Fabrication and characterization of dye doped hollow polymer optical fibre"* International Conference on Fibre Optics and Photonics. December 13-17, 2008, IIT, Delhi.

[2] **M.Kailasnath**, Bikas Ranjan, Nishant Kumar P.Radhakrishnan, VPN.Nampoori "*Direction dependent transmission characteristics of dye mixture doped polymer optical fibre perform"* International Conference on Fibre Optics and Photonics. December 13-17, 2008, IIT,Delhi.

[3] **M.Kailasnath**, Bikas Ranjan, P.Radhakrishnan, VPN.Nampoori and CPG. Vallabhan *Efficient energy transfer in dye mixture doped polymer rods.* Accepted for **PHOTONICS–2006**,International Conference of Fibre Optics, Optoelectronics and Photonics, December 13-16, 2006, Hyderabad, India

[4] **M.Kailasnath**, P.R.John, Rajeshkumar, P.Radhakrishnan, VPN.Nampoori and CPG .Vallabhan. *Fluorescence characterization of dye doped polymer optical fibre preform. International Conference on Optical materials and Thin films for advanced Technology, (**OMTAT-2005**),October 24-27, 2005, Kochi, India.*

[5] **M.Kailasnath**, P.R.John, Rajeshkumar, P.Radhakrishnan, VPN. Nampoori and CPG .Vallabhan. *Fabrication and fluorescence characterization of a Rhodamine B doped graded index polymer optical fibre preform.* International Conference on Optics and Lasers (**ICOL-2005**), December 12-15, 2005, Dehradun, India.

[6] **M.Kailasnath**, G.A.Kumar and VPN.Nampoori "*Energy transfer and Optical gain studies in FDS:Rh.B system under CW laser excitation"*. **PHOTONICS 2004,** International Conference on Fibre Optics, Optoelectronics and Photonics. December 9-11,2004, Kochi

[7] Ravikumar, Krishnamurari, **M. Kailasnath,** P. Radhakrishnan and V.P.N. Nampoori, "*Optical Charactarisation of ZnO nano particles and nano rods prepared by wet chemical technique at low temperature"* Proc. SPIE Vol. 7610, 761011 (2010) SPIE WEST 2010, California, USA.

[8] **M.Kailasnath**, Bikas ranjan, Nishant Kumar, P.Radhakrishnan, VPN.Nampoori "*Influence of solvent on the size and properties of ZnO nanoparticles"* International Conference on Transport and Optical properties of Nanomaterials (ICTOPON-2009). University of Allahabad, India January 5-8, 2008, Allahabad.

National Conference

[1] **M.Kailasnath**, P.Radhakrishnan, and VPN.Nampoori, *"A micro ring multimode laser using hollow polymer optical fibre"* National Laser Symposium, 2010, BARC, Bombay.

[2] **M.Kailasnath, "***Polymer based optical fibres"*, Invited Talk at National Conference on Advanced Materials (NCAM -09), August 27-29, 2009, PSN college of Engineering and Technology, Melathediyur, Thirunelveli, Tamilnadu.

[3] **M.Kailasnath**, Rajeshkumar, P.Radhakrishnan, VPN.Nampoori and CPG .Vallabhan. *"An LED based evanescent wave fiber optic sensor for the trace detection of Fe2+ ions in water"*. National conference on Optics-December,21-22, 2006, IIT Chennai.

[4] **M.Kailasnath**, Bikas Ranjan, P.Radhakrishnan, VPN.Nampoori and CPG .Vallabhan. *"Interferometric measurement of refractive index profile in graded index polymer optical fibre preform"*. National laser symposium-2006-December,5-8, 2006, Raja Ramanna Center for Advanced Technology , Indore.

[5] **M.Kailasnath,** Rajeshkumar, P.Radhakrishnan, VPN.Nampoori, *"Fabrication of a compact polymer optical fibre drawing machine"*. National laser symposium-2006-December,17-20, 2007, M.S.University, Baroda.

……ൠ…..

Contents

.....ꕥ.....

Chapter- 1

Dye doped Polymer optical fibres

Contents

1.1 Introduction

Polymer Optical Fibres (POF) are the most promising solution for the "last 100 m" in data communication. They combine the inherent benefits of all optical fibres such as high bandwidth, total electromagnetic immunity with additionally amazing simplicity in handling. This is mainly due to their relatively large diameter and acceptance angle (or numerical aperture NA). In spite of the outer diameter being in the range of typically 1 mm, the fibre remains flexible because of the use of polymer material, mainly acrylics like polymethyl methacrylate (PMMA). Larger diameter makes splicing of optical fibres much easier and allows the use of lower cost light sources and

connectors leading to very significant economic advantage. POF was introduced by DuPont in the mid 1960s at approximately the same time when glass optical fibre (GOF) was suggested as a transmission medium for optical communications. DuPont's product was a step index fibre with a (PMMA) core and fluoropolymer cladding. Despite the fascinating ability to guide light, POF had a very large attenuation, limited applicability, and negligible commercial value as far as the field of communication was concerned. At that time, even GOFs had attenuation in excess of 1000 dB/km, which made their use in optical communication impractical [1].Mitsubishi Rayon in Japan further developed Dupont's extrusion technology for POF, which led to the introduction of the Eska^{TM} product in 1976[2-4]. The attenuation of this product, which had a PMMA core and poly (fluoroalkyl methacrylate) cladding was still large (300 dB/km) and applicability was limited to low-end uses like illumination.

In 1970, the attenuation of GOF had been reduced to about 20dB/km in the wavelength region near 1μm [5] and by the late 1970s, fibre loss below 1dB/km could be achieved at a wavelength of 1.3μm and thus the era of fibre optic communications commenced. In the mean time, the attenuation of PMMA based POF also had been reduced to about 160 dB/km at a wavelength of 650 nm by process improvements and was further reduced to about 20 dB/km at 680nm by the use of dueterated PMMA (PMMA- d8) [6].All these POFs were step index (SI) POFs. The first graded index (GI) POF was fabricated by Ohtsuka and Hatanaka in 1976 by heat drawing a graded index plastic rod [7]. From the mid 1970s to the early 1980s the graded index plastic rods were made by two different methods namely, two-step co-polymerization[8-10] and photo-copolymerization [11-14]. GI plastic rods made by two-step copolymerization could not be heat drawn due to their cross-linked network structure, where as rods made

by the photo co-polymerization method could be. However GI-POFs made by heat drawing GI plastic rods had rather large attenuation (greater than 1000dB/km at 670nm) and, consequently, more interest at that time was shown in light focusing plastic rod lens for which somewhat larger attenuation could be tolerated. Later when the interfacial gel polymerization method was introduced [15,16], GI-POFs with much smaller attenuation could be fabricated [17-21].

In recent years, solid state dye doped materials have been investigated for constructing a great variety of devices and systems ranging from tunable lasers and amplifiers to nonlinear optical devices such as switches and modulators [22-24]. Organic laser dyes possess a number of outstanding qualities including high values of optical nonlinear coefficients, high quantum efficiency and active media of broad spectral range. In practice the flexibility in selecting from a large number of different dyes permits one to construct many devices operating at a wide range of wavelengths ranging from ultraviolet and visible to infrared. However, devices incorporating these dyes must be in solid form to be employed for useful purposes. Furthermore, laser dyes doped in a solid matrix are easier and safer to handle than those dissolved by organic solvents in liquid form [25]. Optical amplifiers and lasers made of dye-doped fibre require much less pump power than in bulk material because of the effective confinement and long interaction length available in the fibre. Two basic methods for the fabrication of polymer optical fibres are continuous extrusion method [2, 3] and preform method. One important advantage of continuous extrusion method is high production rate. This process, however cannot be run for an indefinitely long period of time because the material being processed thermally degrade over time, and the degraded material contaminates the fibre and deteriorates its optical property. The extrusion method can utilize

ready-made amorphous polymers in pellet form, but contamination associated with materials handling is a serious problem that results in a high attenuation. Consequently, a closed system that integrates purification of monomers, polymerization and extrusion is preferable. In preform method, to obtain any particular refractive index profile along the radial direction of an optical fibre core, a preform with the desired profile can be employed. The preform is a cylinder of the polymer for which refractive index distribution can be made to coincide with that desired for the core of the POF. The preform is drawn in to fibre by the heat-drawing process. Nevertheless, the development of solid state, dye doped materials has been very challenging.

Methyl methacrylate is an organic compound with the formula $CH_2=C(CH_3)COOCH_3$. This colorless liquid which is the methyl ester of methacrylic acid (MMA) is a monomer produced on a large scale for the production of its synthetic polymer, polymethyl methacrylate (PMMA). This process of polymerization shown in figure 1.1 is carried out at a desired temperature in the presence of a suitable polymerization initiator and a chain transfer agent. Dye doped polymers were obtained by incorporating the dyes during the polymerisation. The chemical structures of the laser dyes used in the present study are shown in the figures below.

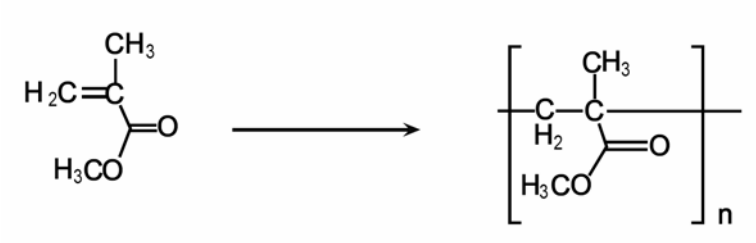

Fig.1.1. The process of polymerization of MMA in to PMMA

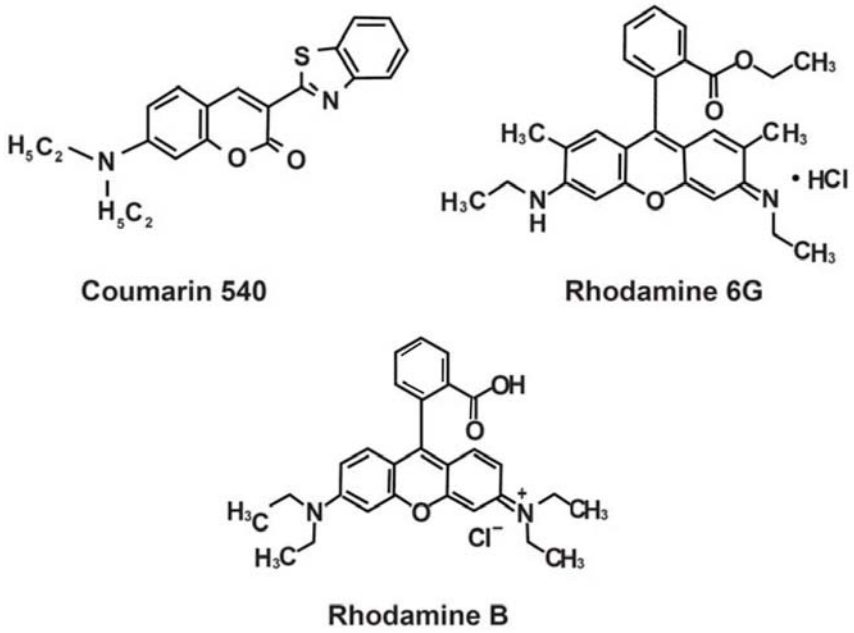

Fig.1.2. The chemical structure of the dyes used.

A dye used in the POF must satisfy the following criteria so that the POF acts as an efficient gain medium. [26]: (a) The dye must have a reasonable quantum yield of fluorescence in the chosen polymer bulk, because this characteristic is intimately related to the probability of stimulated emission. (b) The dye must have high photochemical stability because majority of the POF amplifier configurations require that the dye be capable of undergoing multiple excitation cycles for continued operation. (c) There must be minimal overlap between the dye fluorescence and its absorption spectra, because amplification phenomena rarely occur within the region of overlap because of the self absorption of the dye (d) The dye must absorb the radiation of the pump source and must maintain the population inversion required for stimulated emission. (e) The dye must have adequate solubility and thermal stability in the chosen polymer bulk. Figure 1.2 shows the chemical structures of the laser dyes used for the present study.

1.2 Doping polymer with dye mixtures- Energy transfer mechanisms

Energy transfer dye lasers (ETDLs) have been reported for numerous donor-acceptor pairs by various workers [27-31] during the last three decades. The excitation of dye lasers through energy transfer processes by using appropriate mixture of dyes is very effective in improving the dye laser performance. The extra flexibility is provided by the wavelength shifts due to concentration changes of donor and acceptor dye molecules. The major role in the redistribution of excitation energy between short wavelength(donor) and long wavelength (acceptor) components played by electron energy transfer may either involve the emission of photons or be nonradiative (dipole-dipole interaction) The main mechanisms that have been proposed for such an energy transfer are (1) radiative transfer, i.e., absorption of donor emission by an acceptor; (2) diffusion controlled collisional transfer; and (3) resonance transfer via dipole–dipole interaction . Diffusion controlled transfer occurs over interatomic distances of the order of molecular distances. This mechanism is dependent on the solvent viscosity and temperature. Its probability is very small in the low concentration range [32].

The origin of resonance transfer is the long-range dipole–dipole Coulomb interaction. A good overlap of the emission spectrum of the donor and absorption spectrum of the acceptor is required for radiative transfer and resonance transfer due to long range multipole interaction [33].The radiative energy transfer mechanism is often the dominant mechanism in dilute solution and its occurrence cannot be neglected in the studies of radiationless energy transfer. These two mechanisms can also be distinguished by measuring the donor fluorescence lifetime as a function of acceptor concentration, i.e. if the donor lifetime is little affected by the concentration of the acceptor molecule, radiative transfer mechanism can be considered dominant[34].

To describe the state of the system after excitation, a mathematical description is needed which can be obtained by a kinetic scheme shown in figure 1.3. This scheme corresponds to the singlet states of the donor and acceptor coupled by an energy transfer rate constant $K_{D\to A}$ to account for transfer from first excited singlet state (S_1) of the donor to the ground singlet state (S_o) of the acceptor. Each singlet state is pumped with a short pulse from a laser source of intensity I_p at a rate $\sigma_{01}(p)I_p$. Lasing occurs in the acceptor molecule at a rate $\sigma_e I_L$ where I_L is the generated dye laser intensity. Absorption losses at the dye laser frequency are represented by the rate $\sigma_{01}(L)I_L$ .One can therefore write rate equations for the singlet state levels of the donor and acceptor. Triplet effects are neglected because of the short duration of the pulses (10ns), while photochemical reactions and excited state absorptions (photoquenching effects) are assumed to be insignificant [35]

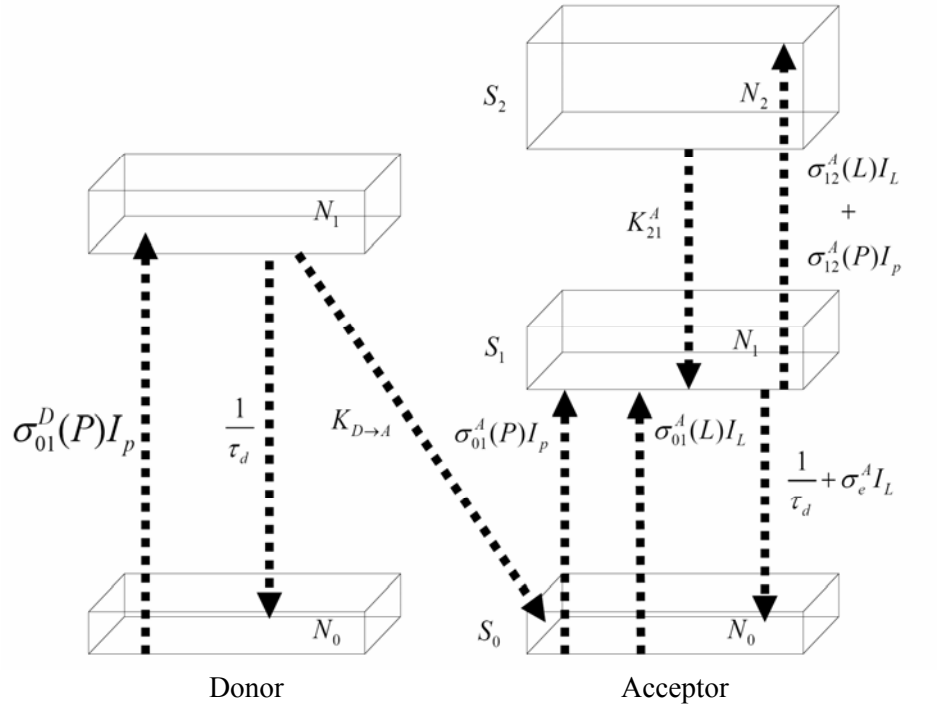

Fig. 1.3. Kinetic scheme for the energy transfer

$$\frac{dN_{1D}}{dt} = N_{0D}\sigma_D W(t) - K_F N_{1D} N_{oA} - \frac{N_{1D}}{\tau_D} \quad \text{.....(1.1)}$$

$$\frac{dN_{1A}}{dt} = N_{0A}\sigma_A W(t) + (K_F + K_R) N_{1D} N_{oA} - \frac{N_{1A}}{\tau_A} \quad \text{.....(1.2)}$$

$$N_D = N_{0D} + N_{1D} \quad , \quad N_A = N_{0A} + N_{1A} \quad , \quad N = N_A + N_D \quad \text{.....(1.3)}$$

where N_{0D}, N_{1D} ,N_{0A} and N_{1A} indicate the state population densities of the respective states, the subscripts 0 and 1 standing for the ground and first singlet states respectively, *W(t)* (photons cm^{-2} s^{-1}) is the pump rate, σ_D and σ_A are the absorption cross sections at the pump wavelength and τ_D and τ_A are the decay times of the singlet states of the donor and acceptor respectively in the absence of transfer. K_F & K_R are the non radiative and radiative rate constants.

The gain of the dye mixture system at wavelength λ in terms of the stimulated and absorption cross sections is given by [36]

$$\gamma(\lambda) = \sigma_e^A N_{1A} - \sigma_a^A N_{0A} + \sigma_e^D N_{1D} - \sigma_a^D N_{0D} \quad \text{.....(1.4)}$$

Since the absorption and emission of donor molecules can be assumed to be negligibly small in the fluorescence spectrum of the acceptor molecule, the gain coefficient can be given by

$$\gamma(\lambda) = \sigma_e^A N_{1A} - \sigma_a^A N_{0A} \quad \text{.....(1.5)}$$

The rate equations (1.1) and (1.2) can be made dimensionless by multiplying with $\frac{\tau_A}{N_A}$ to give

$$\frac{dn_{1D}}{dx} = n_{0D}\alpha_D - K_F N_A n_{1D} n_{oA} \tau_A - \frac{n_{1D}\tau_A}{\tau_D} \quad \text{.....(1.6)}$$

$$\frac{dn_{1A}}{dx} = n_{0A}\alpha_A + (K_F + K_R) N_A n_{1D} n_{oA} \tau_A - n_{1A} \quad \text{.....(1.7)}$$

where

$$x = \frac{t}{\tau_A}, \quad n_{1D} = \frac{N_{1D}}{N_A} \ , \ n_{0D} = \frac{N_{0D}}{N_A}$$

$$\alpha_D = \sigma_D W(t) \tau_A \ , \ \alpha_A = \sigma_A W(t) \tau_A \quad \text{.....(1.8)}$$

Since we are measuring the unsaturated gain, ground state populations are negligibly perturbed. Therefore $N_{0A}=N_A$, i.e.

$$n_{1D} = \frac{N_A}{N_A} = 1 \ , \ n_{0D} = \frac{N_D}{N_A} = F = \frac{F_D}{1 - F_D}$$

where $F_D = \frac{N_D}{(N_A + N_D)}$ is the fractional donor population. Now, under the steady state approximation,

$$\frac{dn_{1D}}{dx} = 0 = \frac{dn_{1A}}{dx}$$

Hence the above equation reduces to

$$n_{1A} = \alpha_A + \frac{K_F + K_R}{K_F N_A + K_D} N_A \frac{F_D}{1 - F_D} \alpha_D \quad \text{.....(1.9)}$$

where $K_D = \frac{1}{\tau_D}$ is the natural decay rate of the donor. Thus the final gain equation becomes

$$\gamma(\lambda)=\left(\sigma_e^A\frac{\alpha_A}{\alpha_D}+(K_F+K_R)\sigma_e^A\frac{F_D}{1-F_D}\frac{N_A}{K_FN_A+K_D}\right)\alpha_DN_A-\sigma_a^AN_A \quad ....(1.10)$$

Equation 1.10 shows that the gain per acceptor molecule of the mixture is increased with the addition of the donor by a factor

$$(K_F+K_R)\sigma_e^A\frac{F_D}{1-F_D}\frac{N_A}{K_FN_A+K_D}\alpha_DN_A \quad .....(1.11)$$

It is evident that $\gamma(\lambda)$ is proportional to the pump power and a plot between the two is a straight line with the slope of the line given by equation (1.11). This slope can also be calculated by subtracting the contribution due to the acceptor alone from that of the mixture. For a known value of K_F the value of K_R can be calculated by equating the experimental value of the slope to the numerical value obtained above.

The non-radiative rate constant K_F can be calculated by the Stern-Volmer equation which in its most familiar form can be written [35,37] as

$$\frac{I_{0D}}{I_D}=1+K_F\tau_{0D}[A] \quad .....(1.12)$$

where I_D and I_{0D} are the fluorescence intensities of the donor in the presence and absence of the acceptor respectively, τ_{0D} is the lifetime of the excited donor in the absence of the acceptor, $[A]$ is the concentration of the acceptor and K_F is the rate constant for the nonradioactive energy transfer from D* to A.

A plot of $\frac{I_{0D}}{I_D}$ vs $[A]$ will be a straight line with a slope equal to $K_F\tau_{0D}$. Knowing the value of τ_{0D}, the rate constant for the nonradiative

transfer of energy from donor to acceptor, K_F can be obtained. The critical separation of the donor and the acceptor, R_0 for which energy transfer from D^* to A and emission from D^* are equally probable, is obtained by using [38]

$$R_0 = 7.35\left([A]_{1/2}\right)^{-1/3} \quad \text{.....(1.13)}$$

where $[A]_{1/2}$ is the half quenching concentration at which $I_D = \frac{1}{2} I_{0D}$. Thus by comparing the rate rate constants for radiative and nonradiative processes, the contribution of the two mechanisms to the overall energy transfer in a mixed solution can be estimated.

1.3 Lifetime measurements-Time correlated single photon counting

Time domain analysis of the dye fluorescence under various conditions is important in characterizing them as laser media. At present most of the time domain measurements are performed using time correlated single photon counting (TCSPC), but other methods can be used when rapid measurements are needed. Many publications on TCSPC have appeared [39-45]. These measurements use high repetition rate mode locked pico second (ps) or femto second (fs) laser light sources, and high speed micro channel plate (MCP) photo multiplier tubes (PMTs). For many applications, these expensive systems are being rapidly replaced by systems using pulsed laser diodes (LDs), light emitting diodes (LEDs) , and small, fast PMTs.

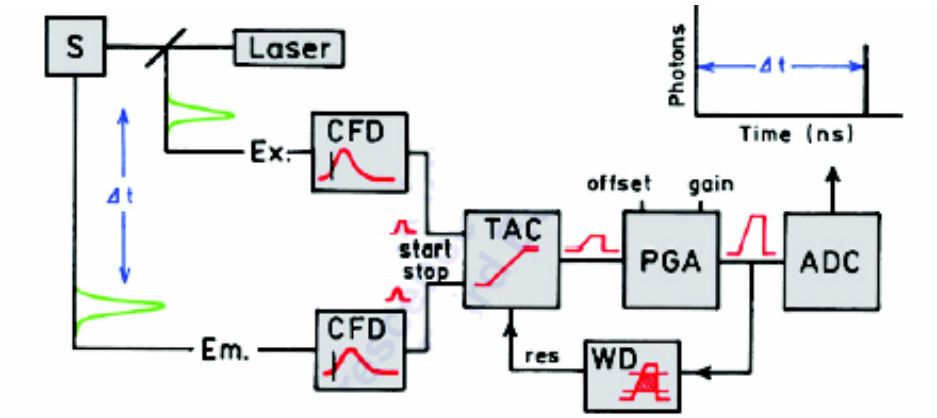

Fig. 1.4. Electronic schematic for the time correlated single photon counting

Principle of Time correlated single photon counting

The principle of TCSPC is shown in figure 1.4. The sample is excited with a pulse of light, resulting in the waveform shown at the top of the figure. This is the waveform that would be observed when many fluorophores are excited and numerous photons are observed. However for TCSPC the conditions are adjusted so that just one photon is detected per laser pulse. In fact the detection rate is typically one photon per 100 excitation pulses. The time duration is measured between the excitation pulse and the observed photon and stored in a histogram. The x axis is the time difference and the y axis gives the number of photons detected for this time difference. When much less than one photon is detected per excitation pulse, the histogram represents the waveform of the decay. If the count rate is higher, the histogram is biased to shorter times. This is because with TCSPC only the first photon can be observed. At present the electronics are not fast enough to measure multiple photons per pulse when the lifetimes are in the nanosecond regime. Multiple photons per pulse can be measured for decay times near a microsecond or longer. Specialized electronics are used for measuring the time delay between the excitation and emission.

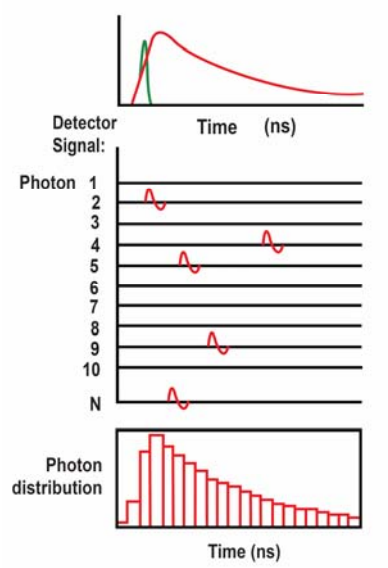

Fig.1.5. Principle of TCSPC. The pulses in the middle panel represent the output from a constant fraction discriminator.

The experiment starts with the excitation pulse that excites the samples and sends a signal to the electronics. This signal is passed through a constant function discriminator (CFD) which accurately measures the arrival time of the pulse. This signal is passed through a time-to-amplitude converter (TAC), which generates a voltage ramp that is a voltage that increases linearly with time on the nanosecond time scale. A second channel detects the pulse from the single detected photon. The arrival time of the signal is accurately determined using a CFD, which sends a signal to stop the voltage ramp. The TAC now contains a voltage proportional to the time delay (Δt) between the excitation and emission signals. As needed the voltage is amplified by a programmable gain amplifier (PGA) and converted to a numerical value by the analog-to-digital converter (ADC). To minimize false readings the signal is restricted to given range of voltages. If the signal is not within the range the event is suppressed by a window discriminator (WD). The voltage is converted to a digital value that

is stored as a single event with the measured time delay. As described in the figure 1.5, a histogram of the decay is measured by repeating this process numerous times with a pulsed light source.

1.4 Fabrication techniques for polymer optical fibres

1.4.1 Step Index Polymer optical fibres

Fabrication of step index polymer optical fibre (SIPOFs) by the preform method involves two stages. In the first stage, a cylindrical preform 1-5cm in diameter and up to 1cm length is made. In the second stage, the preform is drawn into a fibre by the heat drawing process. This is the conventional method for the manufacture of GOFs and the same process, in principle, is applied for the manufacture of POFs as well. For the manufacture of commercial step index fibre, a cylindrical tube is made which serves as the cladding layer by polymerizing the cladding material in a rotating cylindrical reactor. Materials that can be polymerized by the radical polymerization reaction typically are used and the reaction is induced thermally or by UV radiation using a photo initiator. Due to the fast rotational speed of the reactor about its cylindrical axis, a tube of uniform thickness is formed once the reaction is complete. This tube is then removed from the reactor and filled with a core material mixed with an initiator and a chain transfer agent. The core material is then polymerized to make a preform that is drawn into a fibre by the heat drawing process. The tubular cladding layer can also be made by directly extruding a readymade polymer. However contamination can be serious making this approach less preferable.

Advantages of preform method are simplicity and versatility. As the thermal exposure is limited to the heat drawing process, degradation occurs to a lesser degree compared to the continuous extrusion method. In addition, this process is easy to modify and the materials that are used can be readily changed. Despite these advantages this batch process is not prevalent for the manufacture of SI-POFs, probably due to lower production rate than the

continuous method. However, the versatility of the preform method makes it a preferred method for the manufacture of GI-POFs. The SIPOFs used for the present work were fabricated without incorporating any cladding and the surrounding air medium air acts as the cladding.

1.4.2 Graded Index Polymer optical fibres

GIPOF has drawn considerable interest recently as a high bandwidth data transmission medium for short distance applications such as local area networks, office networks and home networks. The bandwidth of GI POF is maximized by optimizing the distribution of the refractive index in the radial direction of the fibre. Theoretically, the refractive index profile is often described by the power-law model [46,47]

$$\begin{aligned} n(r) &= n_1\left[1-2\Delta\left(\frac{r}{R}\right)^{\alpha}\right] \qquad \text{for} \quad r \le R \\ &= n_2 \qquad\qquad\qquad\qquad\quad \text{for} \quad r \ge R \end{aligned} \qquad \text{.....(1.14)}$$

Here, r is the radial distance from the fibre axis, R is the radius of the fibre core, n1 and n2 are the refractive indices at $r = 0$ and $r = R$, respectively, $\Delta = \frac{(n_1^2 - n_2^2)}{2n_1^2}$, and α is the power-law exponent, which determines the refractive index profile as a function of radius. In particular a parabolic index profile corresponds to the case α=2.

The bandwidth of an optical fibre is limited by dispersion, which represents broadening of optical pulses as they propagate through the fibre. The dispersion of an optical fibre is divided into two parts: intermodal (or simply modal) and intramodal. Intramodal dispersion is also called the group velocity dispersion. In a geometrical optics description, the modal

dispersion is attributed to different paths followed by different rays. For example a ray propagating along the fibre axis has the shortest path, whereas the path is longer for oblique rays. Consequently, different rays with different paths arrive at the fibre output at different times unless their velocities are adjusted along their paths through spatial variation of the refractive index as in a GI fibre. For this reason the modal dispersion can also be called as multipath dispersion. Intramodal dispersion has two contributions: material (or chromatic) dispersion and waveguide dispersion. Material dispersion is caused by a finite distribution of the wavelength of incident light and the wavelength dependence of the refractive index of a material. Nonideal incident light always has a wavelength distribution and hence material dispersion occurs unless the material is nondispersive. However, material dispersion is reportedly much smaller than modal dispersion unless the modal dispersion is extremely small, as is the case in single mode fibres. Waveguide dispersion depends on fibre parameters such as core radius R and the fractional index difference Δ . When the refractive index profile is described by the power-law model, the bandwidth is maximized when

$$\alpha = 2 + \varepsilon - \Delta \frac{(4+\varepsilon)(3+\varepsilon)}{5+2\varepsilon} \quad \text{.....(1.15)}$$

where ε is the material dispersion parameter[48]. If the material dispersion is assumed to be negligible, the maximum bandwidth is achieved when $\alpha = (2 - 12\Delta/5)$ .As Δ is small, of the order of 0.01, for a typical GIPOF for fibre optic communications, the optimum α is close to 2 and the refractive index profile is approximately parabolic. Studies indicate that the material dispersion has a significant influence on the bandwidth of GIPOFs, and the

optimum value of α for PMMA based GIPOFs is about 2.3 when material dispersion is taken into account[49,50].

1.4.3 Interfacial-Gel polymerization

The best known method for the fabrication of GI-POFs is the interfacial gel polymerization method, which was pioneered by Koike and his co-workers [15,16]. At first, this method was applied to the co-polymerization of monomer mixtures with different reactivity ratios and different refractive indices as in the photoco-polymerisation process [18,51].Later it was applied to mixtures of a monomer and a non-reacting organic dopant[52].

In this method a transparent polymeric tube (e.g., PMMA) is prepared and this tube is then filled with a mixture of a monomer and a nonreacting dopant (e.g., methyl methacrylate and benzyl butyl phthalate) and is thermally polymerized in an oil bath. The inner wall of the tube is swollen by the monomer as it forms a thin gel phase. The polymerization reaction that takes place by heating is faster in the gel phase; consequently, the thickness of the polymeric tube grows inward, forming a rod. The molecular volume of the dopant is typically larger than that of the monomer, the monomer diffuses into the gel phase faster than the dopant and reacts. Consequently, the dopant is rejected from the polymerization site and its concentration becomes gradually higher towards the center of the preform as the polymerization reaction progresses. Thus a concentration gradient of the dopant is created in the radial direction of the preform. Figure 1.6 show the photographs of the dye doped graded index polymer rod and its cross sectional view.

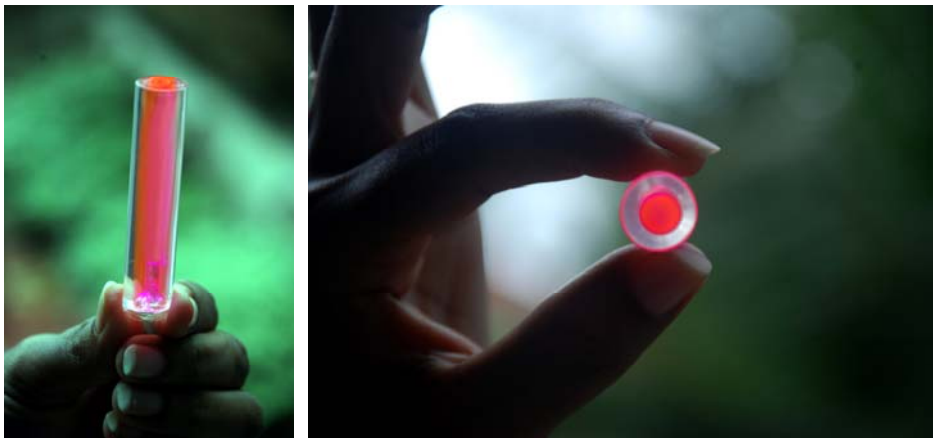

Fig.1.6. Photograph of the dye doped graded index polymer rod

1.4.4 Refractive index profile measurement of the preform rod

The refractive index profile measurement of the solid rod can be done using the slab method where a thin slice of the preform was cut, polished and kept in one of the arms of a Mach Zender interferometer. A He-Ne laser beam along with a beam expander was used as the light source. Thin, polished slabs of the rod of about 1mm thickness were introduced into one of the paths of the interferometer. The light passing through the slab undergoes a phase shift, which depends on the optical path length. The fringe displacements for the points within the central portion of the disc are then measured with respect to the parallel fringes outside the core region. These fringes can be photographed using a high resolution digital camera. The difference in refractive index between various points in the core and cladding region can be calculated from the fringe shift and the parallel fringe spacing (in the cladding) [53]. Figure 1.7 shows the experimental setup and and a typical photograph of the fringe pattern. The profile parameter α of the rod was also calculated from the equation 1.14 for the variation of refractive index n(r) with the distance from the axis for graded index fibres [54].

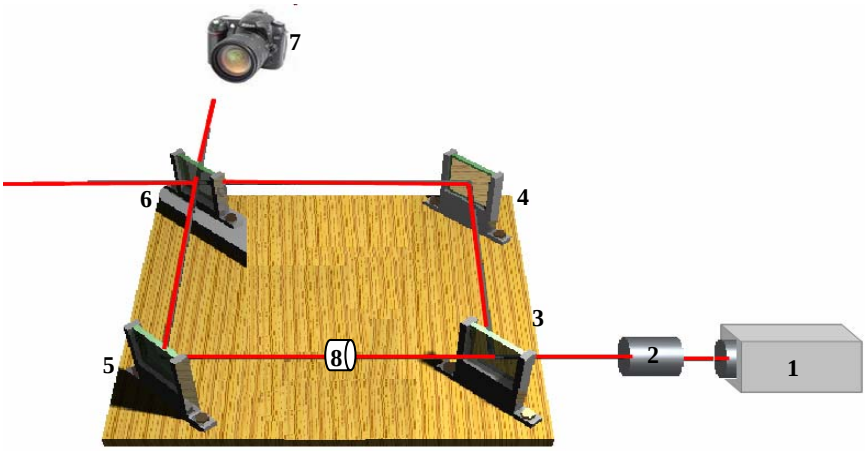

Fig.1.7. The experimental setup for measuring the refractive index profile of the rod. 1. He-Ne Laser, 2. Beam Expander, 3,6. Beam splitters, 4,5. Mirrors, 7. High resolution digital camera, 8.Sample

1.5 Heat drawing process

The manufacture of POF is similar to that of glass fibre, except for two important differences. First, the processing temperature for POF (~200^{0}C) is much lower than that for glass fibre drawing (~2000^{0}C). Second, free convection of air is typical in POF manufacturing, as compared to the forced convection of inert gas, which is used in glass fibre drawing [55]. Three goals motivate the need to accurately predict and understand the initial heating process: minimizing the heating time, minimizing the initial material waste and optimizing the processing conditions for various preform diameters. Understanding the effect that the thermal environment has on the heating characteristics of the preform will allow the calculation of the preform's resulting temperature. Due to the prominence of radiative heat transfer at steady state, the resulting axial temperature profile within the preform is strongly coupled to the corresponding axial temperature.

The heat drawing process is shown schematically in figure 1.8. The preform is positioned vertically in the middle of the furnace where its lower portion is

heated locally to the drawing temperature. Both convective and radiative heat transfer mechanisms are important in heating the preform in the furnace [56-58]. As the rod proceeds through the heating zone, its temperature and viscosity will vary across its axis governed by the input heat distribution.

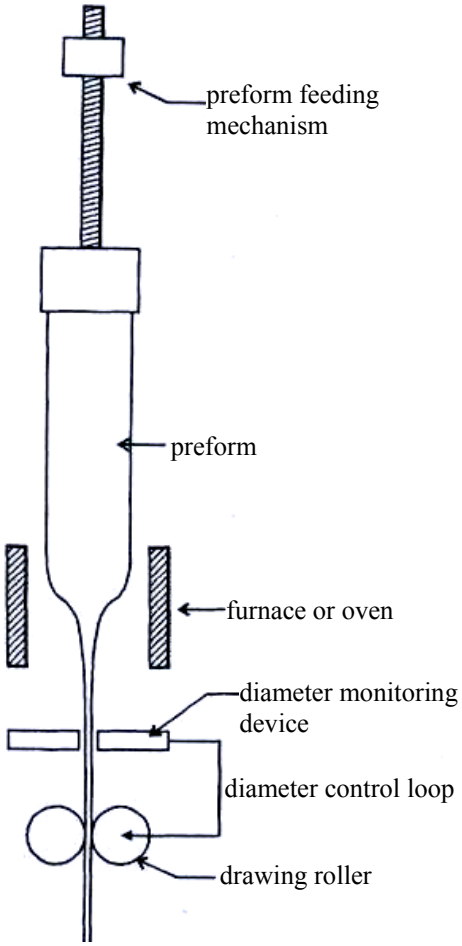

Fig.1.8. The schematic diagram of the fibre heat drawing process.

These conditions along with the extensional deformation caused by the drawing tension yield a "neck-down" shape within the heating zone .This neck down shape is influenced by differing drawing conditions and in turn influences

the fibre diameter uniformity [59]. When the lower part of the preform reaches a temperature beyond its softening point, it necks downwards by its own weight due to gravity. Once this initiation of the drawing process is achieved, tension is applied to the fibre by drawing rollers and the fibre is drawn continuously while the preform is fed at a predetermined rate. Given the rod feed and fibre drawing velocities, the nominal draw down diameter ratio is governed by the conservation of mass [60].

To minimize the transmission loss due to variation of the fibre diameter, it must be controlled stringently [61].The fibre diameter can be continuously monitored and the desired value is maintained by controlling the speed of the drawing roller [62]. The typical diameter of multimode GOFs is about 125-250 μm, whereas that of POFs is in the range of 0.25-1.0mm.whereas the diameter of GOFs must be controlled to within 0.1%, less stringent tolerances of 2-3% are applied to POFs. The steady drawing of fibres is a well-understood process for both glasses [63-65] and polymers [66-68]. As the fibre drawing is characterized by a free surface, it is subjected to a variety of instabilities [69].The most prevalent instability modes are tensile rupture and draw resonance [69-72].Tensile rupture is due to the failure of the material in tension, whereas draw resonance is characterized by periodic oscillation of the fibre diameter that is sustained unless the response is driven to extreme amplitudes. Although the influence of convective heat transfer on draw resonance has been reasonably well documented, the influence of radiative heat transfer has not been rigorously investigated yet [73].

To minimize transmission loss in POFs due to thermal damage, special attention also should be given to furnace design. As the radiative heat transfer is dominant in the furnace, a shorter distance between the preform surface and the inner surface is preferable. In addition, localizing heat to a narrow zone where the preform is melted is preferable to minimize heat exposure. Thus

shorter length of the heating zone is desirable as long as sufficient heating is provided. The step index fibres can be drawn from the dye doped polymer rods obtained by direct polymerization of the dye doped MMA solution in a test tube. Graded index fibres can be fabricated from the dye doped graded index rods. Figure 1.9 shows the photograph of a typical step index fibre doped with Rhodamine B.

Fig. 1.9. The photograph of the drawn dye doped step index fibre.

1.6 Fibre Attenuation measurement- Cut-Back method

Fibre attenuation measurement have been developed in order to determine the total fibre attenuation and this is contributed by both absorption losses and scattering losses. The overall fibre attenuation is of great interest to the system designer but the relative magnitude of the different loss mechanisms is important in the development and fabrication of low loss fibres. Different methods can be employed for measuring attenuation: the insertion loss method (non destructive), the substitution method (non destructive) and the cut-back method (destructive).A commonly used standard technique for determining the total fibre attenuation per unit length is the cut-back or the differential method[74].

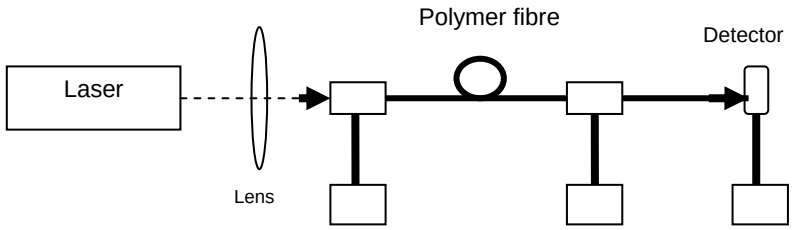

Fig.1.9. Fibre attenuation measurement using cutback method

The cutback method provides more accurate results than the insertion and substitution method .The advantage of this method lies in the fact that launching conditions remain unchanged. A schematic diagram of a typical experimental setup is shown in figure 1.9. Light beam from a 5 mW Helium Neon laser is launched into the fibre with the help of a lens. After polishing the fibre end faces the fibre is firmly held in a suitable holder such that only a small length projects outside. The incident beam is adjusted at the input end of the fibre so that maximum power is obtained at the output end. The output power is measured using a photo detector as $P(L_1)$, where L_1 is the length of the test fibre. Without disturbing the launching conditions, a short length of the fibre from the output end is cut and polished. The output power is again measured as $P(L_2)$ where L_2 is the cut back length of the fibre. Cutting, polishing and measuring process is repeated several times. From these measurements the attenuation can be measured using the relation

$$\alpha_{dB} = \frac{10\log\frac{(P(L_2)}{(P(L_1)}}{L_1 - L_2} \quad \text{..... (1.16)}$$

1.7 Beam profile measurements

The guiding properties of the fabricated SI and GI fibres were tested by launching a He-Ne laser beam in to a 1 meter long fibre and measuring its output profile. The output from the fibre was analyzed using a software. The output beam profiles of the fibres were measured by injecting a Gaussian mode

into the fibres using a DataRay Beam R2 scanning type beam profiler and analyzing the output using the software DR Ver 6.0. A linear scanning probe carries either a single slit, or orthogonal X-Y slits. Light passing through the slit falls on to a Si detector inside the profiler. It can preform real time measurements of the parameters like gaussian beam diameter,Gaussian fit,centroid position, ellipticity, orientation of major axis and beam wander display for the beam dimensions in the range 3μm-45mm with a resolution of 0.5μm. The 2-D and 3-D profiles are reconstructed from the X-Y scan, making the assumption that the measured X beam profile in the same for all the values of Y and that the measured Y beam profile is the same for al values of X.

1.8 Hollow Optical fibres

Stacking and heat drawing hollow polymer optical fibres is one of the methods to fabricate micro structured optical fibres (MOF). Microstructured optical fibre, or photonic crystal fibre [75], offers huge potential in the field of fibre-optic chemical and biochemical sensing. The characteristic micron-sized holes that run along the length of MOF can be filled with a fluid, thereby bringing the species to be quantified in contact with the mode field propagating through the fibre over long lengths. Of particular importance is the ability of MOF to guide whilst being filled with low index materials such as aqueous solutions, which are important for biosensing, and sensing gases. Sensing mechanisms can be based on the modulation of characteristics such as polarization, wavelength, intensity and phase. Light may be guided in MOF by two distinctly different guiding mechanisms: in a solid core surrounded by a microstructured cladding providing index guidance [75], or, alternatively, in a hollow core surrounded by a necessarily regular microstructured region designed such that certain wavelengths cannot propagate through this region and are hence confined to the hollow core [76].Correspondingly, there are several sensing regimes possible using MOFs. An advantageous feature

common to all three cases of MOF chemical sensors is that sample volume required is small, since the volume of the holes of, say, a 50 cm length of MOF is typically of the order of microlitres. In the present work we have fabricated a Rhodamine 6G dye doped hollow polymer optical fibre and the fluorescence emission was characterized after filling the fibre with an aqueous solution of the dye Sodium Fluorescein. The fibre was excited using a 488nm argon ion laser and SHG output at 532nm from an Nd:YAG laser.

1.9 Polymer microring lasers

Optical micro resonators are of great interest for the studies of quantum electrodynamics (QED) modification of spontaneous emission, microlasers and light emitting diodes. As the mode volume of the microresonator decreases and approaches a cubic wavelength, the number of modes interacting with the optically active spectral region in the microresonator approaches unity. This can result in single lasing mode with in the emission spectral width and in strong coupling between the optical field and the gain medium. One of the key advantages of organic materials is the simple solution processing that permits some very novel fabrication methods that are impossible with inorganic semiconductors. Such novel processing has allowed other less conventional microresonator structures in polymer lasers, notably microlasers with annular or even spherical resonator structures. One example of this is the polymer microring laser [77-83] which consists of a thin polymer waveguide deposited around a dielectric or metallic core.

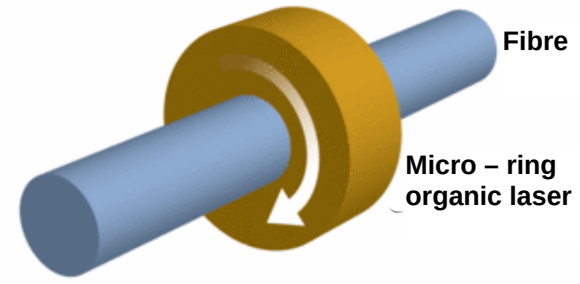

Fig. 1.10. A typical microring organic laser

These structures can be readily fabricated from solution by simply dipping the core, which may be silica optical fibre or metal wire into a concentrated solution of the polymer. As shown in figure 1.10, on withdrawal of the fibre from the solution, an annular droplet surrounding the core dries to deposit a thin polymeric film. An alternative approach is to deposit a polymer on the inner surface of a micro capillary, which has the advantage of encapsulating the organic film [84]. Such films form a type of ring cavity by reflection of light at the interfaces between polymer and surrounding media. These lasers are rather larger in dimension than the planar microcavities, in that the diameters D, of the cores are typically tens to hundreds of micrometers. The round trip path of the resonator is approximately equal to πD, and hence light travels through a much longer part of the gain medium in a round-trip. Assuming that the round trip losses are not substantially greater than in the case of the planar microcavity, this means that a much lower excitation density (~1μJ cm^{-2})[78,81] is required in order to achieve sufficient gain to reach lasing threshold. Lasers with very low threshold pulse energies of 100 pJ have also been reported [79]. Typically these lasers are pumped on one side of the ring (in which pump light is sent down the core of the ring) can lead to reduced threshold densities due to a more uniformly pumped structure. These structures can also be configured as light emitting diodes and have the possibility of electrical excitation for lasers by using gold wire as the core and depositing a partially transmitting outer contact.

The longer round trip however means that there are commonly many more longitudinal modes supported by the cavity, so these lasers tend to oscillate on many closely spaced wavelengths. The feedback mechanism can also be rather complicated [78,82], with a combination of whispering gallery modes in which total internal reflection around the ring can form a closed loop optical path plus other waveguide modes, in which light is trapped in the film by total internal reflection at both polymer air and polymer core interfaces.

Both mechanisms support a distinct set of resonant frequencies which are superimposed to give complicated clusters of closely spaced modes within the gain bandwidth. For sufficiently small diameters, <10μm, these clusters can be engineered to give single frequency lasing. In addition to the often complicated spectral output, these resonators are distinctive in that they do not emit a well defined directional output beam; instead light is emitted uniformly in all radial directions. While this may generally considered an unappealing feature, such an unusual output pattern may have some potential for sensing applications.

Several types of microcavities such as spheres, rings, disks and Fabry-Perot cavities made by semiconductors, organic dye solutions and dye doped polymers have been reported [85-91]. The Q value is used to characterize the quality of a microresonator mode and is defined as 2π times the number of optical cycles required for the cavity mode field to decay to 1/e of its initial value. For many applications it is important to explore novel inexpensive and repeatable fabrication techniques.

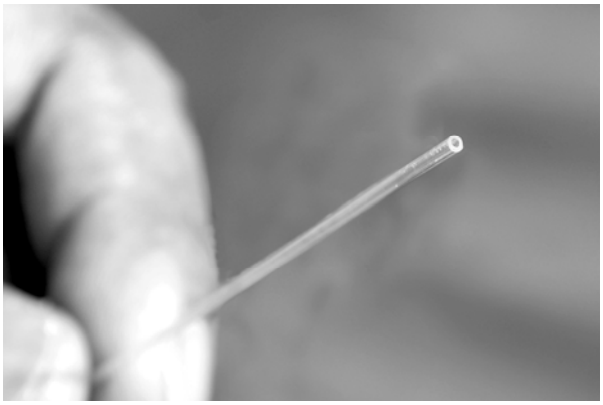

Fig. 1.11. A dye doped hollow polymer optical fibre

It is important to explore new techniques to fabricate ultra high-Q-value resonators for fundamental QED and nonlinear optical studies. In order to realize low threshold lasers, it is necessary to utilize a high Q cavity to confine

the light into a gain region and also to have a strong coupling ratio between field and matter. Whispering gallery modes (WGM) oscillations from microring cavities have the advantage that high Q values are easily obtained even in a very small mode volume and the number of modes contributing to the laser oscillations can be reduced. In the present study, we formed a polymer microring by making use of a hollow dye doped polymer optical fibre which acts as a waveguide forming a ring resonator. The resonant frequencies for the wave guided laser modes for a hollow optical fibre with outer diameter D are given by [92]

$$\nu_m = \frac{mc}{\pi D n} \quad \text{.....(1.17)}$$

where m is an integer, c is the speed of light in vacuum, and n is the refractive index of the polymer. Figure 1.11 shows a dye doped polymer hollow optical fibre which can act as a polymer microcavity.

1.10 Conclusions

A general introduction to polymer optical fibres (POF) and a glimpse of the potential of the doped optical fibres in modern optical communication network has been given. The chemical structure of PMMA and that of the dyes used for doping the POF is discussed. The general fabrication techniques of graded index fibres and polymer microcavities have been discussed. The importance of the use of dye mixtures for doping the POF is explained using a rate equation based theory of energy transfer among dyes. The techniques used in the present investigation for the fabrication and characterization of the dye doped polymer optical fibres with different refractive index profiles have been explained.

References

[1] G.P. Agrawal, "*Fibre Optic Communiation Sytems*" 2nd ed. Wiley-Interscience, NewYork,1997.

[2] Mitsubishi Rayon Co., *U.K. Patent* 1,431,157,1974

[3] Mitsubishi Rayon Co., *U.K. Patent* 1,449,950,1974

[4] C.Emslie, "*Review polymer optical fibres*," J.Mater.Sci. 23,2281 ,1988.

[5] F.P.Kapron,D.B.Keck and R.D.Maurer, "*Radiation Losses in. Glass Optical Waveguides,*"Appl.Phys.Lett.17,423,1970.

[6] T.Kaino, K.Jinguji, and S.Nara, "Low loss poly(methylmethacrylate-d8) core optical fibres" Appl.Phys.Lett.42,567, 1983.

[7] Y.Ohtsuka and Y.Hatanaka, "*Preparation of light-focusing plastic fibre by heat-drawing process*" Appl.Phys.Lett. 29,735 ,1976.

[8] Nippon Selfoc Co.,*U.S Patent* 3,955,015,1976.

[9] Y.Ohtsuka,T.Senga, and H.Yasuda, "*Light-focusing plastic rod with low aberration,*"Appl.Phys.Lett.25,659, 1974.

[10] Y.Ohtsuka,T.Sugano and Y.Terao, "*Studies on the light-focusing plastic rod. 8: Copolymer rod of diethylene glycol bis (allyI carbonate) with methacrylic ester of fluorine containing alcohol*" Appl.Opt. 20,2319,1981.

[11] Y.Ohtsuka and I,Nakamoto, Y.Ohtsuka and I,Nakamoto, "*Light-focusing plastic rod prepared by photocopolymerization of methacrylic esters with vinyl benzoates*" Appl.Phys Lett. 29,559, 1976.

[12] Y.Ohtsuka, Y.Koike and H.Yamazaki, "*Studies on the light-focusing plastic rod. 6: The photocopolymer rod of methyl methacrylate with vinyl benzoate*"Appl.Opt.20,280,1981.

[13] Y.Koike,H.Hatanaka and Y.Ohtsuka, "*Studies on the light-focusing plastic rod. 17: Plastic GRIN rod lens prepared by photocopolymerization of a ternary monomer system*", Appl.Opt.23,1779, 1984.

[14] Y.Ohtsuka and Y.Koike,Appl.Opt. "*Studies on the light-focusing plastic rod. 18: Control of refractive-index distribution of plastic radial gradient-index rod by photocopolymerization*" 24,4316, 1985.

[15] Y.Koike,Y.Takezawa and Y.Ohtsuka, "*New interfacial-gel copolymerization technique for steric GRIN polymer optical waveguides and lens arrays*", Appl.Opt.27,486,1988.

[16] Koike, N.Tanio, E.Nihei and Y.Ohtsuka, *"Gradient-index polymer materials and their optical devices*", Polym.Eng. Sci. 29,1200, 1989.

[17] Y.Koike, "*High-bandwidth graded-index* polymer *optical fibre Polymer*" 32,1737, 1991.

[18] Y.Koike and E.Nihei,*U.S.Patent* 5,253,323, 1993.

[19] T.Ishigure,E.Nihei, and Y.Koike, "*Graded-index polymer optical fibre for high-speed data communication*"Appl.Opt.33,4261,1994.

[20] Y.Koike, T.Ishigure and E.Nihei, J.Lightwave Technol. "*High-bandwidth graded-index polymer optical fibre,"*13, 1475 ,1995.

[21] T.Ishigure,A.Horibe,E.Nihei and Y.Koike, "*High-bandwidth, high-numerical aperture graded-index polymer optical fibre*" J.Lightwave Technol.13,1686,(1995).

[22] M.G Kuzyk, U.C.Prek. and C.W.Dirk, "*Guest-host polymer fibres for nonlinear optics,*" Appl.Phys.Lett,59,902,1991.

[23] D.Bloor, "*Organic materials for Nonlinear Optics*" II, R.A.Hann and D.Bloor, Eds. Cambridge, U.K: Royal Society of Chemistry, pp.3-24,1991.

[24] H.Kanbara, M.Asebe, K.Kubodera, and T.Kaino, "*All-optical picosecond switch using organic single-mode fibre waveguide*" Appl.Phys.Lett. 61,2290,1992.

[25] G.D.Peng,Z.Xiong and P.L.Chu, "*Fluorescence Decay and Recovery in Organic Dye-Doped Polymer Optical Fibres*," J.Lightwave Technol. 16,2365,1998.

[26] A.Tayaga, Y.Koike, E.Nihei,S.Teramoto,K.Fujii,T.Yamamoto and K.Sasaki. "*Basic performance of an organic dye-doped polymer optical fibre amplifier*" Appl.Opt 34,988, 1995.

[27] C.E.Moeller, C.W. Vebrber and A.H. Adelman, "*Laser pumping by excitation transfer in dye mixtures*" Appl.Phys. Lett., 18 , 278,1971.

[28] S.A.Ahmed, J.S.Gergely and D.Infante, "*Energy transfer organic dye mixture lasers*", J.Chem.Phys., 61,1584,1974.

[29] F.B.Dunning and E.D.Stokes, "*The generation of tunable near IR radiation using a nitrogen laser pumped dye laser*", Opt.Commun., 6,160,1972.

[30] R.C.Hilborn and H.C. Brayman, "*Simultaneous two-wavelength output from multiple-dye pulsed tunable dye lasers*" ,J.Appl.Phys., 45, 4912,1974.

[31] A.Dienes and M.Madden, "*Study of excitation transfer in dye mixtures by measurements of gain spectra*" ,J.Appl.Phys., 45,4912,1974.

[32] B.Panoutsopoulos, M.Ali, S.A.Ahmed, "*Experimental verification of a theoretical model for continuous wave energy transfer dye mixture lasers in the near infrared*", Appl. Opt 31,1213,1992.

[33] C.Lin, A.Dienes , "*Study of excitation transfer in laser dye mixtures by direct measurement of fluorescence lifetime*", J. Appl.Phys.,44, 5050,1973.

[34] A.Dienes and M.Madden, "*Study of excitation transfer in dye mixtures by measurements of gain spectra*", J.Appl.Phys., 44 ,4161,1973.

[35] S.Muto, C.Ito and H.Ineba, "*Efficient PPF-αNPO Energy Transfer Dye Laser in Ultraviolet Region*", Jpn. J. Appl. Phys., 21,L535,1982.

[36] O.G.Peterson, J.R.Webb and W.C.McGolgin, Appl. Phys., 42, 917,1971.

[37] M.Orentstein, J.Katriel and S.Speiser, "*Optical bistability in molecular systems exhibiting nonlinear absorption*" Phys.Rev.A, 35,2157,1987.

[38] R.D Singh, A.K.Sharma, N.V.Unnikrishnan and D.Mohan, "*Energy transfer study on coumarin-30-rhodamine-6G dye mixture using a laser fluorimeter*", J.Mod. Opt., 37, 419,1990.

[39] Demas JN, "*Excited state lifetime measurements*", Academic Press New York1983.

[40] O'Connor DV, Philips.D, "*Time correlated Single Photon Counting, Acdemis Press*", NewYork 1984.

[41] Birch DJS, Imhof RE, "*Time domain fluorescence spectroscopy using TCSPC*". In Topics in fluorescence Spectroscopy Vol.1: Techniques, pp.1-95, Ed JR Lakowicz, Plenum Press NewYork 1991. .

[42] Ware WR, "*Transient Luminescence measurements.In Creation and detection of excited state*" Vol 1A, pp. 231-302. Ed AA Lamola, Marcel Dekker NewYork , 1971.

[43] Becker W, Bergmann A, "*Multidimensional Time correlated Single Photon Counting*" In Reviews in Fluorescence Vol. 2. pp. 77-108 ed CD Gedds, JR.Lakowicz, Kluwer Academic/Plenum Publishers NewYork, 2005.

[44] Bassi A, Swartling J, D'Andrea C,Pifferi A, Torricelli A, Cubeddu R, "*Time resolved spectrophotometer for turbid media based on super continuum generation in a photonic crystal fibre*". Opt. Lett 29 (20) 2405-2407,2004.

[45] Karolczak J,Komar D, Kubicki J, Wrozowa T, Dobek K, "*The measurements of picosecond fluorescence lifetimes with high accuracy and subpicosecond precision*" Chem.Phys.Lett. 344, 154,2001.

[46] P.Halley, "*Fibre Optic Systems*," Wiley, NewYork,1987.

[47] R.Olshansky and D.B Keck, "*Pulse broadening in graded-index optical fibres*" Appl.Opt.15,483, 1976.

[48] D.Gloge and E.A.J.Marcatili*, "Bell System Tech.J*." 52,1563 ,1973.

[49] T.Ishigure,E.Nihei, and Y.Koike, "*Optimum refractive-index profile of the graded-index polymer optical fibre, toward gigabit data links*" Appl. Opt.35,2048,1996

[50] T.Ishigure, M.Satoh,O.Takanashi, E.Nihei, T.nyu, S.Yamazaki and Y.Koike, "*Formation of the Refractive Index Profile in the Graded Index Polymer Optical Fibre for Gigabit Data Transmission*" J.lightwave Technol., 15,2095 ,1997.

[51] Y.Koike,E.Nihei, *U.S.Patent* 5,382,488,1995.

[52] T.Koike *Us Patent* 5,541,247,1996.

[53] C.K.Sarkar "*Optoelectronics and Fibre Optics Communication*", New Age International, New Delhi,2001.

[54] John M. Senior "*Optical Fibre Communications*", Prentice-Hall of India, New Delhi,2004.

[55] Hayden.M.Reeve, Proceedings of IMECE , "*Symposium on polymer and composite material processing*", November 11, NewYork,2001.

[56] S.H.K.Lee and Y.Jaluria, J.Mat. *Proc. Manufacturing Sci*. 3, 317, 1995.

[57] S.H.K.Lee and Y.Jaluria, "*Simulation of the transport processes in the neck-down region of a furnace drawn optical fibre*", Int. J. Heat Mass Transfer 40, 843,1997.

[58] A.M.Mescher, H.M.Reeve and J.B.Dixon, "*Proceedings of the International Polymer Optical Fibres Technical Conference*", Cambridge, MA,P 26,2000.

[59] U.C. Paek, R.B.Runk, "*Physical behavior of the neck-down region during furnace drawing of optical fibres*," J.Appl.Phys, 49(8) 4417,1978.

[60] U.C.Paek, "*Laser Drawing of Optical Fibres*" Appl.Opt. 13,1383 ,1974.

[61] D.Markuse, "*Radiation losses of the HE11 mode of a fibre with sinusoidally perturbed core boundary*" Appl.Opt. 14, 3021, 1975.

[62] T.Izawa and S.Sudo, "*Optical fibres: Materials and fabrication*", Kluwer, Boston, 1987.

[63] L.R.Glicksman, **"***The cooling of glass fibres*" Glass Technol. 9, 131,1968.

[64] G. Manfre, *Glass Technol*. 10, 99, 1969.

[65] J.A.Burgman, *Glass Technol*. 11, 110, 1970.

[66] S.Kase and T.Matsuo, **"***Studies on melt spinning. II. Steady-state and transient solutions of fundamental equations compared with experimental results*" J.Appl.Polym.Sci. 11,251 ,1967.

[67] M.M.Denn, **"***Continuous Drawing of Liquids to Form Fibres*", Ann.rev. Fluid Mech. 12, 365 ,1980.

[68] C.W.Park, "*Extensional flow of a two phase fibre*," *AIChE J*. 36,197, 1990.

[69] A.Ziabicki, in "*Man made Fibres*"(M.F.Mark, S.M.Atlas and E.Cernia, Eds.), p.13. Interscience, NewYork, 1967.

[70] J.R.A.Pearson and M.A,Matovich, "*Spinning a molten threadline*", Ind. Eng. Chem. Fund. 8, 605 ,1969.

[71] S.Kase, "*Studies on melt spinning. IV. On the stability of melt spinning*". J.Appl.polym.Sci. 18, 3279, 1974.

[72] W.S.Lee, C.W.Park, "*Stability of a Bicomponent Fibre Spinning Flow*", J.Appl.Mech. 62, 511,1995.

[73] F.T.Geyling and G.M.Homsy, "*Extensional instabilities of* glass *fibre drawing process*,"Glass Technol. 21, 95 ,1980.

[74] Ajoy Ghatak, K,Thyagarajan, "*Introduction to fibre optics*", Cambridge University Press, NewDelhi,2002.

[75] J. C. Knight, T. A. Birks, P. St. J. Russell and D. M. Atkin, "*All-silica singe-mode optical fibre withphotonic crystal cladding*," Opt. Lett. **21**, 1547-1549 ,1996.

[76] R. F. Cregan, B. J. Mangan, J. C. Knight, T. A. Birks, P. St. J. Russell, P. J. Roberts, and D. C. Allen, "*Single-mode photonic bandgap guidance of light in air,*" Science 285, 1537-1539,1999.

[77] A.Schulzgen.,C.Spiegelberg,M.M. Morrell, S.B.Mendes, P.M.Allemand, Y.Kawabe, M.Kuwata Gonokami,S.Honkanen,M.Fallahi,B.Kippelen and N.Peyghambarian. "*Light amplification and laser emission in conjugated polymers*", Opt.Eng. 37,1149,1998.

[78] S.V.Frolov,M.Shkunov,Z.V.Vardeny,K.Yoshino. "*Ring microlasers from conducting polymers*", Phys.Rev.B 56,R4363,1997.

[79] S.V.Frolov, Z.V.Vardeny,K.Yoshino. "*Plastic microring lasers on fibres and wires*", Appl.Phys.Lett. 72,1802,1998.

[80] Y.Kawabe, C.Spiegelberg, A.Schulzgen, M.F.Nabor, B.Kippelen, E.A.Mash, P.M.Allemand, M.Kuwata Gonokami,K. Takeda and N.Peyghambarian. "*Whispering- gallery-mode microring laser using a conjugated polymer*", Appl.Phys.Lett. 72,141,1998.

[81] G.Ramoz-Ortiz,C.Spiegelberg, N.Peyghambarian and B.Kippelen, "*Temperature dependence of the threshold for laser emission in polymer microlasers*", Appl.Phys.Lett. 77,2783,2000.

[82] R.C.Polson,G.Levina,Z.V.Vardeny "*Spectral analysis of polymer microring lasers*", Appl.Phys.Lett. 76,3858,2000.

[83] R.Osterbacka,M.Wohlgenannt,M.Shkunov,D.Chinn,Z.V.Vardeny, "*Excitons, polarons, and laser action in poly(p-phenylene vinylene) films*", J.Chem.Phys. 118,8905,2003.

[84] Y.Yoshida,T.Nishimura, A.Fujii,M.Ozaki,K.Yoshino, "*Lasing of Poly(3-alkylthiophene) in Microcapillary Geometry*", Jpn.J.Appl.Phys Part 2 , 44,L1056,2005.

[85] A.J.Campillo,J.D.Eversole, and H.B.Lin, "*Cavity quantum electrodynamic enhancement of stimulated emission in microdroplets*", Phys.Rev.Lett. 67,437 ,1991.

[86] S.L.McCall,A.F.J.Levi, R.E.Slusher, S.J.Peartson and R.A. Logan, "*Whispering-gallery mode microdisk lasers*",Appl.Phys.Lett,60,289 ,1992.

[87] M.Kuwata-Gonokami,K.Takeda,H.Yasuda and K.Ema, "*Laser Emission from Dye-Doped Polystyrene Microsphere*", Jpn.J.Appl.Phys,part 1 31,L99 ,1992.

[88] J.C.Knight,H.S.T.Driver,R.J.Hutcheon and G.N.Robertson, "*Core-resonance capillary-fibre whispering-gallery-mode laser*", Opt.Lett. 17, 1280, 1992.

[89] M.Osuge and K.Ujihara, "*Spontaneous emission and oscillation in a planar microcavity dye laser*", J.Appl.Phys.76,2588, 1994.

[90] M.Kuwata Gonokami, R.H.Jordan, A.Dodabalapur,H.KKatz, M.L.Schilling, R.E Slusher, and S.Ozawa, "*Polymer microdisk and microring lasers*" Opt.Lett.20,2093 ,1995.

[91] J.P.Zhang, D.Y.Chu,S.L.Wu, S.T.Ho, W.G.Bi, C.W.Tu,and R.C.Tiberio, "*Photonic-Wire Laser*", Phys.Rev.Lett.75,2678 ,1995.

[92] H.P.Weber and R.Ulrich Appl.Phys.Lett. "*A thin Film Ring laser*", 19 38,1971.

……ൠ…..

Chapter- 2

A comparative study of energy transfer in dye mixtures in monomer and polymer matrices under pulsed laser excitation

Contents

2.1 Introduction

Several techniques have been reported for obtaining two or more wavelengths simultaneously from a single dye laser [1-4]. These techniques have used a number of wavelength selective elements in the dye laser cavity. The excitation of dye lasers through energy transfer processes by using an appropriate mixture of dyes is a more convenient means of extending the lasing wavelength region and improving the efficiency. Energy transfer dye lasers (ETDLs) using numerous donor-acceptor pairs have been reported by various workers during last three decades. [5-10]. The primary motivation for the use of mixture of dyes as lasing medium has been either an improvement in the laser performance or the possibility of multi wavelength operation. Dienes et.al [11] developed a simple theoretical model to explain the variation of laser gain with

acceptor concentration and gain measurements done by them on rhodamine 6G:cresyl violet (Rh 6G-CV) mixtures and on CV alone clearly show a higher gain in the mixture as compared to CV alone [12]. This gain, which is the result of an enhanced lifetime of the acceptor, produces a blue shift in the emission peak of the acceptor [13]. As a result of this gain enhancement the conversion efficiency of the dye laser was improved considerably.

Most of the ETDL studies conducted earlier report investigations of energy transfer between dyes in liquid media. The use of a solid matrix for the dye laser gets rid of many of the common problems associated with static or flowing liquid systems such as convective Schlieren, evaporation, flow fluctuation, stagnant films, solvent or dye poisoning and even explosions [14]. One of the important advantages of transparent polymers compared to the traditional optical materials is that it is possible to introduce organic dyes or other compounds that can play the role of active components into the polymers, which appreciably changes the characteristics of the polymer matrix.

Vast majority of optical amplifiers are based on an optic fibre doped with a fraction of a percent of the rare-earth element erbium. Although rare-earth doping has been generally used in silica, many laboratories have been working to develop stable rare-earth doped polymer lasers and amplifiers. The main issue with rare earth doped polymer lasers and amplifiers has been pumping inefficiencies due to the de- excitation of the excited states caused by the IR absorption in the polymer. In bulk form, polymer hosts impregnated with certain dyes have achieved 80% conversion efficiency from pump power to signal power with tuning range close to those in solution [15]. Dye –doped polymer optical fibres can be made into useful fibre amplifiers and lasers that operate at wavelengths other than 1300nm and 1550 nm [16,17]. Optical amplifiers and lasers made of dye-doped fibre require much less pump power

compared to bulk material because of the effective confinement and long interaction length available in the fibre. Since photo bleaching increases with the increase of the exposure intensity, low pump intensity would increase the lifetime of the gain medium. Also, the thin and long geometry of the fibre is ideal for good thermal relaxation to minimize the thermally induced photo bleaching [18]. This chapter gives the details of the comparative study of energy transfer mechanisms in 3 different dye mixtures in monomer and polymer matrices under pulsed laser excitation.

2.2 Theoretical tools

The rate constants for the radiative and Forster type energy transfer mechanisms can be obtained from the Stern-Volmer plots given by the equations [19, 20]

$$\frac{I_{0d}}{I_d} = 1 + K\tau_{0d}[A] \quad \text{.....(2.1)}$$

$$\frac{\phi_{0d}}{\phi_d} = 1 + K_{nr}\tau_{0d}[A] \quad \text{.....(2.2)}$$

where I_{0d} and I_d are the fluorescence intensities of the donor in the absence and presence of acceptor, respectively. ϕ_{0d} and ϕ_d are corresponding quantum yields. τ_{0d} is the fluorescence lifetime of the donor without acceptor. K and K_{nr} are total and nonradiative transfer rate constants respectively. [A] is the acceptor concentration. By knowing the value of τ_{0d}, K and K_{nr} can be calculated from the slopes of I_{0d} / I_d versus [A] curve and ϕ_{0d} / ϕ_d versus [A] curve which are straight lines. The critical transfer radius (R_0), for which energy transfer from the excited donor (D*) to [A] and emission from D* are equally probable, is given by [21]

$$R_0 = \frac{7.35}{\left([A]_{\frac{1}{2}}\right)^{\frac{1}{3}}} \quad \text{..... (2.3)}$$

Where $[A]_{1/2}$ is the half quenching concentration which can be obtained under the condition

$$\frac{I_{0d}}{I_d} = 2$$

Total transfer efficiency η is written as the sum of two parts,

$$\eta = \eta_r + \eta_{nr} \quad \text{..... (2.4)}$$

As is well known, in the presence of acceptor, the fluorescence intensity of the donor is reduced from I_{0d} to I_d by energy transfer to acceptor. A more practical expression for η can be given by [22, 23]

$$\eta = 1 - \frac{I_d}{I_{0d}} \quad \text{..... (2.5)}$$

The nonradiative transfer efficiency η_{nr} is defined as [24]

$$\eta_{nr} = \pi^{\frac{1}{2}} X \exp(X^2)(1 - erfX) \quad \text{..... (2.6)}$$

where $X = \frac{[A]}{[A_0]}$ is the molar concentration expressed relative to the critical molar concentration of the acceptor,

$$[A]_0 = \frac{3000}{2\pi^{3/2} N R_0^3} \quad \text{..... (2.7)}$$

where N is the Avogadro number and

$$erfX = \frac{2}{\pi^{1/2}} \int_0^X \exp(-t^2) dt \quad \text{..... (2.8)}$$

2.3 Experimental

Three types of dye mixtures in MMA with fixed donor concentrations were prepared using laser grade dyes (Exciton, Lambda Physik) and distilled spectroscopic grade methyl methacrylate (Lancaster). The excitation source was an Nd:YAG pumped Optical Parametric Oscillator (Spectra Physics- MOPO 710) of which 445 nm line is employed to pump C 540 which is the donor molecule in the first two dye pairs whereas the Rh6G:RhB dye mixture was pumped using a frequency doubled Nd:YAG laser emitting at 532 nm. The pump wavelength 445 nm was selected since any higher pump wavelength, was found to be absorbed significantly by the Rh.B and Rh 6G which results in the direct excitation of the acceptors. For the first two pairs, the donor concentration [D] was kept fixed at 10^{-5}m /l and for the third pair, [D] was fixed at 10^{-4} m/l while the acceptor concentration was varied.

Dye solution was taken in a quartz cuvette of width 1 cm and it was pumped in a transverse pumping configuration. The fluorescence emission from the solution was collected using an optical fibre and was directed to the entrance slit of an Acton Spectrapro-500i spectrograph having a resolution of 0.03nm coupled with a CCD camera to record the spectrum. Optical absorption spectra of the samples were recorded on a Jasco V-570 spectrophotometer. The solutions were thermally polymerised after adding polymerisation initiator benzoyl peroxide (BPO) 0.4 wt% and the chain transfer agent (n-butyl mercaptan) , 0.1 wt%. One end face of the fabricated rods was cut and polished and it was tightly fixed inside a hole drilled in an aluminium block, which is provided with openings for excitation of the sample and collection of fluorescence. The fluorescence lifetimes of the donor in pure form and in the dye mixture were measured both in MMA as well as PMMA matrices using time-correlated single-photon counting

technique employing a micro channel plate photomultiplier tube (Hamamatsu R 3809 U-50) and a multi channel analyser. The measurement is made using an IBH-5000 Single Photon Counting Spectrometer. Two nano-LEDs (Spectra Physics) emitting at 455 and 495nm with a resolution of 200 ps were used as the excitation sources. The fluorescence decay curves are analyzed using an iterative fitting program provided by IBH.

2.4 Results and Discussion

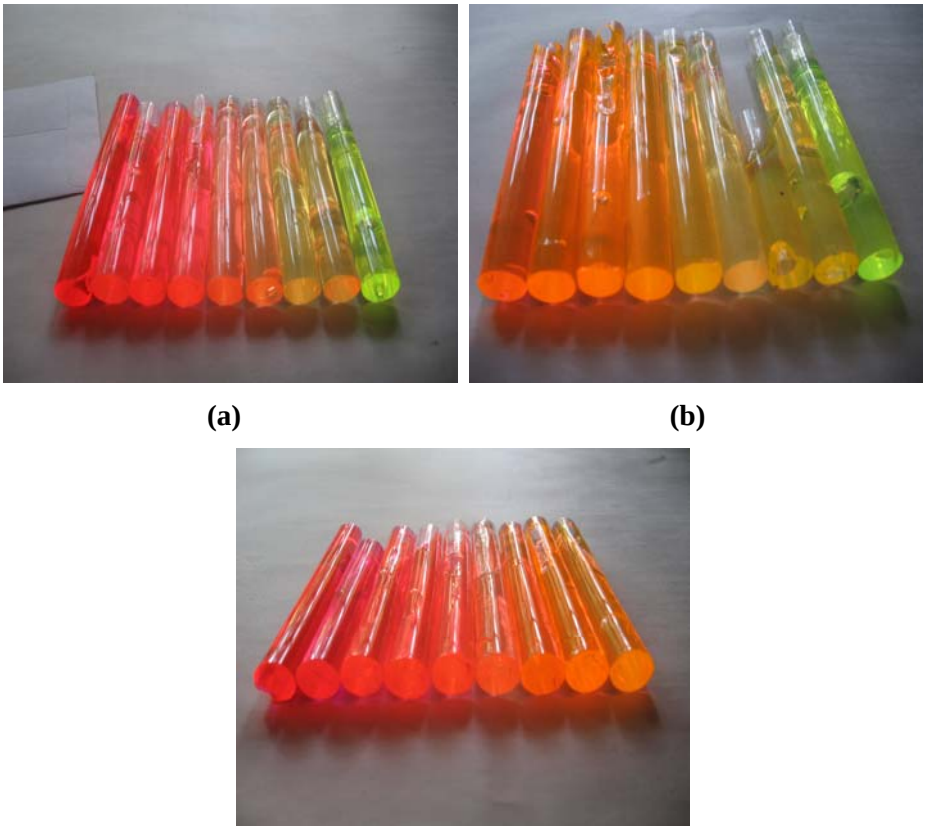

(a) **(b)**

(c)

Fig. 2.1a, 1b, 1c Photographs of all the three sets of fabricated dye mixture doped polymer rods.

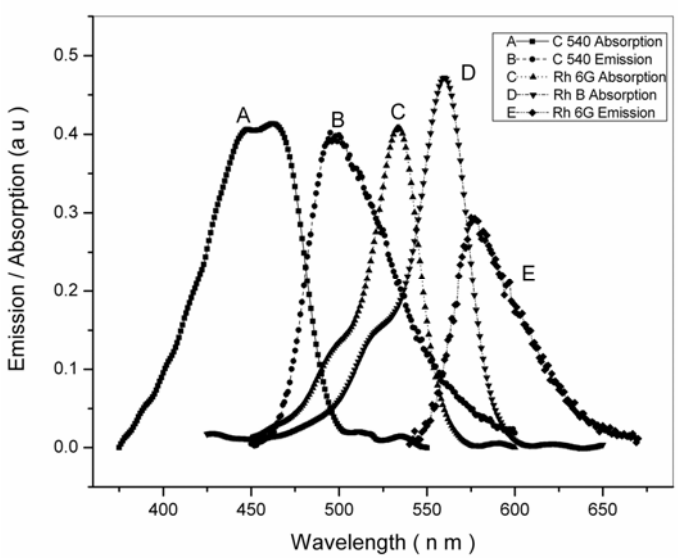

Fig.2.2. Emission spectra of C 540 and Rh 6G along with absorption spectra of C 540, Rh 6G and Rh B in PMMA

The fabricated sets of rods used in the present study are shown in the figure 2.1. (Fig.2.1a-c 540:Rh 2.1b, Fig.2b-1c 540: Rh 6G, Fig. 2c- Rh 6G:RhB). Relevant absorption spectra of C 540, Rh B and Rh 6G as well as the emission spectra of C 540 and Rh 6G in PMMA matrix are presented in figure 2.2. Since most of the area under the emission line shapes of C 540 overlaps with the absorption line shapes of Rh 6G and Rh B, energy transfer from C540 to Rh 6G and Rh B are clearly possible and the extent of this depends on the overlapping area. A similar kind of overlap exists between Rh 6G emission and Rh B absorption also.

Figures 2.3 and 2.4 represent the fluorescence spectra of the three dye pairs, in MMA as well as in PMMA matrices respectively. It can be seen that the intensities and peak wavelengths are different in both matrices. These changes can be attributed to the volume reduction that is happening during the polymerisation of the MMA.

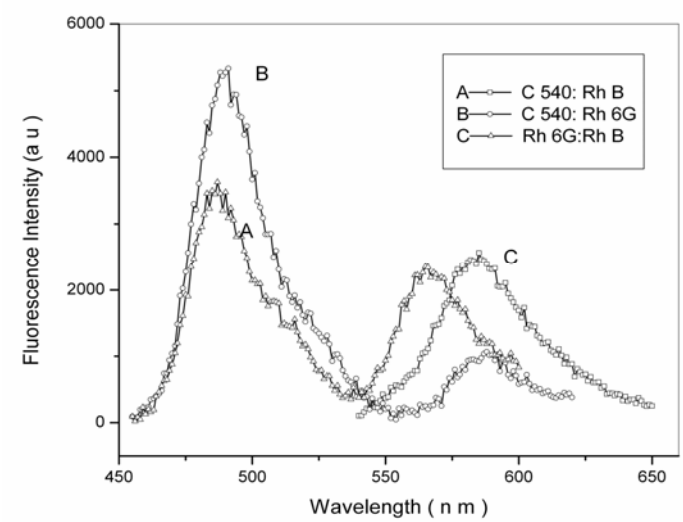

Fig. 2.3. Emission spectra of the dye mixtures in MMA A- [D] =10^{-5} mol l^{-1} and [A] = 7 x10^{-5} mol l^{-1}, B - [D] =10^{-5} mol l^{-1} and [A] = 5 x10^{-4} m/l, C – [D] = 10^{-4} m/l and [A] = 5x10^{-5}m/l

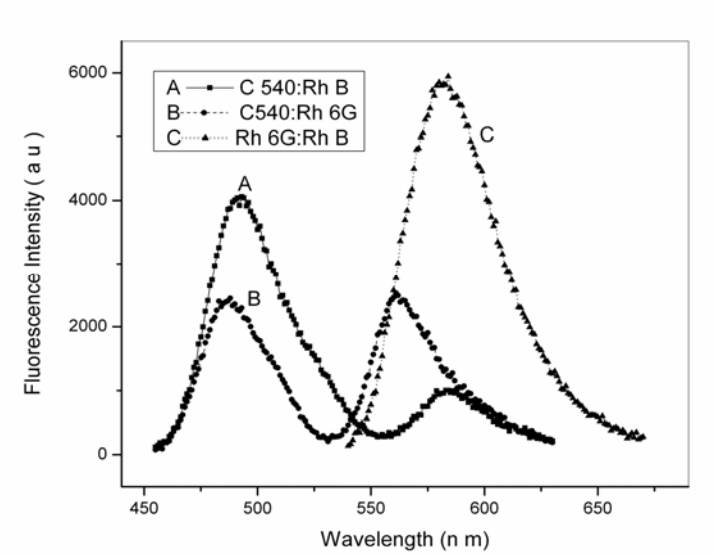

Fig. 2.4. Emission spectra of the dye mixtures in PMMA matrix A- [D] =10^{-5} mol l^{-1} and [A] = 7 x10^{-5} mol l^{-1}, B - [D] =10^{-5} mol l^{-1} and [A] = 5 x10^{-4} m/l, C – [D] = 10-4 m/l and [A] = 5x10^{-5}m/l.

Detailed analysis of the evolution of the peak wavelengths and intensities is possible from the figures 2.5 and 2.6, which are the spectra, recorded in MMA and

PMMA respectively for different acceptor concentrations in the pair C 540: Rh 6G with a fixed donor concentration of 10^{-5} m/l. It is evident that there is considerable decrease in the fluorescence intensity after solidification. Due to the volume reduction, it was also observed that half quenching concentrations of all the three dye pairs have changed appreciably to a lower value. This is attributed to the fact that due to the effect of volume reduction, the donor and acceptor molecules are brought more close together, which enhances the quenching.

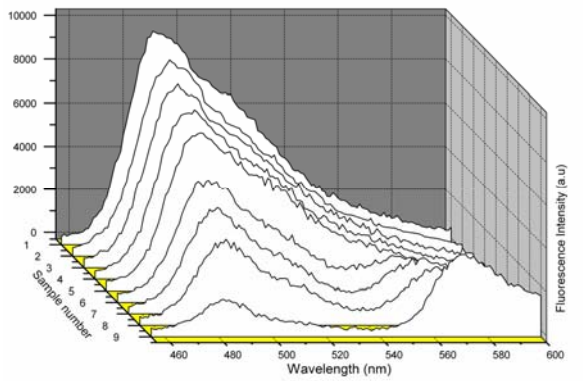

Fig. 2.5. The recorded fluorescence for the pair C 540: Rh 6G in MMA. Sample 1- [D] only 10^{-5}m/l, 2-[A] =7x10^{-6} m/l, 3- [A] = 10^{-5} m/l , 4-[A]= 10^{-5} m/l, 5- [A]= 2.5x 10^{-5} m/l, 6- [A] = 4x 10^{-5} m/l, 7- [A] = 5.5x10^{-5} m/l, 8 – [A] = 7x10^{-5} m/l, 9-[A] = 10^{-4} m/l.

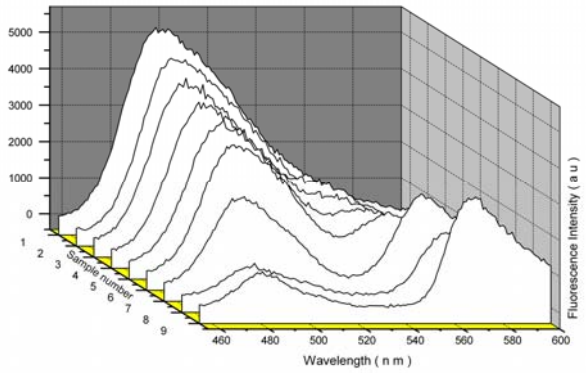

Fig. 2.6. The recorded fluorescence for the pair C 540: Rh 6G.Sample in PMMA 1- [D] only 10^{-5} m/l, 2-[A] =7x10^{-6} m/l , 3- [A] = 10^{-5} m/l, 4-[A]= 10^{-5} m/l, 5- [A]= 2.5x 10^{-5} m/l, 6- [A] = 4x 10^{-5} m/l, 7- [A] = 5.5x10^{-5} m/l, 8 – [A] = 7x10^{-5} m/l, 9-[A] = 10^{-4} m/l.

It was also observed that the acceptor concentration at which the two wavelengths producing comparable intensities are also different in the two matrices. The concentrations are $7x10^{-5}$ m/l , $5.5x10^{-5}$ m/l respectively for MMA and PMMA matrices for the pair C 540- Rh 6G. A similar kind of variation was observed in C 540:Rh B pair as well.

2.4.1 Dependence of peak emission wavelengths on acceptor concentration

From the recorded fluorescence in figure 5 and 6 an important observation is that in the mixture, donor dye always shows a blue shift. In MMA matrix, for the C 540 – Rh 6G pair, the donor blue shift was found to be 9 nm while for the C 540- Rh B pair the shift was about 7 nm. In the absence of donor, the acceptor emission showed a continuous red shift of about 9 nm in the range of concentrations from 10^{-5} m/l to 10^{-4} m/l for the C 540- Rh 6G pair and this red shift was about 11 nm for the pair C 540- Rh B in the concentration range, 10^{-4} m/l to $7x^{-4}$ m/l. But in the presence of donor, both the acceptors showed an initial blue shift followed by a red shift. For the dye pair C 540: Rh 6G, a distinct peak for the acceptor arises at an acceptor concentration $4x10^{-5}$ m/l and this was blue shifted by 4 nm compared to the pure acceptor emission peak at that concentration. Above this acceptor concentration, acceptor emission peaks are red shifted by about 18 nm. A similar behaviour was observed for the C 540 Rh B pair also where distinct peak for the acceptor emission arises at [A] = $5x10^{-4}$ m/l with a blue shift of about 10 nm followed by a red shift of 12 nm up to [A] = $7x10^{-4}$ m/l. The above analysis was not made for the Rh.6G: Rh B pair since there was only a single peak in the emission spectrum. figure 2.7 shows the dependence of donor and acceptor wavelengths on acceptor concentration in MMA as well as PMMA matrices for the pair C 540:Rh 6G. The figure clearly shows that, the blue shifts of the donor emission as well as the red shift in the acceptor emission in the present range of

acceptor concentrations are larger for the dye mixture in PMMA. In MMA, the initial blue shift for the acceptor was about 12 nm, which was followed by a red shift of about 14 nm while for the dye mixture in PMMA, the acceptor shows an initial blue shift of about 15 nm followed by a red shift of 18nm.In PMMA, the donor dye shows a continuous blue shift of about 15 nm. The additional feature in dye mixture in PMMA is that, the acceptor peak becomes more distinct at a lower value of [A].

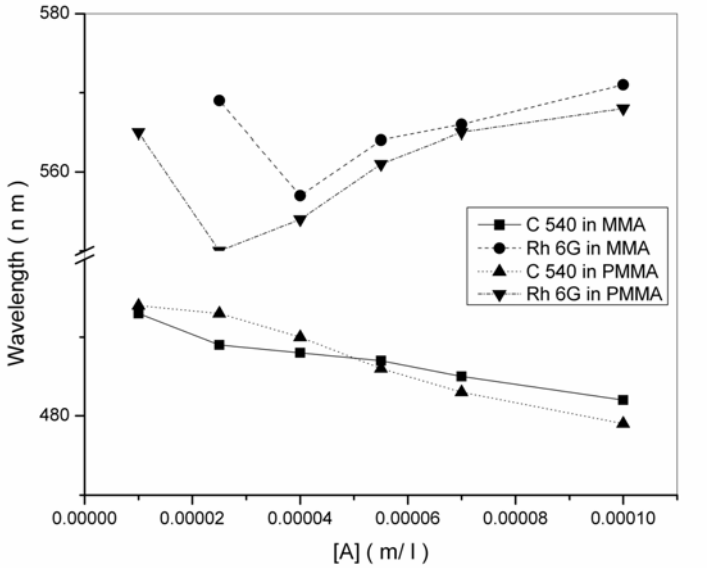

Fig. 2.7. The variation of donor and acceptor emission peak wavelength in the dye mixture C 540-Rh 6G with acceptor concentration.

The blue shift observed in the donor emission can be attributed to the fact that at smaller intermolecular separations, the heat energy generated in the acceptor system will be sufficient to populate the higher excited singlet state of the donor molecule. The sudden blue shift observed for the acceptor molecule is the result of the energy transfer process. The donor-sensitized system was observed to have a higher gain compared to an unsensitised system due to an increase in the effective lifetime [13]. As a result of this, the gain maximum is shifted towards the blue region. The lifetime of the

acceptor will be appreciably increased at low concentrations ($<10^{-3}$ molar) as reported by Urisu et.al [25]. Similar blue shifts have been reported in Rh 6G:Rh B dye mixture in ethanol [26] and also in other dye mixtures [27,28]. At lower [A] values, many acceptor molecules are excited to its higher excited singlet states and the consequent emission gives rise to this blue shift. At higher acceptor concentrations, this effect is not dominant because of the collissional deexcitation**.** The red shift beyond a certain acceptor concentration is also attributed to the fact that with increase in concentration, both absorption and fluorescence intensities increase and a change in the reabsorption pattern occurs. For these concentrations, the acceptor emission depends only on its concentration and the energy transfer effect will not have any dependence on the emission wavelength of the acceptor molecule.

2.4.2 Dependence of peak fluorescence intensity of donor and acceptor on acceptor concentration

It is important to know the relative fluorescence intensities of the two peak emissions in the mixture before the solution is polymerised. In all the three pairs, considerable increase in fluorescence intensities were obtained at the acceptor emission wavelengths compared to the pure acceptor fluorescence. Specifically, in the pair C 540:Rh B, the acceptor dye Rh B starts emission from the [A] = $7x10^{-5}$ m/l onwards whereas in the entire concentration range of the present study, the pure acceptor does not have any emission. Figure 2.8 shows the variation of the emission intensity of the donor and acceptor molecules with acceptor concentration for the present ETDL system. It was observed that, the fluorescence intensity of the acceptor was increased by 4.1 times in the range of acceptor concentrations in the present ETDL system with maximum intensity being at [A] = $1x10^{-4}$ m/l.

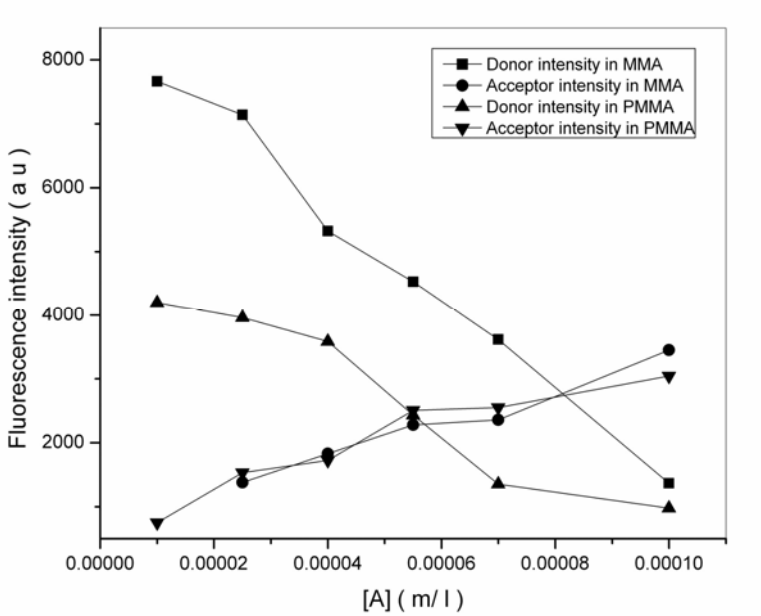

Fig. 2.8. The variation of donor and acceptor fluorescence with acceptor concentration for the C 540: Rh 6G pair.

But at very high acceptor concentrations (>1x10^{-4}m/l), curves show a decrease in slope, which is due to the self-quenching acceptor-acceptor interaction. At the same time, the donor emission intensity decreases considerably with increasing acceptor concentrations. It also clearly depicts the enhancement of the acceptor fluorescence in the range of concentrations of the present study compared to the pure acceptor. A similar enhancement in the acceptor emission was also observed in C 540:Rh B pair also.

For the Rh 6G:Rh B pair, even though there were no distinct peaks for donor and acceptor, the intensity measurements at the donor and acceptor wavelengths showed almost a similar behaviour.

It may be pointed out that the pure acceptors Rh 6G and Rh B are not having any emission at 445nm excitation even though there is a little fluorescence from the Rh 6G at higher acceptor concentrations (≥ 10^{-4} m/l). In the presence of donor, the

acceptor emission becomes more efficient due to effective energy transfer from the donor. Another important feature is that there is a comparable intensity for the acceptor both in MMA as well as PMMA matrices even though there is considerable reduction in the intensity for the donor after polymerisation.

The comparable intensity for acceptor in the two matrices as shown in figure 2.8 is attributed to the fact that polymerization in the present experiment results in higher values of radiative and nonradiative energy transfer rate constants from donor to acceptor which in turn compensates the possible decrease in acceptor intensity after polymerization.

2.4.3 Energy transfer rate constants

In the presence of acceptor dye, the fluorescence intensity of the donor dye is reduced from I_{0d} to I_d. The energy transfer efficiency and the transfer rate constants for the ETDL system in MMA and PMMA matrices can be calculated by studying the relative fluorescence intensities of the donor (I_{0d} / I_d). In MMA matrix, for the pair C 540:Rh 6G, the transfer efficiency assumes maximum values at the highest acceptor concentration. It starts from a minimum value (~0.26) at the lowest acceptor concentration 10^{-5} m/l to a maximum value (~0.63) at the highest concentration 10^{-4} m/l. For the pair C 540: Rh B, the transfer efficiency varies form (~0.23) at [A] = 10^{-4} m/l to (~0.56) at $7x10^{-4}$ m/l. In the case of Rh. 6G: Rh B pair, the transfer efficiency was 0.25 at [A] = $3.5x10^{-5}$m/l to 0.8 at [A] = 10^{-4} m/l. The maximum values of efficiencies in the PMMA matrix were 0.76, 0.64 and 0.87 for C 540:Rh6G, C540:Rh B and Rh.6G:Rh B pairs respectively. Knowing the value of $[A]_{1/2}$ the half quenching concentration at which $I_d = I_{od}/2$, the value of critical radius R_0 can be evaluated using equation (2.3) for the three dye pairs.

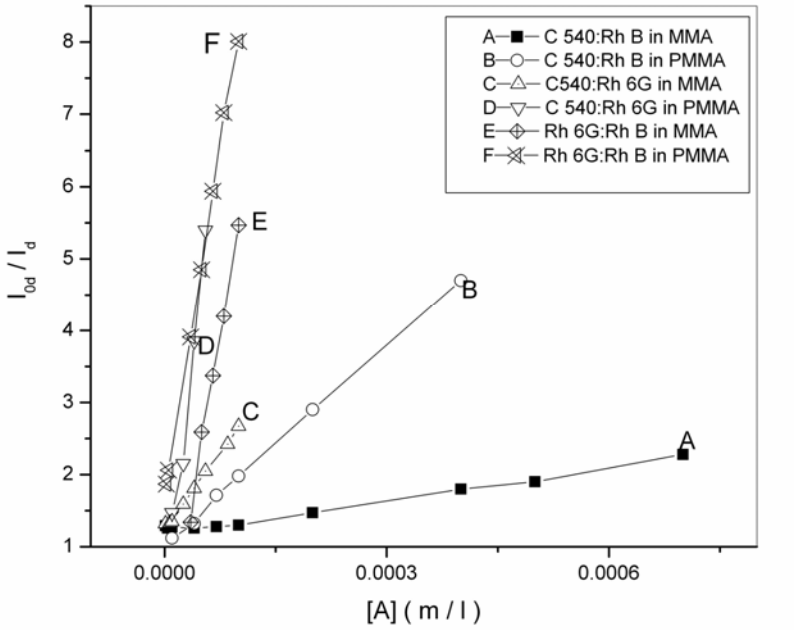

Fig. 2.9. The Stern Volmer plots for the present ETDL systems

After polymerisation, all the samples show a faster quenching compared to the dye mixtures in monomer. Figure 2.9 shows the Stern-Volmer plots obtained for the dye mixtures both in MMA as well as PMMA. There is a clear indication of the change in slope after the medium is solidified which essentially leads to changes in the energy transfer characteristics of the system

The values obtained for R_0 clearly shows that the non-radiative transfer involved in the dye mixture is of dipole-dipole in nature. There are noticeable changes in the R_0 values in PMMA as compared with the values in MMA. For C 540:Rh 6G pair, R_0 changed from 195 A^0 to 242 A^0. The changes in the other dye pairs were 91 A^0 to 156 A^0 and 210 A^0 to 340 A^0 for C540:Rh B and Rh 6G:RhB pairs respectively. The fluorescence lifetimes of the pure donor molecules in MMA as well as PMMA were

measured experimentally using time-correlated single photon counting technique. Figures 2.10 and 11 shows fluorescence decay curves of the pure donor molecules in MMA. The measured values of the lifetimes were τ_{0d} = 4.96 ns, 8.00 ns for C 540 and Rh. 6G respectively. Figures 2.12 and 2.13 depict the decay curves for donor molecules in the PMMA giving the lifetime values as 4.99 ns and 9.95 ns for C 540 and Rh. 6G respectively. Using these values of τ_{0d}, the total energy transfer rate constants (K_T) were calculated from the slopes of the Stern–Volmer plots.

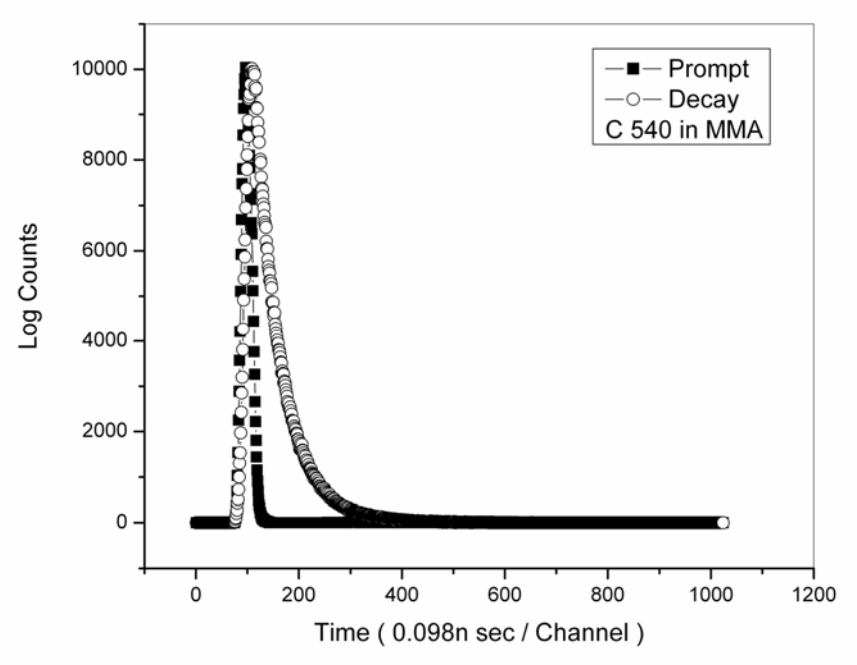

Fig. 2.10. The fluorescence decay curve of the donor C 540 in MMA

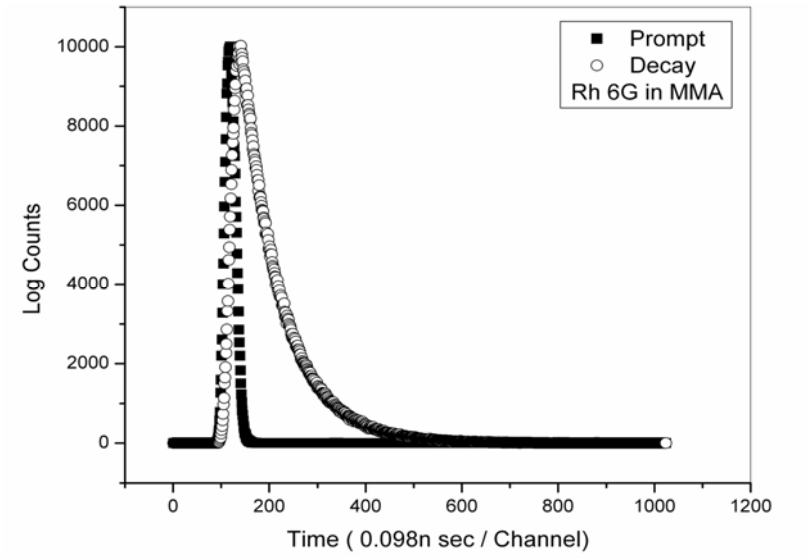

Fig. 2.11. The fluorescence decay curve of the donor Rh.6G in MMA

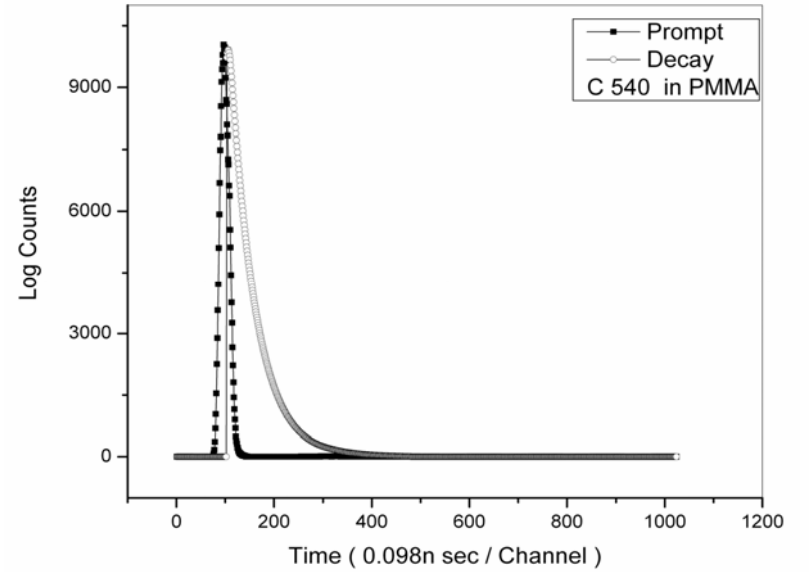

Fig. 2.12. The fluorescence decay curve of the donor C 540 in PMMA

The non-radiative transfer efficiencies were evaluated using the equation (2.6) for different [A] values and hence a comparison between the radiative and non-radiative contributions to the energy transfer mechanism can be made by plotting a graph between η_r/η_{nr} and [A]. Figure 2.14 and 2.15 shows such

graphs and the minimum value of the ratio η_r/η_{nr} was found to be ~ 14 for the dye pair, C 540:Rh 6G in PMMA.

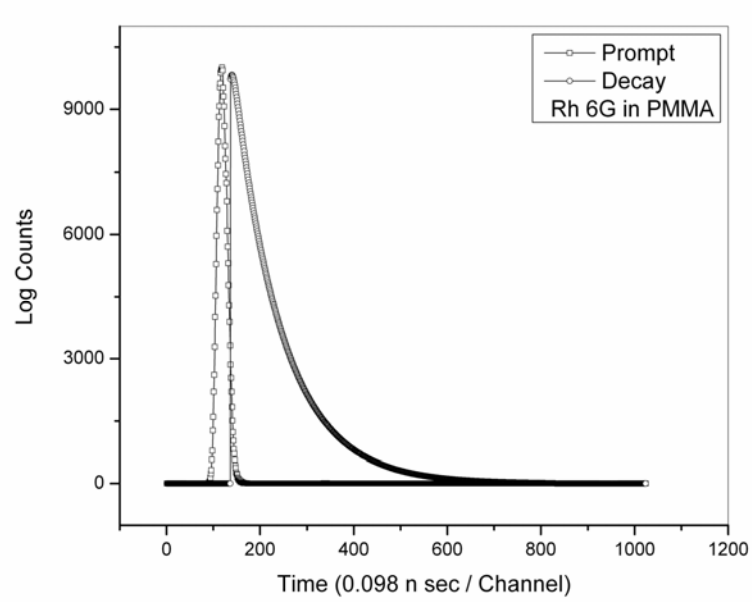

Fig. 2.13. The fluorescence decay curve of the donor Rh 6G in PMMA

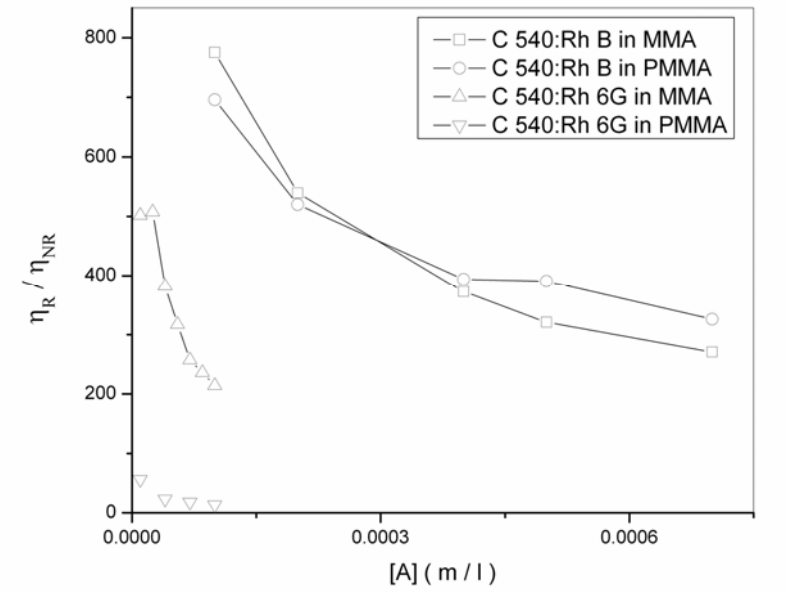

Fig. 2.14. Plot of η_r / η_{nr} vs. [A] for C 540:Rh 6G ,C 540: Rh B pairs in MMA and PMMA

The present study gives us a clear idea about the relative magnitudes of the energy transfer mechanisms occurring in the mixtures. The result clearly indicate that non-radiative transfer part is comparatively less important than the radiative transfer mechanism in the present ETDL systems even though the non-radiative part shows an increase in its values at higher acceptor concentrations. For the pair, C 540:Rh6G in PMMA, it was observed that the nonradiative part is considerably increased compared to the mixture in MMA. This can be the reason for the fast quenching in this dye pair compared to the other two. In the figure 2.15, for the dye mixture in MMA, both η_r and η_{nr} have low magnitudes so that η_r / η_{nr} is lower at low acceptor concentrations. At higher acceptor concentrations, η_{nr} enhances which is clear as in the figure.

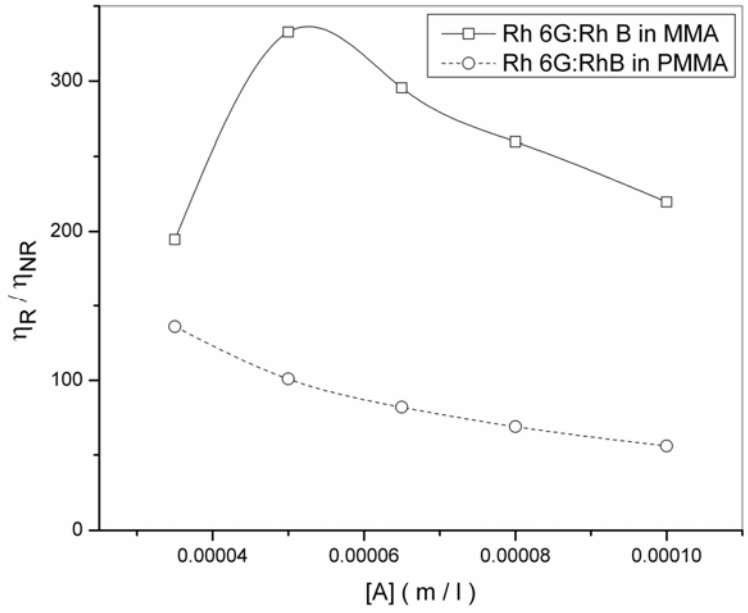

Fig. 2.15. Plot of η_r/η_{nr} vs. [A] for Rh 6G : Rh B pair

By knowing the value of η_{nr} at different acceptor concentrations, the relative quantum yields of the donor molecules (ϕ_{0d}/ϕ_d) in MMA as well as

PMMA were calculated. The values of non-radiative transfer rate K_{nr} can be directly evaluated from the slope of the graph between ϕ_{0d}/ϕ_d and [A] (Fig.2.16) which is also a straight line obeying the Stern- Volmer expression.

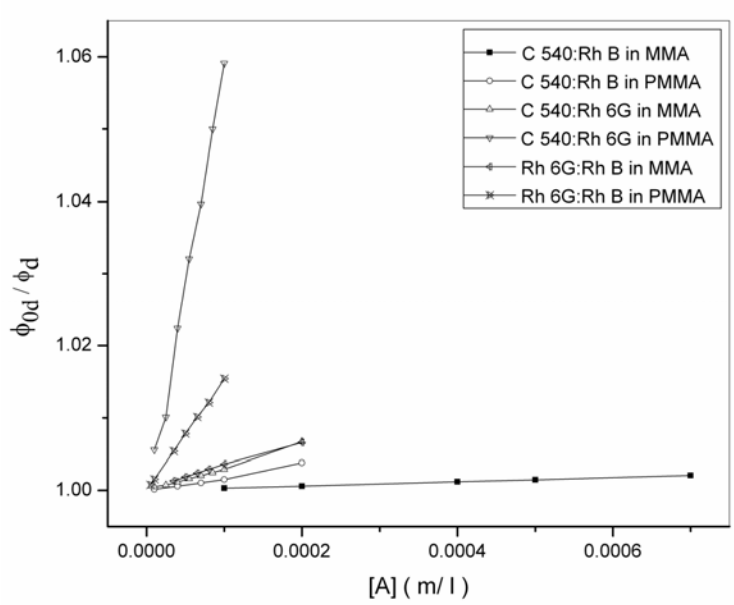

Fig.2.16. Plot of ϕ_{0d}/ϕ_d vs. [A] for the three dye pairs in MMA and PMMA

Also by knowing the values of τ_{0d} and ϕ_{0d}/ϕ_d, the value of τ_d, the fluorescence lifetime of the donor in the presence of acceptor at various acceptor concentrations can be evaluated. Figure 2.17 and 2.18 shows the variation in the lifetimes of the donor molecules in the presence of acceptors. It is clear that the fluorescence lifetime of the donor molecules are not affected much due to the energy transfer mechanism, which again confirms the dominance of radiative type of energy transfer except for the pair, C 540:Rh 6G in PMMA where there is a considerable nonradiative contribution. The kind of changes in the donor lifetime shows that there is noticeable increase in the nonradiative energy transfer mechanism in this system.

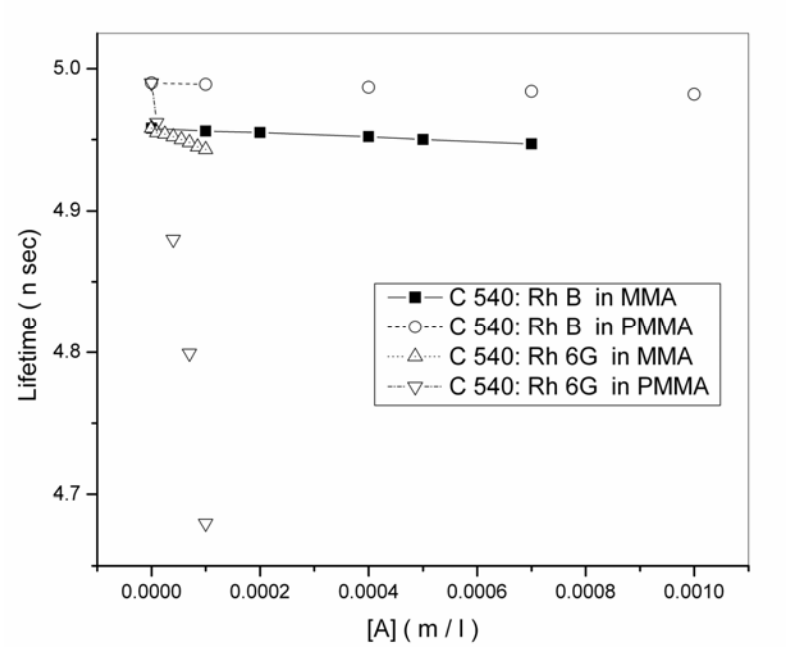

Fig.2.17. Plot of τ_d vs. [A] for the C 540:Rh 6G and C 540: Rh B pairs

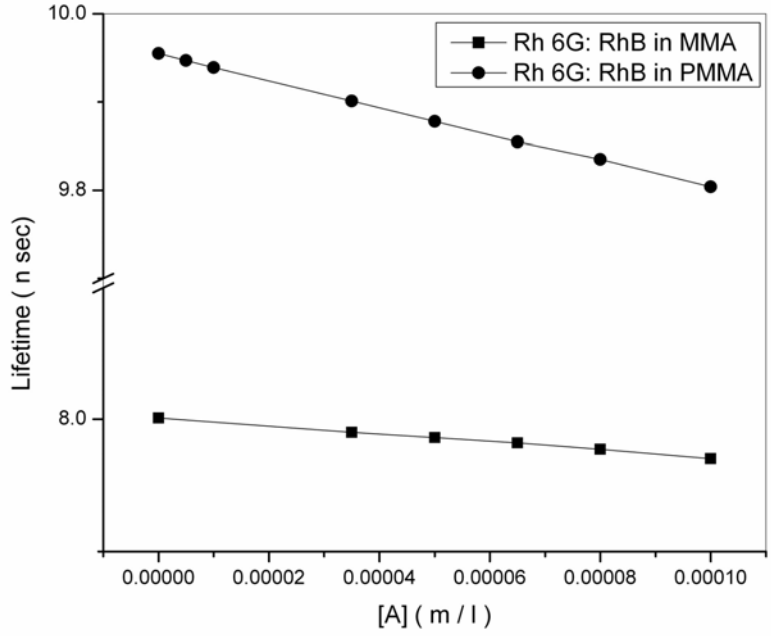

Fig.2.18. Plot of τ_d vs. [A] for the Rh 6G:Rh B pair

Another observation is that, the pure donors showed an enhancement in the lifetime after the polymerisation. The changes were from 4.96, 8.00 ns to 4.99, 9.95 ns respectively for the C 540 and Rh 6G respectively. The calculated values of τ_d in MMA as well as PMMA for the pair C 540:Rh. 6G at [A] = $4x10^{-5}$ m/l were about 4.95 ns and 4.88ns respectively. These values of τ_d were also measured experimentally using the transient single photon counting technique and was found to be 4.96 ns and 4.84. Table 2.1 summarises the various calculated parameters of the dye mixture in MMA and PMMA.

Table 2.1. Calculated parameters for the energy transfer

Parameter	**Dye pair**					
	C540:Rh.B	**C540:Rh.B**	**C540:Rh.6G**	**C540:Rh.6G**	**Rh6G:RhB**	**Rh6G:RhB**
Matrix	MMA	PMMA	MMA	PMMA	MMA	PMMA
K_r (x 10^9 S^{-1})	322	485	2836	8893	7699	6824
K_{nr} (x 10^9 S^{-1})	0.59	0.67	5.53	118	4.37	15.4
R_0 (A^0)	90.7	94.5	195	242	210	340
$[A]_{1/2}$ (M)	$5.38x10^{-4}$	$4.7x10^{-4}$	$5.3x10^{-5}$	$2.8x10^{-5}$	$4.3x10^{-5}$	$1.01x10^{-5}$
τ_{0d} (x10^{-9} Sec)	4.96	4.99	4.96	4.99	8.00	9.96
τ_d (x10^{-9} Sec) (at [A] = $7x10^{-4}$M)	4.94	4.97	4.95 (at [A] = $7x10^{-5}$M)	4.79	7.97 (at [A] = $7x10^{-4}$M)	9.86

2.5 Conclusions

A series of dye mixture doped polymer rods were fabricated which simultaneously emit two wavelengths at different relative intensities. The shifts in these wavelengths with acceptor concentration provides a wide range tunability.

A detailed analysis of the energy transfer process in the dye pairs C 540:Rh 6G, C 540:Rh B and Rh 6G:Rh B in methyl methacrylate and poly (methyl methacrylate) has been done. The lifetimes of the pure donor and the dye mixture in MMA and PMMA were experimentally determined. Enhancements of lifetimes were observed for the pure donor dyes in PMMA matrix. It was observed that, the fluorescence intensity of the acceptor dyes were increased many times within the range of acceptor concentrations studied. Acceptor concentration dependence of the energy transfer, the blue shift in the donor molecules and the variations in the donor lifetime clearly show that the radiative energy transfer process is having a major contribution in the present ETDL system. By suppressing the undesirable triplet state formation, the immobilisation of the dye molecules in PMMA leads to overall enhancement in the efficiency of the system. We recognize that our results could forecast suitable concentration regions for the wavelength shifts and intensity variations with the acceptor concentration for the dye mixture. The shifts in the wavelengths of both donors as well as acceptors were also studied which will enable us to choose from a variety of polymer rods to fabricate solid-state dye lasers and polymer optical fibre amplifiers operating in multi wavelength regime.

References

[1] D.J.Taylor, S.E Harris, S.T.K Nieh and T.W.Hansch, "*Tuning of a Dye Laser Using the Acousto-Optic Filter*", Appl.Phys. Lett 19, 269 ,1971.

[2] E.F.Salewski and R.A.Keller, "*Tunable Multiple Wavelength Organic-Dye Laser*", Appl.Opt. 10,2773, 1971.

[3] H.S.Pilloff, "*Simultaneous two wavelength selection in the N_2 laser pumped dye laser*", Appl. Phys. Lett, 21, 339, 1972.

[4] C.Y. Wu and J.R.Lombardi, "*Simultaneous two-frequency oscillation in a dye laser system*", Opt.Commun. 7, 233, 1973.

[5] G Peterson, B B Snavelly, Bull. Am. phy.soc.13, 397, 1968.

[6] S A Ahmed, J S Gergerly, "*Energy transfer organic dye mixture laser*" J Chem. Phy. 61 ,1584, 1974.

[7] Y Yap, T Tou and K Kwek, "*Measurements of time delays in superradiant laser emissions from binary dye mixtures*," Jpn. J . Appl. Phys. 35, 1996.

[8] P Burlsmacchi, H F R Sandoval, "*Characteristics of a multicolor dye laser,"* Opt. Commun. 31, 185, 1979.

[9] Y Saito, N Nakai, A Nomura and T Kano, "*Spectral characteristics of a short-pulse red-green-blue dye mixture laser."*Appl. Opt. 31, 4298, 1992.

[10] C E Moller, C M Verber, A H Adelman, "*Laser pumping by excitation transfer in dye mixtures."* Appl. Phys. Lett.18, 278, 1971.

[11] A Dienes, M. Madden, "*Study of excitation transfer in dye mixtures by measurements of gain spectra*".J Appl .Phy. 44, 4161,1973.

[12] C Lin, A. Dienes, "*Study of excitation transfer in laser dye mixtures by direct measurement of fluorescence lifetime,"* J. Appl. Phys 44, 5050,1973.

[13] T Urisu, K Kajiyama," *Concentration dependence of the gain spectrum in energy transfer dye mixtures,"* J. Appl. Phys. 47 , 3563,1976.

[14] D.A Gramov, K.M.Dyumaev, A.A.Manenkov, A.P.Maslyakov,"*Efficient plastic-host dye lasers*",J.Opt.Soc. Am. B 2 , 1028,1985.

[15] R.E Hermes, "*Lasing performance of pyrromethene-BF2 laser dyes in a solid polymer host,*" SPIE, 2116, 178,1994.

[16] M.Rajesh, K.Geetha, C.P.G.Vallabhan, P.Radhakrishnan and V.P.N.Nampoori, "*Fabrication and characterization of dye-doped polymer optical fibre as a light amplifier*", Applied Optics, 46,1, 106,2007.

[17] Akihiro Tayaga, Shigehiro Teramoto, Tsuyoshi Yamamoto, Kazuhito Fujii, Eisuke Nihei, Yasuhiro Koike and Keisuke Sasaki, "*Theoretical and experimental investigation of rhodamine B-doped polymer optical fibre amplifiers*", IEEE Journal of Quantum Electronics 31, 12, 2215,1995.

[18] Gang Ding Peng, Zhengjun Xiong, Peng, Pak L.Chu, "*Fluorescence Decay and Recovery in Organic Dye-Doped Polymer Optical Fibres*", Journal of Light wave Technology, 16, 12, 2365,1998.

[19] M.A.Ali, S.A Ahmed, "*Comprehensive examination of radiationless energy transfer models in dyes: Comparisons of theory and experiment*" J.Chem.Phys.90, 1484,1989.

[20] D.Mohan, S.Sanghi, R.D.Singh, "*Energy transfer excitation in an N_2-laser-pumped coumarin 485-rhodamine B dye mixture through optical gain characteristics*", J.Photochem. Photobio A:Chem.68 ,77,1992.

[21] R.D.Singh, A.K.Sharma, N.V.Unnikrishnan and D.Mohan, "*Time resolved spectra of coumarin 30-rhodamine 6G dye mixture*." Pramana-J.Phys.34, 77,1990.

[22] M.A.Ali, S.A Ahmed, "*Practical method for obtaining spectral distribution of gain in energy transfer dye lasers: comparison of theory and experiment*", Appl.Optics 29,4494,1990.

[23] J.B.Birks and M.S.S.C.P.Leite, "*Effects of diffusion on transfer efficiency"*, J.Phys.B 3, 513,1970.

[24] T.Govindanunny and B.M.Sivaram, "*Gain studies on a uranine-damc dye mixture laser under nitrogen laser pumping*" J.Lumin.21,397, 1980.

[25] T Urisu, K Kajiyama, "*Concentration dependence of the gain spectrum in methanol solutions of rhodamine 6G*" J. Appl. Phys. 47,3559, 1976.

[26] P J Sebastian, K Sathyanandan, "*Donor concentration dependence of the emission peak in rhodamine 6G -Rhodamine B energy transfer dye laser*", Opt. Comm. 35,113, 1980.

[27] G.A.Kumar,N.V.Unnikrishnan, "*Energy transfer and optical gain studies of FDS: Rh B dye mixture investigated under cw laser excitation*", J. Photochem. Photobiol A 144,107, 2001.

[28] M.Kailasnath,G.A.Kumar amd VPN.Nampoori. "*Proceedings of Photonics 2004, Seventh Intetrnational Conference on Optoelectronics, fibre optics and Photonics*," Kochi India,9-11 December 2004, pp400

[29] F P Schater, "*Dye lasers*," Springs Verlag, Newyork ,1977.

[30] S.J.Strickler, R.A.Berg. "*Relationship between Absorption Intensity and Fluorescence Lifetime of Molecules*", J.Chem.Phys. 37, 814, 1962.

……ൠ…..

Chapter- 3

Excitation wavelength dependence of energy transfer in dye mixture doped polymer optical fibre preforms

Contents

3.1 Introduction

Intermolecular energy transfer between two distinct molecular species in the condensed phase has been observed in numerous molecular systems [1]. Following the introduction of dye lasers, energy transfer between dye molecules has been used to exploit the absorption properties of a lasing dye mixture for matching with the emission spectrum of the optical pump source. The primary motivation for the use of mixture of dyes as lasing medium was either an improvement in the laser performance or the possibility of multi frequency operation [2]. Even though a number of techniques exist for obtaining two or more wavelengths simultaneously from a single dye laser, they use several wavelength selective elements in the dye laser cavity. [3-5]. The use of dye mixture doped transparent polymers in solid-state dye lasers and polymer optical fibre amplifiers can be a very good method to extend these conventional approaches.

One of the important advantages of transparent polymers compared to the traditional optical materials is that it is possible to introduce organic dyes or other compounds that can play the role of active components into the polymers, which appreciably changes the characteristics of the polymer matrix [6,7]. Optical amplifiers and lasers made of dye-doped fibre require much less pump power compared with bulk material because of the effective confinement and long interaction length available in the fibre. Since photo bleaching increases with the increase of the exposure intensity, low pump intensity would increase the lifespan of the gain medium. Also, the thin and long geometry of the fibre is ideal for good thermal relaxation so as to minimize the thermally induced photo bleaching [8]. Recently, we have observed an enhancement in the radiative energy transfer efficiency in the polymer phase of C 540- Rh B dye mixture compared to monomer when excited with a 445 nm laser beam [9]**.** However, the emission wavelengths and relative intensities can vary with excitation wavelength in such cases. This chapter explains the excitation wavelength dependence of the fluorescence emission and energy transfer mechanism using coumarin 540 dye as donor in C 540- Rh B dye mixture doped PMMA rods.

Theory

Detailed theory of energy transfer dye laser is discussed elsewhere [10]. The rate constants for the radiative and nonradiative energy transfer mechanisms are given by Stern-Volmer plots given by the equations

$$I_{0d}/I_d = 1 + K\tau_{od}[A] \quad \text{.....(3.1)}$$

$$\varphi_{0d}/\varphi_d = 1 + K_{nr}\tau_{0d}[A] \quad \text{.....(3.2)}$$

where I_{0d} and I_d are the fluorescence intensities of the donor in the absence and presence of acceptor, respectively while φ_{0d} and φ_d are corresponding quantum

yields. τ_{0d} is the fluorescence lifetime of the donor without acceptor and [A] is the acceptor concentration. K and K_{nr} are total and non-radiative transfer rate constants respectively. According to the Forster Dexter theory, the critical radius for resonant energy transfer between the donor and acceptor molecules are given by the expression [11],

$$R_0 = \left[8.8 \times 10^{23} \kappa^2 n^{-4} \phi_{0d} J(\lambda)\right]^{1/6} \quad {}^{0}\!A \quad \text{..... (3.3)}$$

where κ^2 is the dipole orientation factor, n is the refractive index of the medium,ϕ_{0d} is the fluorescence quantum yield of the donor in the absence of acceptor and J(λ) is the spectral overlap integral given by

$$J(\lambda) = \int \varepsilon_A(\lambda) F_D(\lambda) \lambda^4 d\lambda \ \ cm^3 \ \mathrm{M}^{-1} \quad \text{..... (3.4)}$$

where, $\varepsilon_A(\lambda)$ is the extinction coefficient of acceptor and $F_D(\lambda)$ is the fluorescence emission intensity of the donor as a function of the total integrated intensity. Evidently, any variation in the values of $\varepsilon_A(\lambda)$ and $F_D(\lambda)$ will result in a corresponding change in the energy transfer parameters. However, the fluorescence emission spectrum is independent of excitation wavelength as long as the excitation wavelength is well within the absorption spectrum of the molecule. Hence $J(\lambda)$ will not have significant dependence on the donor excitation wavelength.

3.2 Experimental

A series of dye mixture doped polymer rods were fabricated by the standard procedure for making the polymer optical fibre preforms without cladding [16]. The donor concentration was kept constant at 10^{-5} m/l whereas the acceptor concentration was varied from $4\text{x}10^{-5}$ m/l to $7\text{x}10^{-4}$ m/l. The fluorescence emission from the rods was measured using a Varian Cary-Eclipse fluorescence spectrophotometer with excitation wavelengths 445nm, 465nm,

488nm and 532nm. Here, 445 nm is the longest excitation wavelength, which was found to be suitable for avoiding any direct excitation of the acceptor molecules. The wavelength 488nm coincides with the prominent argon ion laser emission but not well within the absorption spectrum of the donor while 532 nm matches with the frequency doubled Nd:YAG laser wavelength, which is at the absorption maximum of the acceptor molecule. Finally, 465 nm is an intermediate wavelength, which ensures a multi wavelength emission from the fabricated rods. The excitation spectra of the samples were also recorded in the fluorescence spectrophotometer for the peak emission wavelengths of 495nm, 580nm of the donor and acceptor respectively. Optical absorption spectra of the samples were recorded on a Jasco V-570 spectrophotometer. The fluorescence lifetimes of the donor in pure form and in the presence of acceptor in PMMA matrix were measured using time-correlated single-photon counting technique employing a micro channel plate photomultiplier tube (Hamamatsu R 3809 U-50) and a multi channel analyser. The measurement is made using an IBH-5000 Single Photon Counting Spectrometer. A nano-LED (Spectra Physics) emitting at 455 nm with a resolution of 200 ps was used as the excitation source. The fluorescence decay curves were analyzed using an iterative fitting program provided by IBH and no further deconvolution was made.

3.3 Results and discussion

Fig.3.1. A photograph of the fabricated preforms

Figure 3.1 shows the photograph of the fabricated polymer optical fibre preforms doped with dye mixture with varying acceptor concentrations. Individual absorption spectra of Rh B (10^{-4} mol/l) and C 540 (10^{-5} mol/l)in PMMA are presented in figure 3.2 along with the emission spectrum of C 540 with a 445 nm excitation. Since a considerable area under the emission line shapes of C 540 at 445nm excitation overlaps with the absorption line shapes of Rh B, energy transfer from C540 to Rh B is clearly possible, the extend of this being depended on the overlapping area. Figure 3.3 depicts the net absorption spectra of the samples, which clearly shows that there are significant modifications in the absorption pattern with acceptor concentration. We attribute these changes in the absorption spectra as due to the process of energy transfer as well as due to the presence of aggregations like dimers and trimers in the samples.

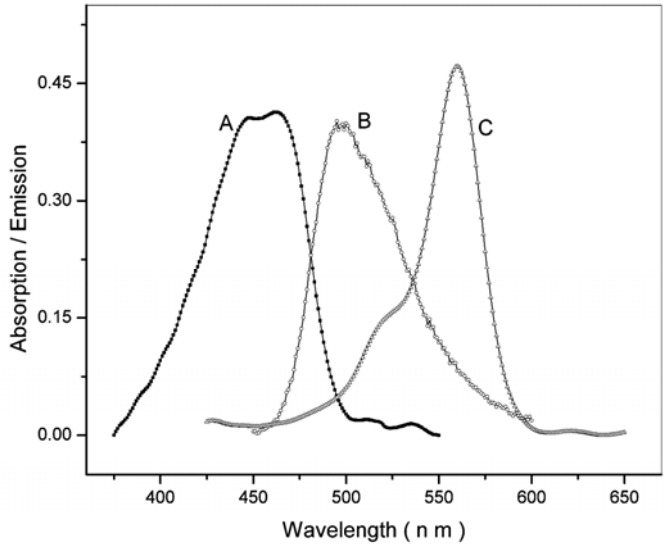

Fig.3.2. Overlapping of absorption and emission spectra. in PMMA matrix. A- absorption spectrum of C 540, B- emission spectrum of C 540 for 445 nm excitation and C- absorption spectrum of Rh.B

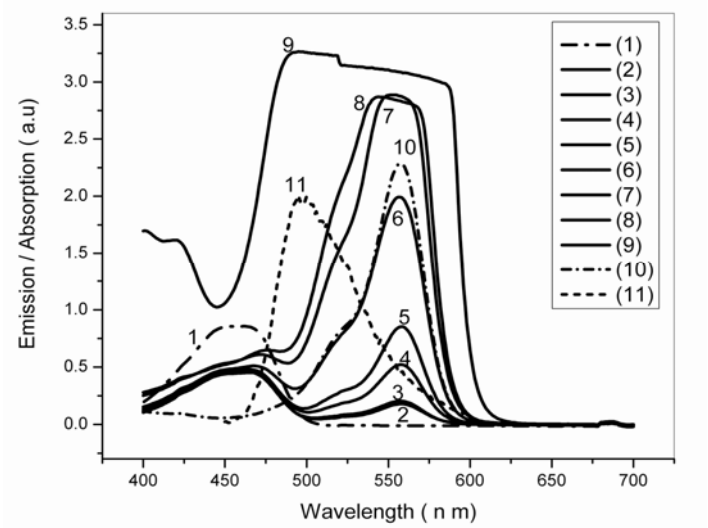

Fig. 3.3. Net absorption spectra of dye mixture doped PMMA rods along with pure donor emission. 1- Donor only ($5x10^{-5}$ m/l), 2-[A] =$4x10^{-5}$, 3- [A] = $7x10^{-5}$, 4-[A]= 10^{-4}, 5- [A]= $2x\ 10^{-4}$, 6-[A] = $4x\ 10^{-4}$, 7- [A] = $5x10^{-4}$, 8 – [A] = $6x10^{-4}$, 9-[A] = $7x10^{-4}$, 10- acceptor (10^{-4} m/l) only, 11- donor emission

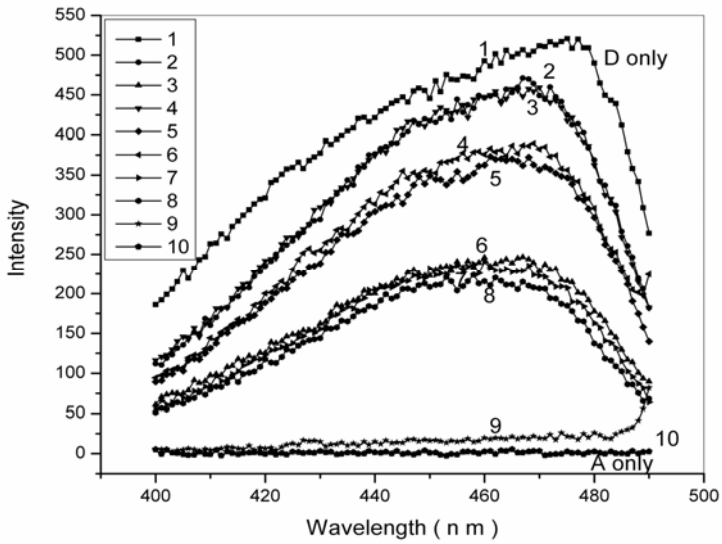

Fig. 4.4. Excitation spectra of dye mixture doped PMMA for 495nm emission. 1- Donor only ($5x10^{-5}$ m/l), 2-[A] =$4x10^{-5}$m/l, 3- [A] = $7x10^{-5}$ m/l, 4-[A]= 10^{-4} m/l, 5- [A]= $2x\ 10^{-4}$ m/l, 6- [A] = $4x\ 10^{-4}$ m/l, 7- [A] = $5x10^{-4}$ m/l, 8 – [A] = $6x10^{-4}$ m/l, 9-[A] = $7x10^{-4}$ m/l, 10-acceptor (10^{-4} m/l) only.

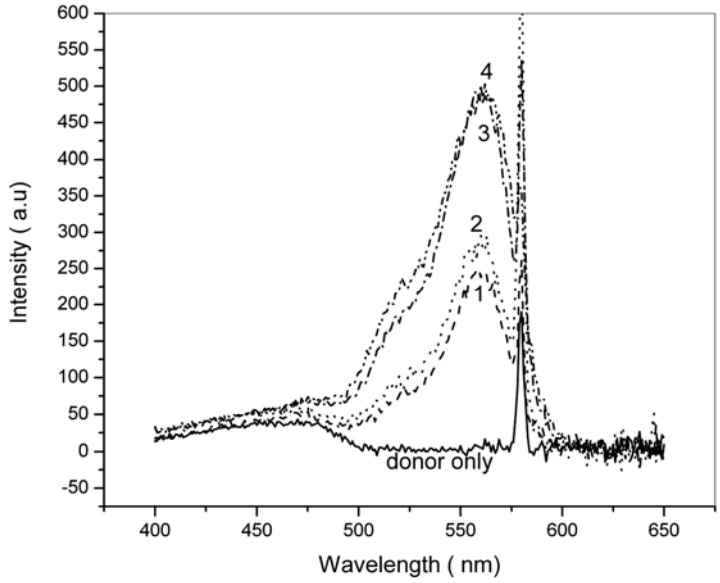

Fig. 3.5a. Excitation spectra of dye mixture doped PMMA for 580nm emission.1-[A] =$4x10^{-5}$m/l, 2- [A] = $7x10^{-5}$ m/l, 3-[A]= 10^{-4} m/l, 4- [A]= $2x\ 10^{-4}$m/l

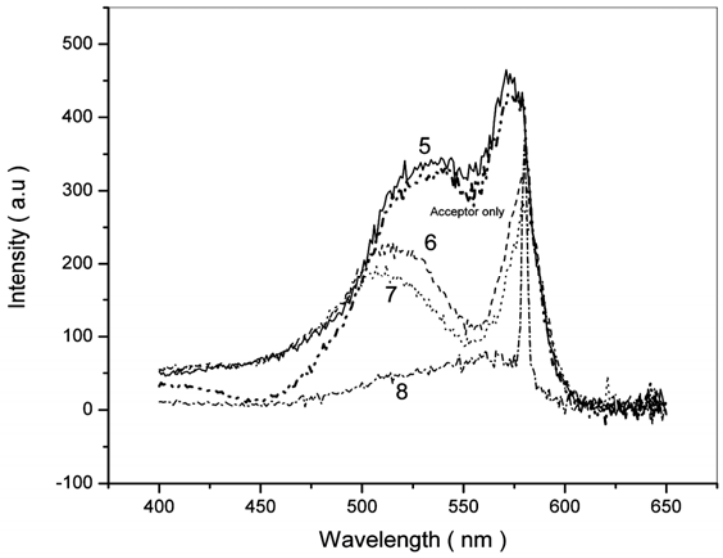

Fig.3.5b. Excitation spectra of dye mixture doped PMMA for 580nm emission. 5- [A] = $4x\ 10^{-4}$m/l, 6- [A] = $5x10^{-4}$m/l, 7 – [A] = $6x10^{-4}$m/l, 8-[A] = $7x10^{-4}$m/l

The excitation spectrum of the rods at 495nm, is depicted in figure 3.4. It is clear that there is a significant shift in the peak wavelength of excitation for emission at this wavelength with acceptor concentration. From the pure donor, efficient fluorescence can be expected at an excitation wavelength of about 475nm. This value continuously reduces to 453nm with an acceptor concentration of $6x10^{-4}$ m/l. With increasing acceptor concentration the long wavelength tail of the donor emission increasingly gets absorbed by the acceptor. Also there is no efficient wavelength of excitation for emission at 490nm from the pure acceptor. Figure 5a and b shows the excitation spectra of the samples at the emission maximum of the acceptor, i.e. 580 nm. A new peak appears in the excitation spectra in the 570 - 580 nm region. As shown in figures 3.6, 3.7 and 3.8, the fluorescence spectrum of dye mixture exhibit double peak in the intermediate acceptor concentrations corresponding to characteristic donor and acceptor emission. The peak emission from the acceptor shift to higher wavelengths with increasing acceptor concentration [A] and it appears around 605nm at highest [A]. In the excitation spectrum, at highest acceptor concentration as well as with pure donor, the sharp peak at 580 nm results from the scattering of the excitation radiation. At intermediate concentrations, there is fluorescence emission around 570- 580 nm and the given peak is due to the resonant fluorescence under 580 nm excitation. At highest acceptor concentration, the peak is shifted to higher wavelength and the emission from this sample is no more around 580 nm. Evidently, the emission wavelength from this sample is beyond 600 nm as seen in the fluorescence spectra.

Figure 3.6 indicates the available wavelengths that can be produced from the fabricated polymer rods with varying relative intensities for an excitation wavelength of 445 nm. In the present study we have noticed that both relative intensities and peak emission wavelengths are different at various excitation wavelengths. Figures 3.7, 3.8 and 3.9 represent the emission spectra for 465, 488 and 532 nm excitations respectively.

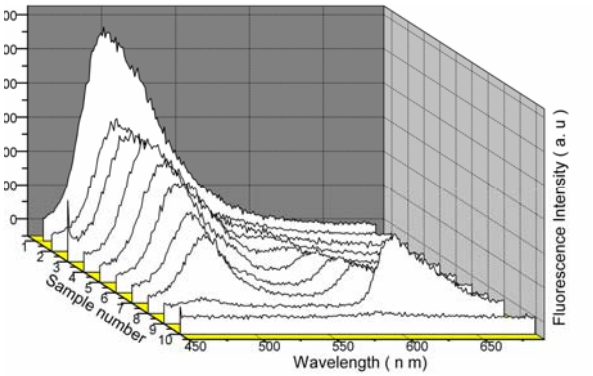

Fig. 3.6. The recorded fluorescence from dye mixture doped PMMA with 445 nm excitation. Sample 1- Donor only, sample 2-[A] =$4x10^{-5}$m/l, sample 3- [A] = $7x10^{-5}$ m/l, sample 4-[A]= 10^{-4} m/l, sample 5- [A]= $2x\ 10^{-4}$ m/l, sample 6- [A] = $4x\ 10^{-4}$ m/l, Sample 7- [A] = $5x10^{-4}$ m/l, Sample 8 – [A] = $6x10^{-4}$ m/l, sample 9-[A] = $7x10^{-4}$ m/l, sample 10-acceptor only(10^{-4} m/l).

For the excitations at 445 nm and 465 nm, donor fluorescence shows a continuous blue shift of about 20 nm in the range of acceptor concentrations used in the present study. Meanwhile, the acceptor shows a continuous red shift of about 15 nm up to [A] = $5x10^{-4}$ m/ l which is then blue shifted by about 5 nm. Beyond this [A] value, the acceptor emission was red shifted.

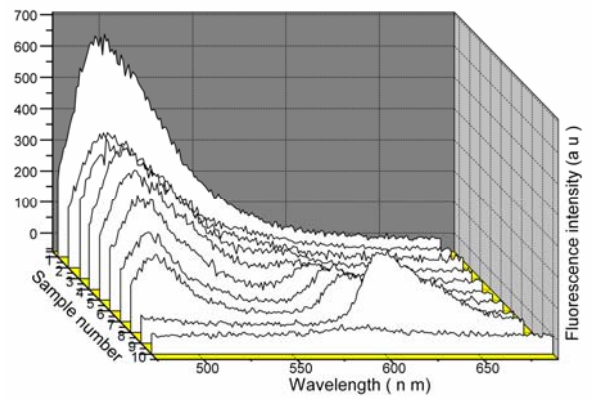

Fig. 3.7. The recorded fluorescence from dye mixture doped PMMA with 465 nm excitation. Sample 1- Donor only, sample 2-[A] =$4x10^{-5}$ m/l, sample 3- [A] = $7x10^{-5}$ m/l, sample 4-[A]= 10^{-4} m/l, sample 5- [A]= $2x\ 10^{-4}$ m/l, sample 6- [A] = $4x\ 10^{-4}$ m/l, sample 7- [A] = $5x10^{-4}$ m/l, sample 8 – [A] = $6x10^{-4}$ m/l, sample 9-[A] = $7x10^{-4}$ m/l, sample 10-acceptor only (10^{-4} m/l).

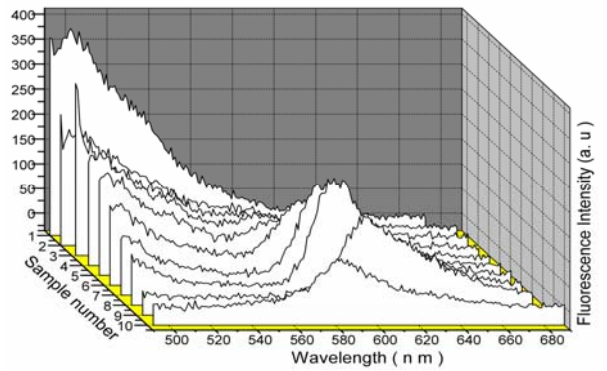

Fig. 3.8. The recorded fluorescence from dye mixture doped PMMA with 488 nm excitation. Sample 1- Donor only, sample 2-[A] =$4x10^{-5}$ m/l, sample 3- [A] = $7x10^{-5}$ m/l, sample 4-[A]= 10^{-4} m/l, sample 5- [A]= $2x\ 10^{-4}$ m/l, sample 6- [A] = $4x\ 10^{-4}$ m/l, sample 7- [A] = $5x10^{-4}$ m/l, sample 8 – [A] = $6x10^{-4}$ m/l, sample 9-[A] = $7x10^{-4}$ m/l, sample 10-acceptor only (10^{-4} m/l).

In the absence of donor, the acceptor showed a continuous red shift of about 13 nm. It may be pointed out that the pure acceptor has no emission with 445nm and 465nm excitations even though there is a little emission for 488nm excitation. For 488nm excitation, we could not notice much blue shift for the donor but the acceptor emission was again red shifted by about 15 nm.

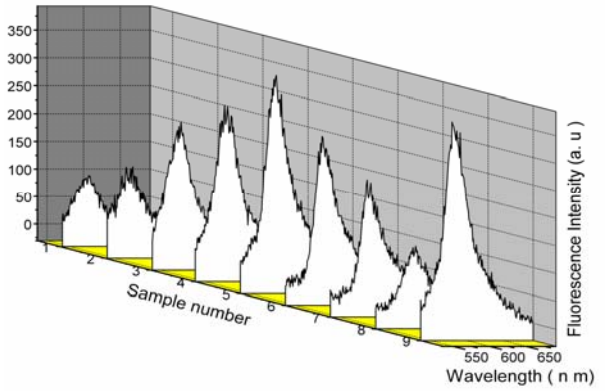

Fig. 3.9. The recorded fluorescence from dye mixture doped PMMA with 532 nm excitation. sample 1-[A] =$4x10^{-5}$m/l, sample 2-[A] = $7x10^{-5}$ m/l, sample 3-[A]= 10^{-4} m/l, sample 4- [A]= $2x\ 10^{-4}$ m/l, sample 5- [A] = $4x\ 10^{-4}$ m/l, sample 6- [A] = $5x10^{-4}$ m/l, sample 7 – [A] = $6x10^{-4}$ m/l, sample 8-[A] = $7x10^{-4}$ m/l, sample 9-acceptor only(10^{-4} m/l).

These results for the 445 and 465nm excitations are in good agreement with our earlier investigation on the wavelength shifts with a 445 nm laser excitation [9].

At an optimum concentration of the acceptor for the energy transfer, the acceptor emission shows a blue shift. The donor-sensitized system was observed to have a higher gain compared to an unsensitised system due to an increase in the effective lifetime. As a result of this, the gain maximum is shifted to the blue region [17, 18]. At higher acceptor concentrations, this effect was absent because of the dominance of collisional de-excitation. At 488 nm, there were no significant blue shifts from both donor and acceptor. At this wavelength donor excitation is not much efficient and there is a possibility for the direct excitation of the acceptor as well. The 532nm excitation was found to be absorbed by acceptor alone and the corresponding emission showed a continuous red shift of about 15nm. Figure 3.10 shows the variations of the simultaneous emission wavelengths exhibited by the rods.

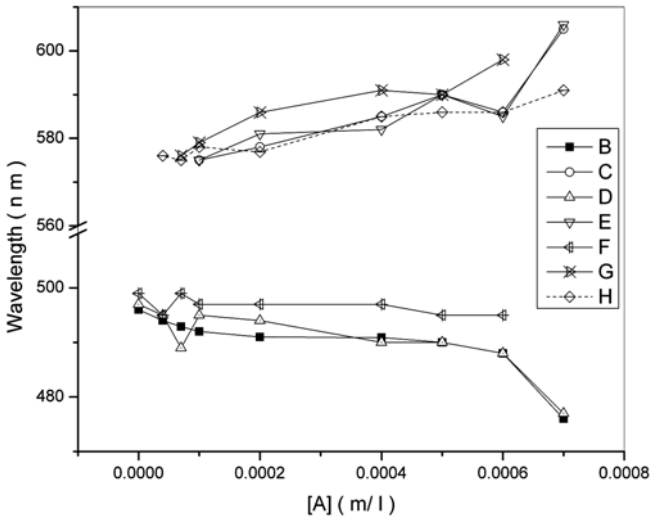

Fig.3.10. Simultaneous peak emission wavelengths available from the rods fabricated with different acceptor concentrations. B- Donor emission at 445nm excitation, C-Acceptor emission at 445nm excitation, D- Donor emission at 465nm excitation, E-Acceptor emission at 465nm excitation, F- Donor emission at 488nm excitation, G-Acceptor emission at 488nm excitation – Emission at 532 nm excitation.

Energy transfer rate constants

The excitation wavelength dependence of energy transfer efficiency and the transfer rate constant for the present system can be calculated by studying the relative fluorescence intensities of the donor (I_{0d} / I_d) at various excitation wavelengths. As seen in figure 3.11, there is a noticeable change in the slope of the Stern - Volmer plot for the 488 nm excitation. At this wavelength, the donor emission was found to be rapidly quenched by the acceptor. In the present study, the maximum value of radiative energy transfer rate constant was found to be $6.6x10^{11}$ sec^{-1} with an excitation wavelength 465nm. The rate constants for 445nm and 488nm excitations were $5.4x10^{11}$ $sec^{-1}$and $3.5x10^{11}$ sec^{-1}respectively. This result is attributed to the fact that, both 445 and 465nm, excitations come well outside the donor emission while 488nm is partly absorbed by both donor and acceptor. This is clear from the excitation spectra at 495nm, which shows finite absorption at 488nm by the samples. Thus the calculated parameters for the dye mixture with 488 nm may vary much from the values for the other two wavelengths of excitation.

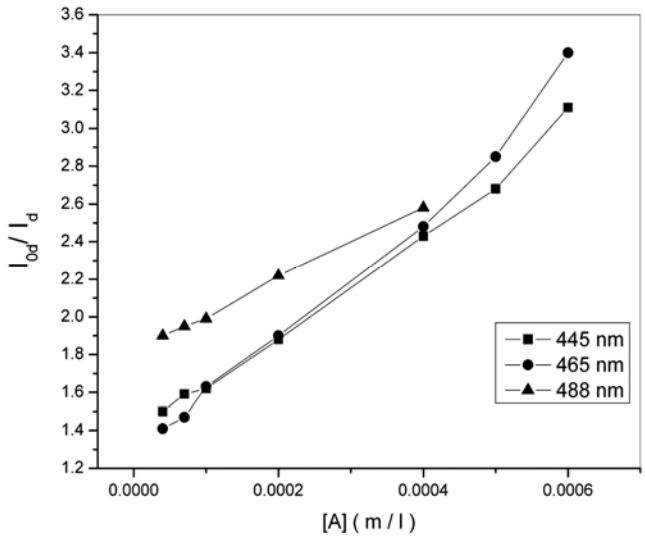

Fig .3.11. The Stern- Volmer plot for the present ETDL system

Knowing the value of $[A]_{1/2}$ the half quenching concentration at which $I_d = I_{od}/2$,the values of the critical radii R_0 can be evaluated[11]. The values obtained for R_0 clearly shows that the non-radiative transfer involved in the dye mixture is of dipole-dipole in nature.

The fluorescence lifetime of the pure donor was measured experimentally using transient single photon counting technique. Figure 3.12 shows the fluorescence decay curve of the donor, which gives lifetime of the donor in the absence of the acceptor as 4.99ns when embedded in PMMA. Also a very little decrease in the lifetime was noticed due to the presence of acceptor, which is a signature of radiative type of energy transfer in the rods. Figure 3.13 shows the decay curve of the donor in the presence of acceptor ($7x10^{-4}$ m/l) giving a lifetime of 4.83 nsec.

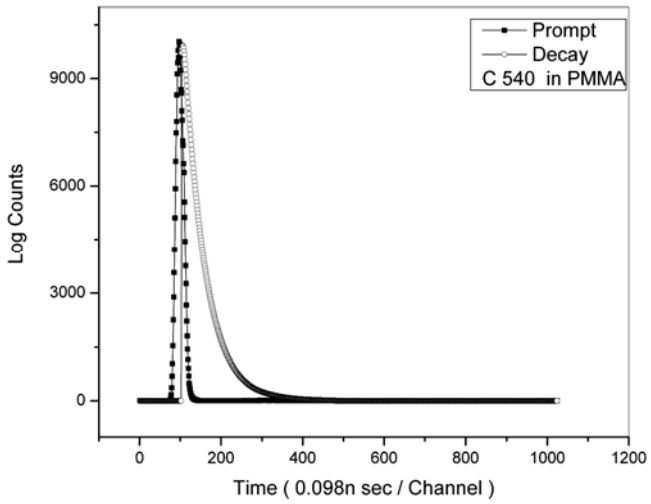

Fig. 3.12. The fluorescence decay curve of the donor C 540 in PMMA matrix

Using this value of τ_{0d}, the total energy transfer rate constant K_T is calculated and a comparison between the radiative and non-radiative contributions to the energy transfer can be made by plotting a graph between η_r/η_{nr} and [A].

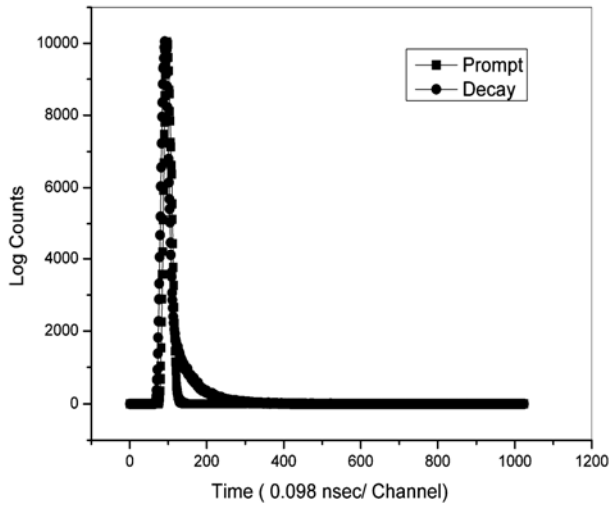

Fig. 3.13. The fluorescence decay curve of the donor C 540 in the presence of Rh.B (10^{-5} m/l) in PMMA matrix.

Figure 3.14 shows such a graph and the minimum value of the ratio η_r/η_{nr} was found to be ~ 9 occurring at 488 nm excitation. The result clearly indicates that, at all the three wavelengths of excitation, non-radiative transfer part is comparatively less important than the radiative transfer mechanism in the present ETDL system even though the non-radiative part shows an increase in its values at higher acceptor concentrations.

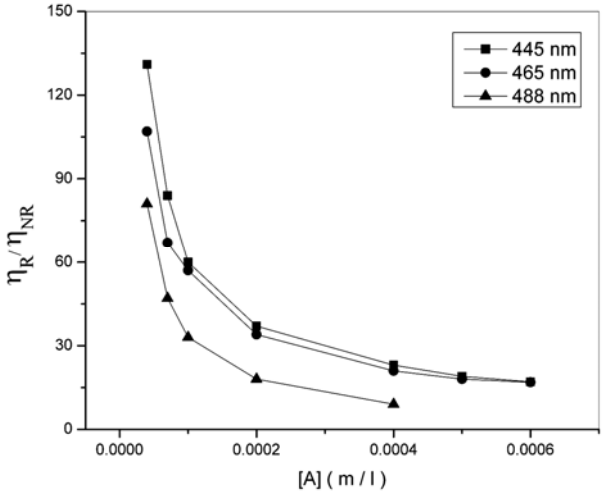

Fig. 3.14 Plot of η_r/η_{nr} vs. [A]

By knowing the values of τ_{0d} and ϕ_{0d}/ϕ_d, the value of τ_d, the fluorescence lifetime of the donor in the presence of acceptor at various acceptor concentrations can be evaluated. Figure 3.15 shows the graph between lifetime and acceptor concentration. Again, for 488nm excitation, the calculated donor lifetime 4.71nsec with [A] = $7x10^{-4}$ m/l is shorter than the experimentally measured value while for the other two excitation wavelengths, the calculated values are around 4.8 nsec which agrees with the measurement. With 445 and 465nm excitations, nonradiative relaxations taking place in the S_1 manifold before the energy gets transferred to the acceptor can result in a longer lifetime. Such relaxations may not be that much important in the case of 488nm excitation resulting in rapid energy transfer. The results clearly show the importance of the selection of the excitation wavelength in the context of the energy transfer studies. Table 3.1 summarises the various calculated parameters of the dye mixture doped rods for the three excitation wavelengths.

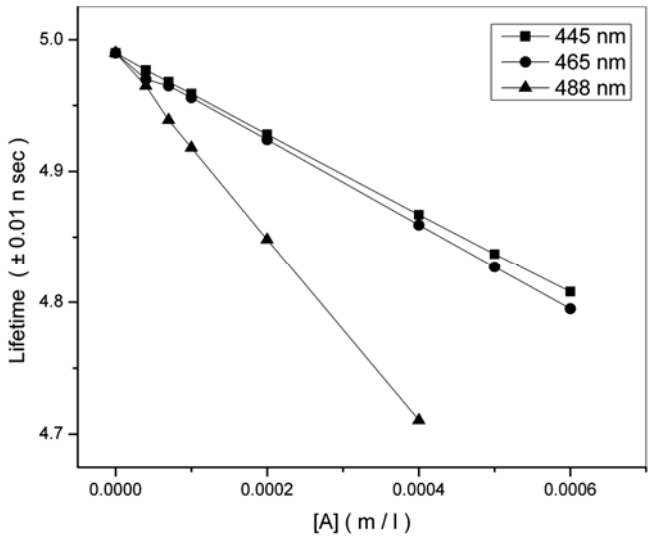

Fig.3.15. Variation of donor lifetime with [A]

Table 3.1 Calculated parameters of the dye mixture

Parameter	445nm	465nm	488nm
K_r (x 10^9 S^{-1})	542	661	355
K_{nr} (x 10^9 S^{-1})	12	13	29
R_0 (A^0)	116.3	119	154
$[A]_{1/2}$ (M) x10^{-4}	2.52	2.35	1.07
$\tau_{d\ (x10^{-9}\ Sec)}$ (at [A] = 7x10^{-4}M)	4.808	4.795	4.711

3.4 Conclusions

The excitation wavelength dependence of the fluorescence emission from C 540 - Rh B dye mixture system in PMMA rods has been analysed. For the pump wavelengths 445 and 465nm, many of the fabricated rods emit at two peak wavelengths simultaneously. A comparable relative intensity for the simultaneous peak emission wavelengths was observed from a rod with acceptor concentration 6x10^{-4}m/l when excited with 445nm and 465nm whereas for a 488nm excitation, the rod with acceptor concentration 4x10^{-4} m/l exhibits such a property. These rods can also offer single peak emission outputs ranging from 576nm to 591nm with a frequency doubled Nd: YAG laser excitation. Calculated parameters at 445 and 465nm excitation are in close agreement with the experimental results.

Reference

[1] A.J.Cox, Brian K. Matise. "*Energy transfer between coumarins in a dye laser*", Chem. Phys Letters, 76,1,125,1980.

[2] Sucharitha Sinha, Alok K Ray, Soumitra Kundu, Sasikumar, Tamal B.Pal, Sivagiriyal K.S.Nair and Kamalesh Dasguptha "*Spectral Characteristics of a Binary Dye-Mixture Laser*", Appl.Opt. 41, 7006,2002

[3] D.J.Taylor, S.E Harris, S.T.K Nieh and T.W.Hansch, "*Electronic Tuning of a Dye Laser Using the Acousto-Optic Filter*"Appl.Phys. Lett 19, 269,1971.

[4] E.F.Zalewski and R.A.Keller, "*Tunable Multiple Wavelength Organic-Dye Laser*", Appl.Opt. 10, 2773,1971.

[5] H.S.Pilloff, "*Simultaneous two wavelength selection in the N_2 laser pumped dye laser*", Appl. Phys. Lett, 21, 339,1972.

[6] G. A. Kumar, Vinoy Thomas, Gijo Jose, N. V. Unnikrishnan, V. P. N. Nampoori, "*Energy transfer in Rh 6G:Rh B system in PMMA matrix under cw laser excitation*", J. Photochem. Photobiol. A 153,145, 2002.

[7] M.Kailasnath, T.S.Sreejaya, Rajesh Kumar, P.Radhakrishnan, V.P.N.Nampoori, C.P.G. Vallabhan, "*Fluorescence characterization and gain studies on a dye-doped graded index polymer optical-fibre preform*", J.Opt.Las.Tech. 40,687,2008.

[8] G.D.Peng, Zhengjun Xiong ,P.L.Chu, "*Fluorescence Decay and Recovery in Organic Dye-Doped Polymer Optical Fibres*", J.Lightwave Technol., 16, 2365,1998.

[9] M.Kailasnath, P.R.John, P.Radhakrishnan, VPN.Nampoori, CPG.Vallabhan, "*A comparative study of energy transfer in dye mixtures in monomer and polymer matrices under pulsed laser excitation*," J. Photochem. Photobiol A : Chem. 195 , 135, 2008.

[10] G.A.Kumar,N.V.Unnikrishnan,"*Energy transfer and optical gain studies of FDS: Rh B dye mixture investigated under cw laser excitation*", J. Photochem. Photobiol A : Chem. 144,107,2001.

[11] Joseph.R.Lakowicz, "*Principles of fluorescence spectroscopy, third edition,*" Springer 2006.

[12] S.Speiser, R.Katraro, "*Computer simulation of an energy transfer dye laser (ETDL)*", Opt.Comm.27,287,1978.

[13] M.A.Ali, S.A Ahmed, "*Practical method for obtaining spectral distribution of gain in energy transfer dye lasers: comparison of theory and experiment*", Appl.Optics 29 ,4494,1990.

[14] J.B.Birks and M.S.S.C.P.Leite, *"Effects of diffusion on transfer efficiency,"* J.Phys.B 3,513,1970.

[15] T.Govindanunny and B.M.Sivaram, "*Gain studies on a uranine-damc dye mixture laser under nitrogen laser pumping*" J.Lumin.21,397,1980.

[16] M.Rajesh, K.Geetha, C.P.G.Vallabhan, P.Radhakrishnan, V.P.N.Nampoori, "*Fabrication and characterization of dye-doped polymer optical fibre as a light amplifier*", Appl. Opt.46 (1), 106,2007.

[17] T Urisu, K Kajiyama, "*Concentration dependence of the gain spectrum in energy transfer dye mixturesJ*. " Appl. Phys. 47,3563,1976.

[18] P J Sebastian, K Sathyanandan, "*Donor concentration dependence of the emission peak in rhodamine 6G -Rhodamine B energy transfer dye laser*", Opt. Comm. 35,113,1980.

[19] T Urisu, K Kajiyama, "*Concentration dependence of the gain spectrum in methanol solutions of rhodamine 6G*" J. Appl. Phys. 47,3559,1976.

[20] M.A.Ali , S.A Ahmed, "*Comprehensive examination of radiationless energy transfer models in dyes: Comparisons of theory and experiment*" J.Chem.Phys.90,1484,1989.

[21] Akihiro Tayaga, Shigehiro Teramoto, Tsuyoshi Yamamoto, Kazuhito Fujii, Eisuke Nihei, Yasuhiro Koike and Keisuke Sasaki, "*Theoretical and experimental investigation of rhodamine B-doped polymer optical fibre amplifiers*", IEEE Journal of Quantum Electronics 31, 12, 2215, 1995.

[22] Gang Ding Peng, Zhengjun Xiong, Peng, Pak L.Chu, "*Fluorescence Decay and Recovery in Organic Dye-Doped Polymer Optical Fibres*", Journal of Light wave Technology, 16, 12, 2365,1998.

[23] D.Mohan, S.Sanghi, R.D.Singh, "*Energy transfer excitation in an N_2-laser-pumped coumarin 485-rhodamine B dye mixture through optical gain characteristics*", J.Photochem. Photobio A:Chem.68,77,1992.

[24] R.D.Singh, A.K.Sharma, N.V.Unnikrishnan and D.Mohan, "*Time resolved spectra of coumarin 30-rhodamine 6G dye mixture*." Pramana-J.Phys.34, 77,1990.

……ൠ…..

Chapter- 4

Fabrication and characterization of dye doped graded index and hollow polymer optical fibres

Contents

4.1 Introduction

Graded Index (GI) polymers have recently attracted considerable attention in the light of their highly promising potential in optical fibre communication [1]. Although the loss in polymer optical fibre (POF) is still much higher than that in silica optical fibre, recent progress has led to the development of polymer based POF with a loss less than 100 dB/km, low enough for many short-range applications [2]. Vast majority of optical amplifiers are based on an optic fibre doped with a fraction of a percent of the rare-earth element erbium. Although rare-earth doping has been generally used in silica, many laboratories have been working to develop stable rare-earth

doped polymer lasers and amplifiers. The main issue with rare earth doped polymer lasers and amplifiers has been pumping inefficiencies due to the de-excitation of the excited states caused by the IR absorption in the polymer. In bulk form, polymer hosts impregnated with certain dyes have now achieved 80% conversion efficiency from pump power to signal power with tuning range close to those in solution. Dye –doped POFs can be made into useful fibre amplifiers and lasers that operate in the visible region [3-6]. Optical amplifiers and lasers made of dye-doped fibre require much less pump power than in bulk material because of the effective confinement and long interaction length available in the fibre. Since photo bleaching increases with the increase of the exposure intensity, low pump intensity would increase the lifetime of the gain medium. Also, the thin and long geometry of the fibre is ideal for good thermal relaxation to minimize the thermally induced photo bleaching as well [7]. The first part of this chapter, details the fabrication of a dye doped graded index polymer optical fibre preform by interfacial gel polymerization and its characterization. The second part of this chapter gives the details of the fabrication and thermal characterization of a compact polymer optical fibre drawing machine which was used for the drawing of polymer optical fibres of different refractive index profiles used in the present investigation. The fabrication and characterization of the step index, graded index and hollow optical fibres are explained as the third part of this chapter

4.1.1 Theory and experiment for the fabrication of graded index preforms

The dye doped graded index polymer optical fibre preform was prepared by the well-known interfacial gel polymerization technique [8]. The monomer was purified as follows: inhibitors in the monomer was removed by rinsing with a 0.5 N NaOH aqueous solution, followed by repeated washing with distilled water to remove the remaining NaOH. The monomer was dried over $CaCl_2$, distilled under reduced pressure and filterd through a 0.2- μm membrane filter. Initially a hollow

polymer tube was prepared. There are many methods for the polymer tube fabrication. First method is to rapidly rotate a glass tube containing monomer using a centrifugation (3000 rpm) in a furnace at 70 ^{0}C which results in a PMMA tube after polymerization [9]. The second method is hole in rod technique in which a hole is drilled in to the cladding polymer rod [10]. The first method requires specialized equipment and the second one results in a preform with large scattering losses since the core cladding interface may not be smooth because of the drilling. We have used the Teflon technique for the PMMA tube fabrication [11]. In this technique, we use a Teflon rod of diameter 6mm that is properly fixed at the center of a glass tube of inner diameter 13mm. One end of the tube is sealed and then it is filled with a mixture of monomer (MMA), 0.4 wt% of polymerisation initiator benzoyl peroxide (BPO), 0.1 wt% of the chain transfer agent (n-butyl mercaptan). The thermal polymerization of the filled tube is carried out in an oil bath where its temperature is properly controlled. After the monomer was fully polymerized and heat-treated, the Teflon was removed and we obtain a polymer tube. The non-sticking property of Teflon as well its chemical and thermal stability results in a smooth finish to the inner surface of the tube. The uniformity of the inner diameter of the tube was tested by making slices from the different parts of the rod. No non-uniformity was observed in diameters verifying the reliability of this technique.

Next, the polymerised tube was heat treated at 100^{0}C in an oven for 24 hours. The bottom side of this tube is sealed and the hole is then filled with a mixture of monomer (MMA), 0.4 wt% of polymerisation initiator benzoyl peroxide (BPO), 0.1 wt% of the chain transfer agent (n-butyl mercaptan), 5 wt% of a high refractive index organic compound diphenyl phthalate (DPP), the laser dye Rhodamine B (10^{-5} m/l) and 1 wt % of dimethyl sulfoxide (DMSO). Here DMSO enhances the solubility of Rhodamine B in MMA [12]. The filled tube was placed in an oven at 80^{0}C for 24 hours and at 90^{0}C for another 10 hours. Here the inner wall of the polymer tube is slightly swollen by

the monomer and a gel phase is formed in this region. Since the rate of polymerisation reaction inside the gel is faster than that in the monomer liquid owing to the gel effect, polymerisation occurs on the inner wall of the tube. Due to the selective diffusion process, the dopant molecules are gradually concentrated along the axis of the tube [9]. Finally the contents of the polymer tube are solidified up to the central axis. After this a heat treatment was carried out at 110^0C for 24 hours to yield the desired preform.

To obtain, any particular refractive index profile along the radial direction of a fibre core, a preform with the desired profile can be employed. The preform is a cylinder of polymer whose refractive index distribution can be made to coincide with that desired for the core of the POF. Interferometry is an accurate method for determining the refractive index profile of both preforms and fibres [13,14]. We have measured the refractive index profile of the solid rod using the slab method where a thin slice of the preform was cut, polished and kept in one of the arms of a Mach Zender interferometer. The light passing through the slab undergoes a phase shift, which depends on the optical path length. The fringe displacements for the points within the central portion of the disc are then measured with respect to the parallel fringes outside the core region. The difference in refractive index between various points in the core and cladding region can be calculated from the fringe shift S(r) and the parallel fringe spacing D (in the cladding) according to the relationship [15]

$$n(r) - n_2 = \frac{\lambda S(r)}{Dd} \quad \text{..... (4.1)}$$

where λ is the wavelength of the measuring light, d is the slab thickness. The parameter S(r) is the central field deviation at a distance r measured from the baseline connecting the same cladding fringe at both sides of the core as shown in figure 4.1.

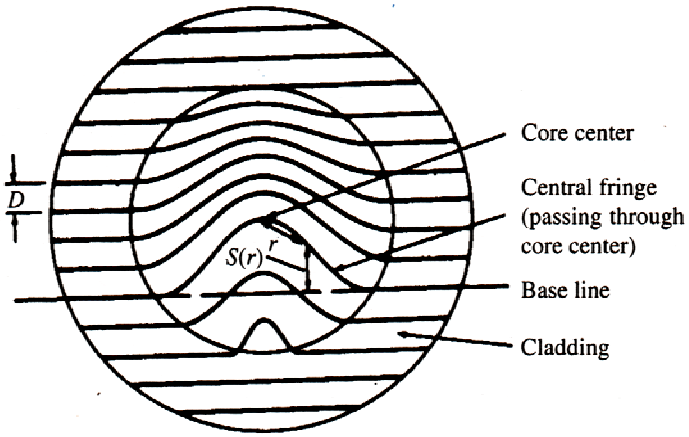

Fig.4.1. Displacements of locus of equal phase shift for different points in the slice.

The profile parameter α of the rod was also calculated from the expression [16,17] for the variation of refractive index n(r) with the distance from the axis for graded index fibres

$$n(r) = n_0\left[1 - 2\Delta\left(\frac{r}{a}\right)^{\alpha}\right]^{\frac{1}{2}} \quad \text{for} \quad r \le a \qquad \text{.....(4.2)}$$

$$= n_0\left[1 - 2\Delta\right]^{\frac{1}{2}} \qquad \text{for} \quad b \ge r \ge a$$

where n(r) is the refractive index at radius r, a is the core radius, b is the radius of the cladding, n_0 is the maximum value of refractive index along the axis of the core and Δ is the relative refractive index difference given by the expression[17]

$$\Delta = \frac{\left(n_0^2 - n_c^2\right)}{2n_0^2} \approx \frac{\left(n_0 - n_c\right)}{n_0} \qquad \text{..... (4.3)}$$

where n_c is the refractive index of the cladding. The value of α for the rod was found as the slope of the graph between ln (r/a) and ln g(r)

where $g(r) = \frac{1}{2\Delta}\left(1 - \left(\frac{n(r)}{n(0)}\right)^2\right)$ ..... (4.4)

For a preform with length 3.5 cms and diameter 1.3 cms, the fluorescence emission was recorded using a (frequency doubled) Diode Pumped Solid State (DPSS) laser emitting at 532 nm as the excitation source. The laser was mounted on a translational stage and the preform was kept stationary. The technique of side illumination fluorescence was used for recording the fluorescence spectrum. The laser beam was focussed using a convex lens along the axis of the preform and various points and the fluorescence signal was collected from one end face of the preform [18]. At each point of illumination the fluorescence spectrum was recorded using a Acton Spectrapro-500i Spectrograph coupled with a CCD camera having a resolution of 0.03nm.

The single pass gain measurement using the ASE method proposed by Shank et.al [19] is applied to calculate the gain in the above mentioned polymer rod. The second harmonic output from an Nd:YAG laser was focused by a cylindrical quartz lens of focal length 5 cm on the rod. A two mm thick aluminium sheet, mounted on a micrometer arrangement served as beam block. The rod was kept in a slanting position to avoid feedback and the output was recorded using a Acton Spectrapro-500i spectrograph coupled with a CCD camera. The dye laser intensities I_1 and I_2 for two lengths l_1 and l_2 of the active medium were measured for different pump intensities. The gain per unit length G (λ) of the dye doped polymer rod was determined using the Newton_Raphson numerical method.

$$\frac{I_1(\lambda)}{I_2(\lambda)} = \frac{[(\exp(G(\lambda)l_1) - 1]}{[(\exp(G(\lambda)l_2) - 1]} \quad \text{..... (4.5)}$$

4.1.2 Step index and Hollow preforms

Hollow polymer optical fibre preform can be fabricated by following a similar route as mentioned for the graded index preform in section 4.1.1. As

discussed in section 5.3, this involves the use of a Teflon rod during the polymerisation.

The laser dye Rhodamine B (10^{-5} m/l)was also incorporated during the fabrication of hollow PMMA tube to get a dye doped hollow preform. This can be heat drawn as a hollow optical fibre. A single process of polymerisation of the laser dye Rhodamine B (10^{-5} m/l) doped MMA in a test tube results in a dye doped polymer rod that can be used for fabricating dye doped step index polymer optical fibres.

4.1.3 Results and discussion for the preforms

Using interfacial gel polymerisation technique, dye doped graded index polymer fibre preforms were fabricated. Figure 4.2 shows the photograph of a graded index preform doped with Rhodamine B.

Fig. 4.2. Dye doped graded index polymer rod.

The refractive index profile of the rod can be measured using the method explained in section 1.4.4 and the experimental setup shown in figure 1.7. A thin slice of the polished preform was prepared and placed in one of the arms of a Mach-Zender interferometer.The shift in the fringes for various positions of the slice was found by taking a photograph of the fringe pattern. Figure 4.3 shows

the photograph of central portion of such a pattern obtained for a sample of thickness 1.19 mm.

Fig.4.3. The photograph of the fringe pattern

Figure 4.4 shows the transmitted fluorescence light as a function of propagation distance through the preform. It is seen that the output intensity decreases with the propagation distance. It was also observed that the peaks exhibit a red shift of about 10 nm while varying the point of excitation through a distance of 3.2 cm.

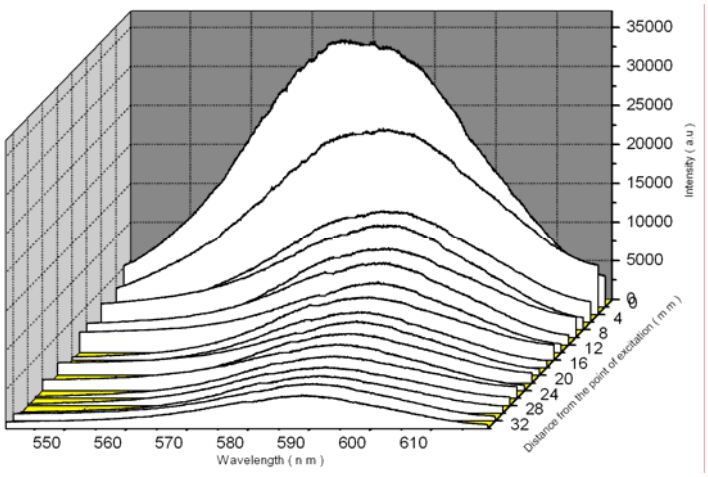

Fig. 4.4. The transmitted fluorescence light using side illumination

The red shift of the fluorescence signal is produced by the self-absorption of the dye due to the overlapping of the absorption and fluorescence spectra of the RhB. After a distance of 3.2 cms, the red shift shows saturation.

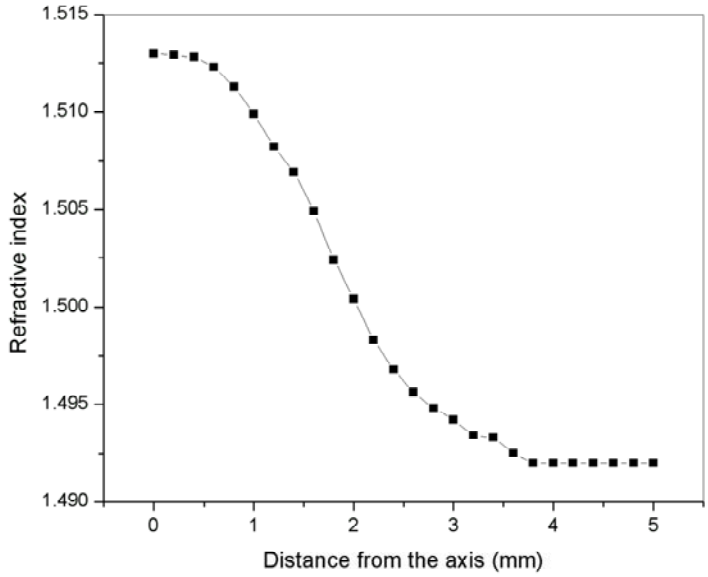

Fig. 4.5. Refractive index profile of the rod

Figure 4.5 shows the refractive index profile of a typical specimen of the fabricated preform. It was found that the maximum difference in the refractive indices between the core and the cladding is 0.021± (0.002) and it occurs along the axis of the preform and it gradually decreases towards the cladding. Figure 4.6 shows the curve obtained for the evaluation of the profile parameter. The curve is very close to a straight line up to an (r/a) value 0.47 and the profile parameter is 1.96. For higher values of r, there is a considerable reduction in slope and the profile parameter vary much from 2. This drastic variation in the refractive index gradient can be attributed to the formation of aberrations at the inner wall of the polymer

tube during the interfacial gel polymerisation. This gives us an idea of the actual diameter of the graded index polymer rod that can be used as a good preform. The outer regions of the rod can be removed by machining before the fibre is drawn. Keeping all other parameters constant, similar rods were prepared by doping with Rhodamine 6G and also Rhodamine 6G:Rhodamine B mixture. A deviation from the parabolic index profile was observed for these samples also. The calculated profile parameters for these rods were found to be 1.81 and 1.87 respectively.

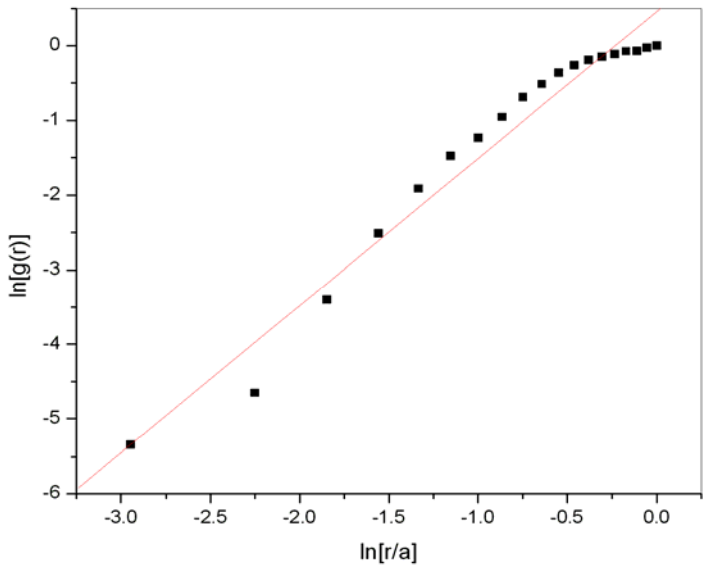

Fig 4.6. Log – log plot of g (r) Vs r/a

Figure 4.7 shows the pump power dependence of the gain of the rod doped with Rh.B. From the figure it is clear that at lower pump powers the gain of the preform shows a linear increase while above 0.04 Watts, gain tends to saturate.

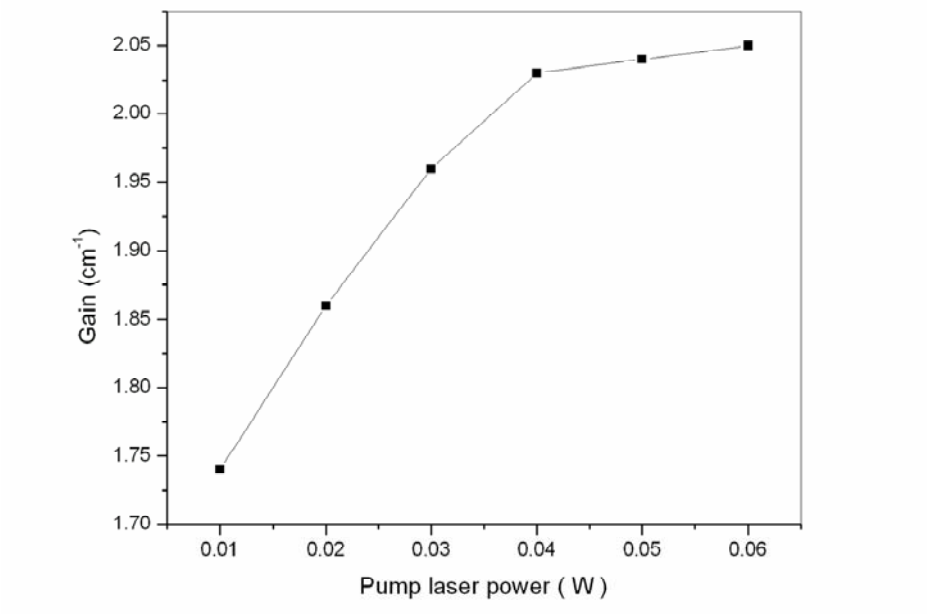

Fig 4.7. Variation of gain with second harmonic output of Nd: YAG laser power

After proper calibration, the spatial variation of the doping concentration of the dye rhodamine B was also studied. The axial excitation of a thin slice of the rod using white light and measurement of the fluorescence signal at 590 nm at various points showed maximum fluorescence along its axis. Figure 4.8 shows the fluorescence intensity variation across the dye doped region. The result indicate that the maximum extent of doping of the dye molecules occur along the axis of the rod. Figure 4.9 shows the schematic representation of the dye distribution in the rod.

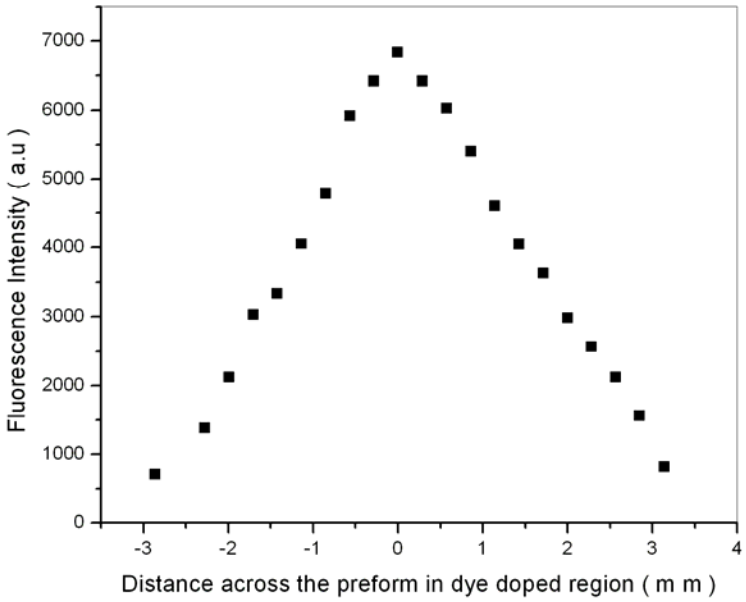

Fig. 4.8. Fluorescence intensity variation across the dye doped region of the preform

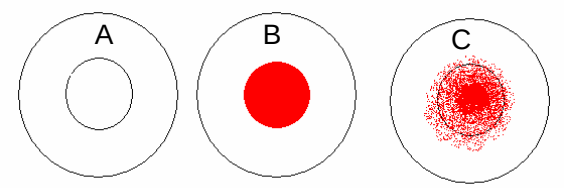

Fig.4.9. Dye distribution inside the preform : A- Hollow polymer tube, B- after filling with dye solution and C- After polymerisation

Step index and hollow polymer rods were fabricated using the method explained in section 4.1.2. No further characterizations were performed for step index and hollow optical fibre preforms. Studies on the optical fibres fabricated using these preforms are discussed separately in chapters 5, 6 and 7.

4.2 Design and fabrication of a compact polymer optical fibre drawing machine

A compact cylindrical furnace for heating the polymer optical fibre preform was developed and its temperature profile was measured along the axis for different set temperatures and furnace voltages. Due to the prominence of radiative heat transfer at steady state, the resulting axial temperature profile within the preform is strongly coupled to the corresponding axial temperature profile of the furnace. As shown in figure 4.10, the furnace was fabricated using machined aluminium, a refractories tube, a heating coil and insulating ceramics. It is 12cm in height and 8cm in diameter. Temperature profile along the axis of the furnace was studied for various set temperatures and furnace voltages.

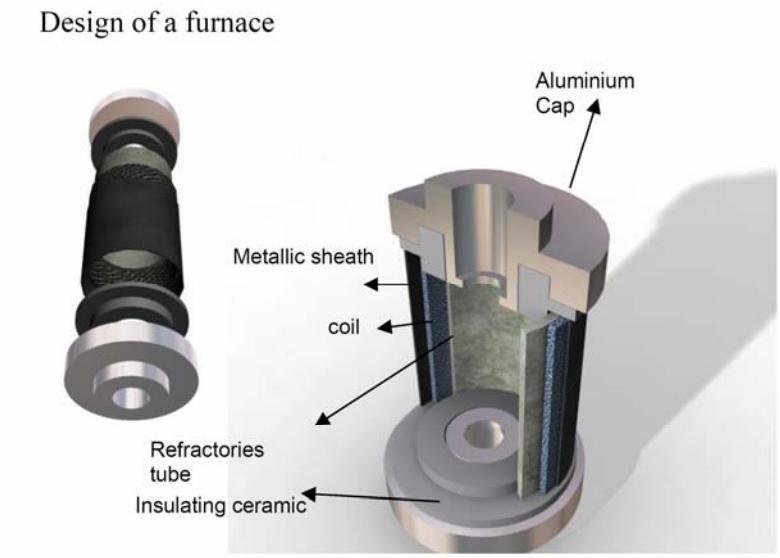

Fig. 4.10. A compact cylindrical furnace used for the machine

With the present design, measurements indicate that the temperature remains almost constant along a length of 2cm at the furnace top with a slightly higher value occurring at about 2cm from the top. Thereafter the temperature variation along the axis up to the bottom is almost linear. Most of the fibres were

heat drawn at 170^{o}C at a furnace voltage of 50 V. A PIC 16F 873A chip is used for controlling the stepper motor driver A3955B which is a 1/8 th stepper IC.A visual basic software was developed to control the device. Figure 4.11 shows the axial temperature profile of the furnace at different input voltages and set temperatures.

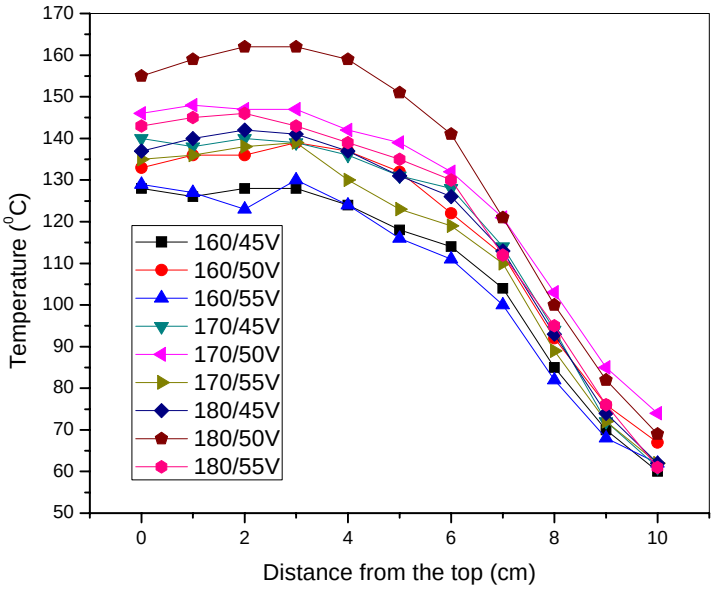

Fig. 4.11. Axial temperature profile inside the furnace

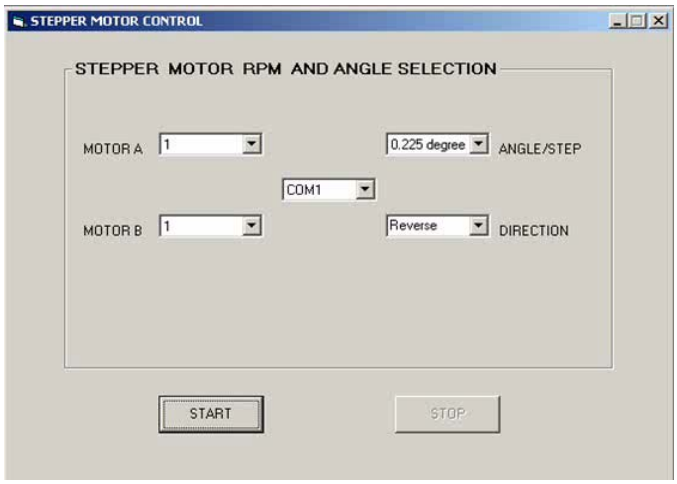

Fig. 4.12. The graphical interface for the device

The stepper motors used for the present device are DFM57SH51-1A.001, which is of a 1.8^0/step type. The driver is capable of reducing this step size up to 0.225^0/step thereby minimizing any possible vibration during the fibre drawing process. At this step size, the motor takes 1600 steps for completing a full rotation. We can choose three more step sizes viz; 0.45, 0.9and 1.8^0/step. In each one, the speed can be varied from $V_{max}/255$ to V_{max} independently for the feeder and drawing motors there by effectively allowing the fibre diameter tailorability. The feeding motor is coupled to a translational stage to get smooth linear downward motion of the preform. Figure 4.12 shows the graphical interface developed to control the device. An autotune PID controller (Radix P48U) was used to control the furnace temperature. It is a microcontroller based user programmable autotune PID controller with 4 digit LED display for displaying measured values and another 4 digit LED display for displaying the set point with a control accuracy of $\pm 1^0 C$.

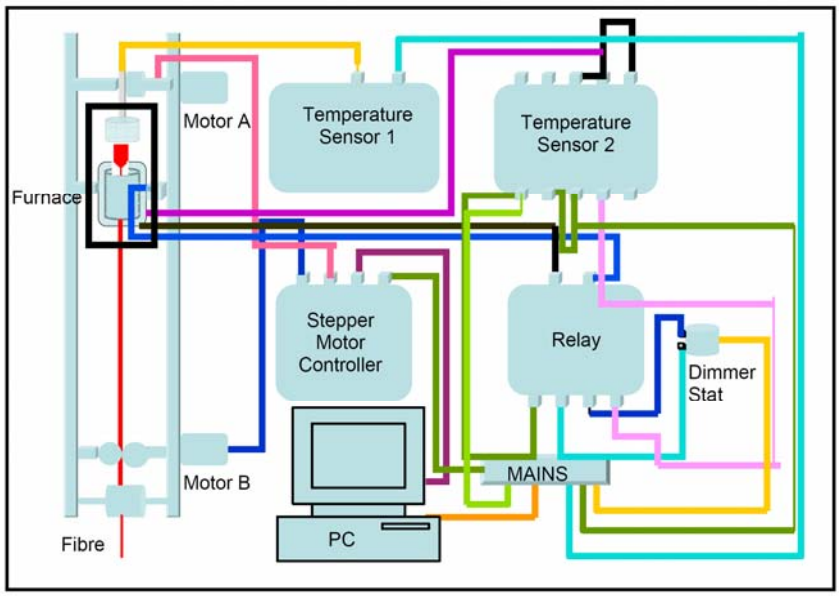

Fig. 4.13. The schematic diagram of the fibre drawing setup

Figure 4.13 shows the schematic diagram of the entire setup. The furnace draws about 1A current almost independent of the temperature of the furnace.

Maximum speed of the feeding and pulling are 0.6 mm/sec and 72.6 mm/sec respectively. Figure 4.14 shows the photograph of the fibre drawing setup.

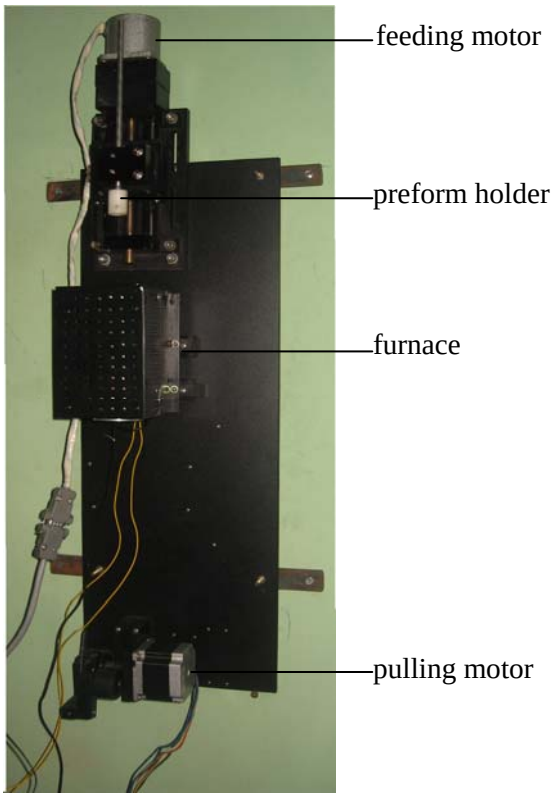

Fig. 4.14. The photograph of the fibre drawing setup

4.3 Fabrication and Characterisation of the optical fibres

Most of the fibres were heat drawn at a temperature of about 170^0C. The preforms were introduced 15 minutes earlier into the furnace which is kept at a lower temperature of about 150^0C for the purpose of preheating. During the next 5 minutes, the temperature was gradually increased to 180^0C. When the preform necks downward by its own weight due to gravity, the furnace temperature was slightly brought down to 170^0C for stabilized melting of the preform. Step index, graded index and hollow polymer optical fibres were drawn from step index ,graded index and hollow polymer optical fibre preforms.

4.3.1 Beam profile measurements

The output beam profiles of the 1 metre long fibres were measured by injecting a Gaussian mode into the fibres using a DataRay Beam R2 scanning type beam profiler and analyzing the output using the software DR Ver 6.0. A linear scanning probe carries either a single slit, or orthogonal X-Y slits. Light passing through the slit falls on to a Si detector inside the profiler. It can perform real time measurements of the parameters like gaussian beam diameter,Gaussian fit,centroid position, ellipticity, orientation of major axis and beam wander display. For the beam dimensions in the range 3µm-45mm the equipment has a resolution of 0.5µm. The 2-D and 3-D profiles are reconstructed from the X-Y scan, making the assumption that the measured X beam profile is the same for all the values of Y and that the measured Y beam profile is the same for all values of X.

It was found that 1m long step index and graded index fibres were maintaining the profile. Figures 4.15 and 4.16 show the results obtained for the profile measurement for graded index and step index fibres. The measured ellipticities for the fibres were found to be 1.06 and 1.01 respectively.

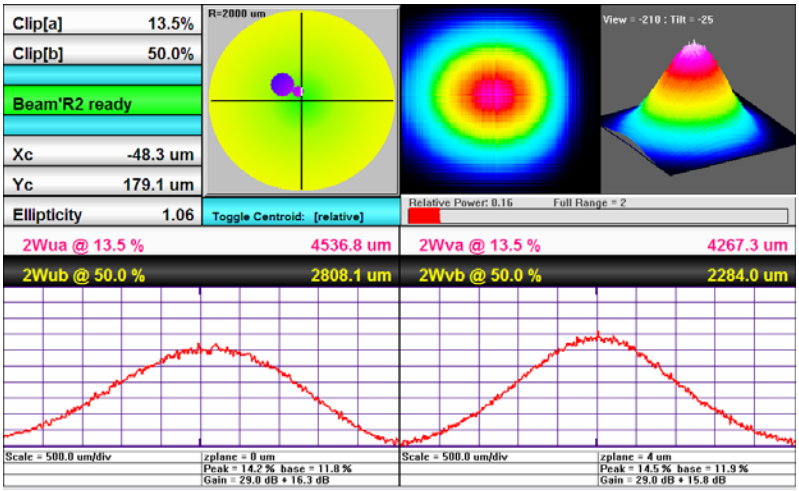

Fig.4.15. Result of the profile measurement for a dye doped graded index fibre GI fibre (600µ)

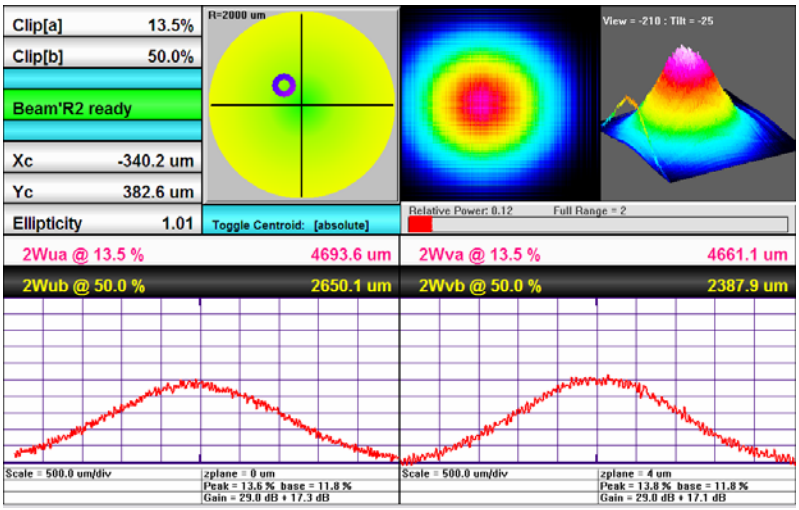

Fig. 4.16.Result of the profile measurement for a dye doped step index fibre (800μ)

4.3.2 Fibre Attenuation measurement- Cut-Back method

Fibre attenuation measurement have been developed in order to determine the total fibre attenuation and this is contributed by both absorption losses and scattering losses. The overall fibre attenuation is of great interest to the system designer but the relative magnitude of the different loss mechanisms is important in the development and fabrication of low loss fibres. Different methods can be employed for measuring attenuation: the insertion loss method (non destructive), the substitution method (non destructive) and the cut-back method (destructive).A commonly used standard technique for determining the total fibre attenuation per unit length is the cut-back or the differential method[20].

The cutback method provides more accurate results than the insertion and substitution method .The advantage of this method lies in the fact that launching conditions remain unchanged. A schematic diagram of a typical experimental setup is shown in figure 1.9. Light beam from a 10 mW Helium

Neon laser (632.8nm) and 10mw diode pumped solid state laser (532nm) were used for the measurements. The light was launched into the fibre with the help of a lens. After polishing the fibre end faces the fibre is firmly held in a suitable holder such that only a small length projects outside. The incident beam is adjusted at the input end of the fibre so that maximum power is obtained at the output end. The output power is measured using a photo detector as $P(L_1)$, where L_1 is the length of the test fibre. Without disturbing the launching conditions, a short length of the fibre from the output end is cut and polished. The output power is again measured as $P(L_2)$ where L_2 is the cut back length of the fibre. Cutting, polishing and measuring process is repeated several times. From these measurements the attenuation can be calculated using the relation.

$$\alpha_{dB} = \frac{10\log\frac{(P(L_2)}{(P(L_1)}}{L_1 - L_2} \quad \text{.....(4.6)}$$

Table 4.1. Shows the details of the loss measurement performed at 632.8nm and 532nm wavelengths (Best values)

Fibre Type	Loss dB/cm at 632.8 nm	Loss dB/cm at 532 nm
Undoped step index	0.21	0.19
Undoped graded index	0.22	0.17
Rh B doped step index	0.23	0.31
Rh B doped grded index	0.27	0.33
Rh 6G doped step index	0.24	0.30
Rh 6G doped graded index	0.25	0.32
Rh 6G;RhB mixture doped Step index	0.27	0.33
Rh 6G;RhB mixture doped graded index	0.26	0.32

The values in the table show that the fabricated fibres have large attenuation compared to the commercial polymer optical fibres. The undoped fibres exhibit the smallest attenuation for both the excitation wavelengths .Again at 632.8nm excitation, attenuation values are slightly higher. This is attributed to the fact that PMMA transmission loss is large at 632.8nm in comparison with 532nm. In the case of doped fibres, attenuation is less at 632.8nm compared to 532nm. The large absorption cross section of the dyes, Rhodamine 6G and Rhodamine B at 532nm results in comparatively larger attenuation at this wavelength.

4.4 Conclusions

Dye doped graded index polymer optical fibre preforms were fabricated using the interfacial gel polymerisation technique and their refractive index profiles were measured using the interferometric technique. Dye doped step index and hollow optical fibres were also fabricated. The best value of profile parameter obtained for the Rhodamine B doped graded index rod in the present study was found to be 1.96 for the inner 47% of the graded index region. The fluorescence characterization of this preform shows that it exhibits a red shift of about 10 nm while varying the point of excitation through a distance of 3.2 cm. It was also seen that the dye concentration and the fluorescence intensity are maximum along the axis of the preform. Pump power dependence of the gain of this rod shows the gain of the rod tends to saturate above 0.04 Watts. A compact polymer optical fibre drawing machine was fabricated and its thermal characterization was done. Dye doped GI, SI and hollow polymer optical fibres were fabricated using this machine. The fabricated preforms were characterized by performing beam profile and attenuation measurements. Undoped SI and GI fibres have minimum attenuation at wavelength 532 and 632nm.This suggests that one can fabricate dye doped step index, graded index and hollow polymer optical fibres using above procedure. Such dye doped optical fibre can be employed to develop fibre amplifiers in the visible region.

References

[1] Xinhua Dai ,Jun He, Zhimin Liu, Xicheng Ai, Guanying Yang, Buxing Han, Jian Xu, "*Stability of high-bandwidth graded-index polymer optical fibre*",Journal of Applied Polymer Science 91,2330,2004.

[2] Jui-Hsiang Liu, Hung-Yu Wang and Chia-Hwa Ho, "*Fabrication and Characterization of Gradient Refractive Index Plastic Rods Containing Inorganic Nanoparticles*", Journal of Polymer Research,10,13,2003.

[3] E.De La rosa-Cruz C.W. Dirk and O. Rodriguez, V.M. Castano, "*Characterization of Fluorescence Induced by Side Illumination of Rhodamine B Doped Plastic Optical Fibres*",Fibre and Integrated Optics, 20 (5),457,2001.

[4] "*Plastic Optical Fibre of the year 2001*" Market Survey, KMI Corp , 1994

[5] Y.Koike, T.Ishigure, and E.Nihei, "*High-bandwidth graded-index polymer optical fibre,*" IEEE J.Lightwave. Technol., 13,1475,1995.

[6] Popov.S "*Dye Photodestruction in a Solid-State Dye Laser with a Polymeric Gain Medium*", Appl.Opt. 37,6449,1998.

[7] J.S.Vrentas, C.M.Vrentas,"*Solvent Self-Diffusion in Glassy Polymer-Solvent Systems*",Macromolecules,27,5570,1994.

[8] Y.Koike,Y.Takezawa and Y.Ohtsuka, "*New interfacial-gel copolymerization technique for steric GRIN polymer optical waveguides and lens arrays*", Appl.Opt.27,486 (1988)

[9] Akihiro Tayaga, Yasuhiro Koike, Eisuke Nihei, Shigehiro Teramoto, Kazuhito Fujii, Tsuyoshi Yamamoto and Keisuke Sasaki, "*Basic performance of an organic dye-doped polymer optical fibre amplifier* ", Applied Optics, 34, 988,1995.

[10] M.G.Kuzyk, U.C.Paek and C.W.Dirk, "*Guest-host polymer fibres for nonlinear optics*",Appl. Phys.Lett, 59, 902,1991.

[11] G.D.Peng, P.L.Chu, X.Lou and R.A. Chaplin, "*Fabrication and characterization of polymer optical fibre*", J. Elec. Electron. Eng. Australia, 15, 289,1995.

[12] Akihiro Tayaga, Shigehiro Teramoto, Eisuke Nihei, Keisuke Sasaki and Yasuhiro Koike, "*High-power and high-gain organic dye-doped polymer optical fibre amplifiers: novel techniques for preparation and spectral investigation*", Applied Optics, 36, 572 ,1997.

[13] M.Kailasnath, P.R.John, Rajeshkumar, "*Proceedings of International Conference on Optoelectronic materials and thin films for advanced technology*" October 24-27, 2005, Kochi, India

[14] M.Kailasnath, P.R.John, Rajeshkumar, "*Proceedings of International Conference on Optics and Optoelectronics,*" December 12-15,2005, Dehradun, India.

[15] C.K.Sarkar, "*Optoelectronics and Fibre Optics Communication"* 2001, New Age International, New Delhi.

[16] R.P. Khare, "*Fibre Optics and Optoelectronics*", 2004, Oxford University Press

[17] John M. Senior "*Optical Fibre Communications*" 2004, Prentice-Hall of India, New Delhi.

[18] Kruhlak,R.J, M G Kuzyk, "*Side-illumination fluorescence spectroscopy. I. Principles*", J.Opt.Soc.Am.B 16,1749,1999.

[19] Shank.C.V, Diener. A, Silfvast .W.T, "*Single pass gain of exciplex 4-MU and rhodamine 6G dye laser amplifiers*",ppl.Phys. Lett, 17, 307,1970.

[20] Ajoy Ghatak, K,Thyagarajan, "*Introduction to fibre optics*", Cambridge University Press, NewDelhi,2002.

[21] Y.Koike, "*High-bandwidth graded-index* polymer *optical fibre*" Polymer 32,1737,1991.

[22] Y.Koike and E.Nihei,*U.S.Patent* 5,253,323, 1993.

[23] T.Ishigure, E.Nihei, and Y.Koike, "*Graded-index polymer optical fibre for high-speed data communication*" Appl.Opt.33,4261,1994.

[24] T.Ishigure,A.Horibe,E.Nihei and Y.Koike, "*High-bandwidth, high-numerical aperture graded-index polymer optical fibre*" J.Lightwave Technol.13,1686, 1995.

[25] A.M.Mescher, H.M.Reeve and J.B.Dixon, "*Proceedings of the International Polymer Optical Fibres Technical Conference*", Cambridge, MA,P 26,2000.

[26] U.C. Paek, R.B.Runk, "*Physical behavior of the neck-down region during furnace drawing of optical fibres,*" J.Appl.Phys, 49(8) 4417,1978.

[27] T.Izawa and S.Sudo, "*Optical fibres: Materials and fabrication*", Kluwer, Boston, 1987.

[28] Y.Koike, N.Tanio, E.Nihei and Y.Ohtsuka, "*Gradient-index polymer materials and their optical devices*", Polym.Eng. Sci. 29,1200, 1989.

……ജോ…..

Chapter- 5

Fabrication and characterization of free standing polymer micro ring cavity multimode laser

Contents

5.1 Introduction

Optical microcavities are natural candidates for very low threshold microlasers and for the observation of interesting quantum optical behaviour [1]. From the view point of semiconductor facbrication technology, the simplest of the cavities may be the planar dielectric Bragg mirror cavity. A difficulty with the planar dielectric cavity is that, there is no lateral confinement of the mode, and as such the transverse modes of the cavity are poorly defined, and consequently, results in a small spontaneous emission coupling factor [2].High Q value optical microresonators with strong optical confinement to the gain region can be obtained by the use of the whispering –gallery resonator modes propagating around the edge of a sphere, disk, cylinder or ring[3]. These techniques may be applicable to a wide range of material systems since low optical cavity loss is obtained from a simple curved surface instead of multiple layer dielectric mirrors.

The optically pumped polymer based devices show lasing at relatively low excitation intensity threshold and are usually a demonstration of the

superior polymer optical properties that allow high optical gain. Laser dye doped poly (methyl methacrylate) is found to be a highly efficient medium either for laser sources with narrow pulse width and wide tunable range or for optical amplifier with high gain, high power conversion and broad spectral band width[4]. Dye doped optical fibres have also been fabricated in conjunction with fibre lasers and fibre amplifiers [5,6]. The first optical amplification in dye doped fibers was demonstrated by researchers in Japan[7,8] in which they demonstrated that efficient conversion as well as long lifetime of the gain medium can be achieved in a Rhodamine B dye doped polymer optical fibre. Exceptionally thin microcavities can in principle exhibit threshold less lasing even though ideal micro cavities are difficult to fabricate. The usual method of fabrication of a cylindrical polymer microcavity is by making a coating of few microns thick conducting polymer or a dye doped transparent polymer of high refractive index over a glass optical fibre [9].This chapter deals with the observation of whispering gallery mode (WGM) structure at room temperature from a ring cavity made up of Rhodamine B dye doped hollow poly(methyl methacrylate) optical fibre pumped by a frequency doubled Q switched Nd:YAG laser .

5.2 Theory of micro ring cavities

Three factors determine the effective length and thus the resonant wavelength of a micro cavity viz. the separation of the mirrors, the phase change of light on reflection of light from mirrors and the refractive indices of the materials inside the cavity [10].The spectral peak of the polymer ring laser is at the maximum of the optical gain spectrum $\gamma(\lambda)$. Lasing occurs at λ where $\gamma(\lambda)$ exceeds the optical losses; this condition is given by [11],

$$\gamma \geq \frac{2\pi n_p}{\lambda Q} \quad \text{.....(5.1)}$$

where n_p is the refractive index of the polymer and Q is the cavity quality factor. Q is usually used to characterize the quality of a resonator mode and is defined as 2π times the number of optical cycles required for the cavity mode field to decay to 1/e of its initial value[12].There are three contributions to Q: Q_{abs} is the absorption limited quality factor given by $2\pi/\alpha\lambda$, where α is the absorption coefficient; Q_{scat} is determined by scattering losses in the polymer film and its surface due to imperfections.; and Q_{cav} is the cavity finesse determined by the microcavity geometry. These Q's are added as follows:

$$Q^{-1} = Q_{abs}^{-1} + Q_{scat}^{-1} + Q_{cav}^{-1} \quad \text{.....(5.2)}$$

For cylindrical microcavities, Q_{cav} is in the range of 10^4-10^8 [13,14]. Q_{scat} strongly depends on the polymer film quality and in principle, may be made so large as to eliminate the Q_{scat}^{-1} contribution in Eqn. (5.2); however it is the least controllable parameter.

The hollow fibre acts as a waveguide forming a ring resonator similar to a polymer film coated on a glass optical fibre. The resonant frequencies ν_m for the waveguided laser modes are given by[15],

$$\nu_m = \frac{mc}{\pi D n_{eff}} \quad \text{.....(5.3)}$$

where m is an integer, c is the speed of light in vacuum, D is the outer diameter of the fibre and n is the effective index of refraction of the hollow waveguide. As shown in figure 5.6, for a relatively thick polymer film, as in our case, n_{eff} may be approximated by[16],

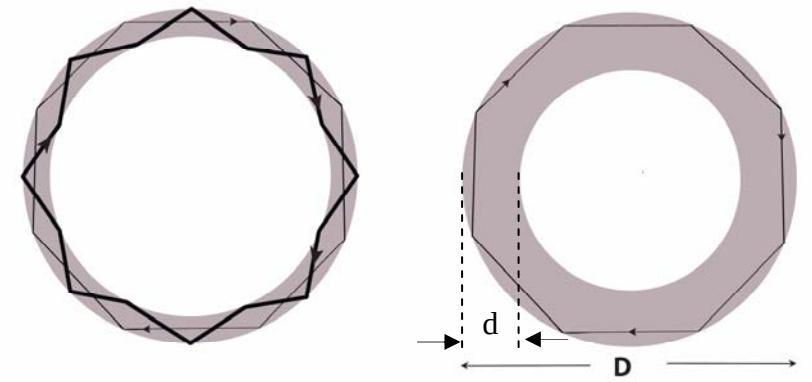

Cross section of a thin waveguide Cross section of a thick waveguide $\frac{d}{D} \geq 0.2$

Fig.5.6. Cross section of a thin and thick dye doped hollow fibre.

$$n_{eff} \approx n_p\left(1-\frac{d}{D}\right) \approx n_p \qquad \text{.....(5.4)}$$

where d is the thickness of the film. Using this approximation we calculate the intermodal spectral spacing

$$\Delta\lambda = \frac{\lambda^2}{\pi D n_p} \qquad \text{.....(5.5)}$$

Figure 5.6 depicts the cross section of a thin and a thick hollow waveguide and the difference in the supported resonant modes in these structures. In thicker polymer rings, (d/D ≥ 0.2), the resonant modes are no longer guided waves [16]. In fact these optical modes never reach the film core interface and therefore are dubbed whispering gallery modes[13,14].The light in this case is confined by total internal reflection at the film air interface, and the mode intensity distribution is concentrated on the outer edge of the fibre. The WGM wavelengths are still given by (5.5). A different approach to understanding the whispering gallery modes has been previously reported [16] by transforming the curved structure into a straight one using the conformal

transformation technique. As a result, the refractive index within the transformed guide is represented by the following dependence on the radius:

$$n(r) = n(\rho)e^{r/R} \quad \text{.....(5.6)}$$

where $n(\rho)$ is the initial index distribution and R the radius of the structure that has been transformed. This expression illustrates that the transformed refractive index increases towards the outside of the hollow fibre, so that the lower order modes will follow the peak of $n(r)$ and travel along the outer wall. The omission of the inner boundary reduces the scattering losses and facilitates heat dissipation [17].

5.3 Experiment

A typical procedure for the fabrication of dye doped hollow polymer optical fibre is as follows: In the first step, a Teflon rod of diameter 6mm is properly fixed at the centre of a glass test tube of inner diameter13mm.The tube is then filled with a mixture of monomer (MMA),0.4 wt% of polymerization initiator benzoyl peroxide (BPO) ,Rhodamine B (10^{-4} m/l)and 0.1 wt% of the chain transfer agent (n-butyl mercaptan).The polymerization is carried out at 80^0C for 48 hours. After polymerization, the Teflon rod was removed to get a dye doped polymer tube. The preform tube thus obtained was placed in an oven at 110^0C for 24 hours for the complete polymerization. Finally, the preform tube was heat drawn into a fibre at 180^0C [18]. Dye doped hollow polymer optical fibres of different diameters were drawn by adjusting the speed of feeding as well as the pulling motor.

The cross section of the drawn hollow fibre that is used for the present study is like a microring with an outer diameter 340μm and inner diameter 157 μm. A 1cm length of the fibre was transversely pumped at 532 nm with a

frequency doubled Q switched Nd:YAG laser (Spectra Physics) with 8ns pulses at 10Hz repetition rate. The pump beam was focused by a cylindrical lens exciting a narrow stripe of 0.6mm width and different excitation lengths on the hollow fibre surface. The fluorescence was collected using a collection fibre and given to a CCD monochromator assembly which has a resolution of 0.03nm. Figure 5.7 shows the experimental setup for the measurement of fluorescence from the dye doped hollow fibre.

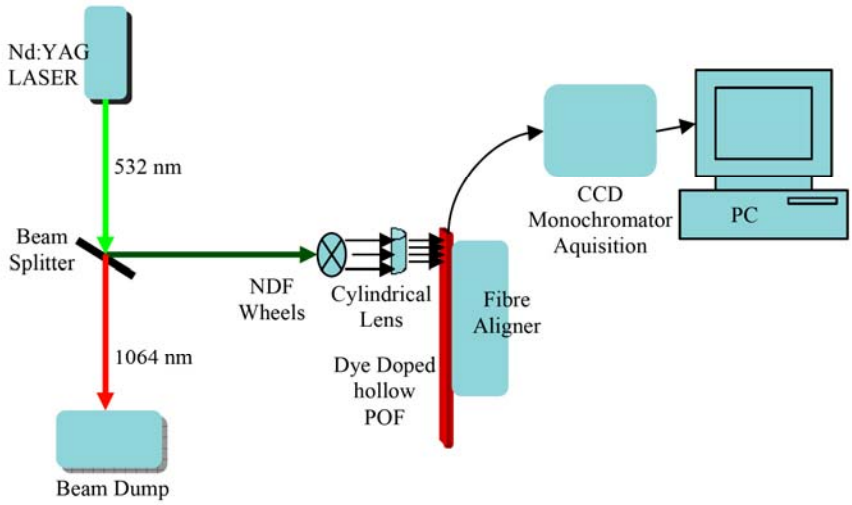

Fig.5.7. Experimental setup used for the study

5.4 Results

Figure 5.8 shows the fluorescence emission from a 1cm long, 340 μm thick hollow fibre doped with Rhodamine B for excitation lengths 2mm and 4mm respectively. As seen from the diagram, for an excitation length of 2mm, fibre exhibits normal fluorescence up to a pump beam average power of 0.049 W. The amplified spontaneous emission begins at 0.081 W and the FWHM decreases continuously up to 0.220W when laser emission was also observed with a multimode structure. Beyond this pump power the fluorescence intensity was found to decrease with a blue shift in the spectrum. At these higher pump

intensities; the multimode structure also starts disappearing. This result is attributed to the degradation of the dye molecule at higher pump powers.

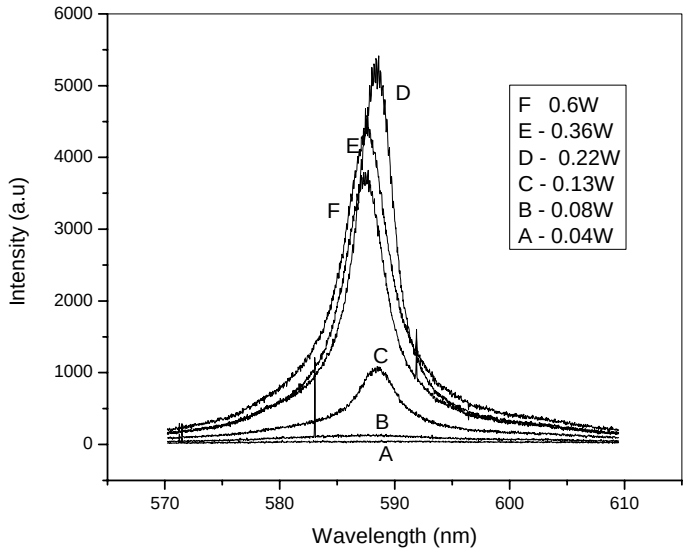

Fig.5.8. Emission spectrum of a 1cm long, 340μm diameter Rhodamine B doped hollow polymer optical fibre for an excitation length 2mm.

Figure 5.9 shows the expanded peaks of the three curves in figure 5.8 for the highest three pump powers. At a pump power of 0.22W, the mode structure is clearly resolved. The wavelength spacing between the modes in the present observation at 0.22W was in agreement with that of the whispering gallery modes in the micro cavity ring lasers given by equation 5.5. The $\Delta\lambda$ in the present study was found to be 0.176nm which is in close agreement with the theoretical calculation of 0.172nm. The longer round trip distance means that there are many longitudinal modes supported by the cavity. The feed back mechanism is rather complicated with a combination of whispering gallery modes confined at the outer surface plus the other waveguided modes in which light is trapped in the film by total internal reflection from both inner and outer air polymer interfaces.[9,19].Each mechanism supports a distinct set of resonant frequencies .These modes can superimpose to give complicated

clusters of closely spaced modes within the polymer gain bandwidth. The dominance of WGM in the present study may be attributed to the considerably larger thickness of the polymer tube (92μm)[20].

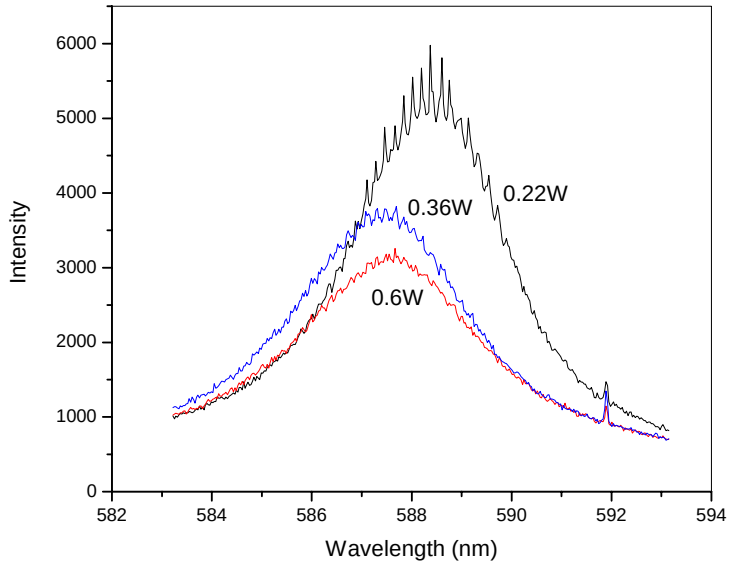

Fig.5.9. Expanded recording of modes in figure 5.8 for excitation length of 2mm

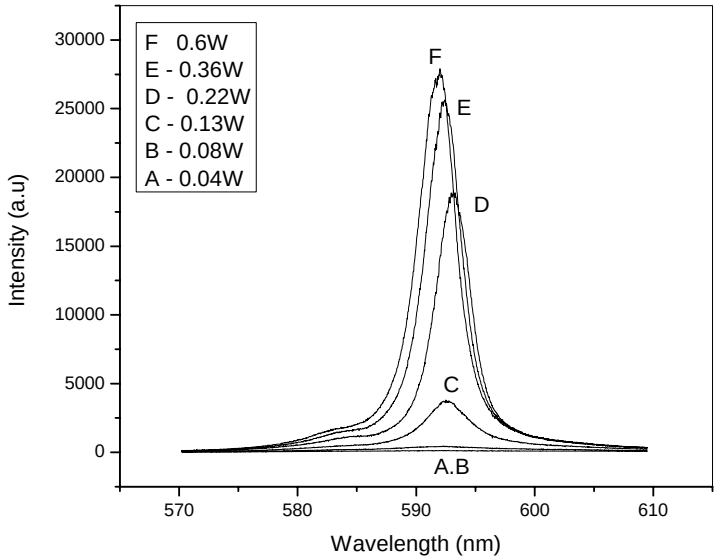

Fig.5.10. Emission spectrum of a 1cm long, 340μm diameter Rhodamine B doped hollow polymer optical fibre for an excitation length 4mm.

The experiment was repeated by increasing the excitation length to 4mm. The emission spectrum shown in figure 5.10 gives rise to an enhancement in the fluorescence intensity when the excitation length was increased to 4mm but the mode structure was absent in this case. Also, there is no decrease in emission intensity with pump power in this case resulting in a minimum FWHM of 3.6nm at 0.6W compared to the 3.73 nm at 0.22 W for the 2mm excitation. As the length of the excitation is increased the number of possible modes becomes very large and the separation between them becomes very small. As a result individual modes are absent in this case and only an enhancement in the fluorescence intensity is observed.

The ASE peak emission wavelength of the hollow fibre as seen from figure 5.11 depends on the pump power and the excitation length. For both 2mm and 4mm excitations, the emission wavelength peak was found to be continuously blue shifted up to a pump power 0. 6 W . For the 4mm excitation the peak was blue shifted by 1.2 nm and for 2mm excitation, blue shift was 1.5nm.

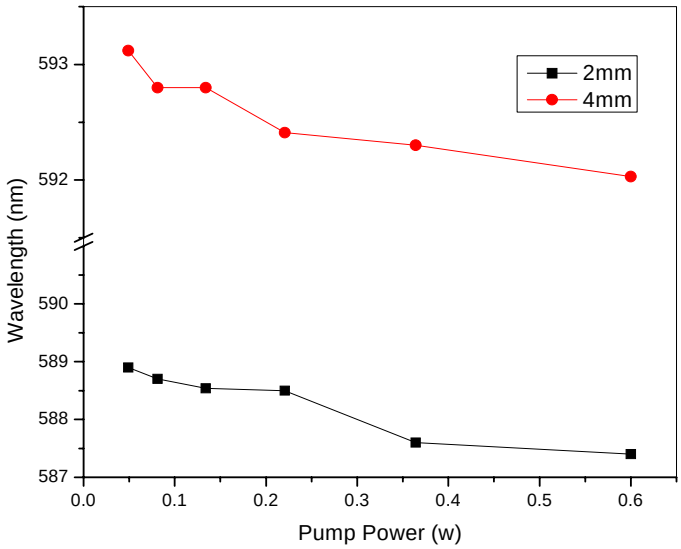

Fig.5.11. The pump power dependence of peak wavelength for 340 μm diameter hollow fibre for different excitation lengths.

A close examination of the fluorescence spectra at low pump power shows a small kink in the lower wavelength side indicating the presence of an additional band corresponding to deexcitation from a higher vibronic level. As the pump power is increased, the radiative transition probability gets enhanced at shorter wavelength side of the spectrum by energy transfer from mode at low energy side to high energy side creating an apparent shift in the spectrum towards the blue side. Further increase in the power does not lead to any shift in the wavelength except that the overall power is decreased.

The dependence of the emission characteristics of the fibre on its diameter was studied using two more fibres with diameters 158 and 615μm. Figures 5.12 and 5.13 shows, for a fibre with 615μm, only an enhancement in the fluorescence intensity was observed with no sign of ASE at both the excitation lengths. There is continuous increase in the fluorescence intensity with pump power. This result is attributed to the fact that a larger diameter fibre requires a higher threshold pump power for ASE and lasing.

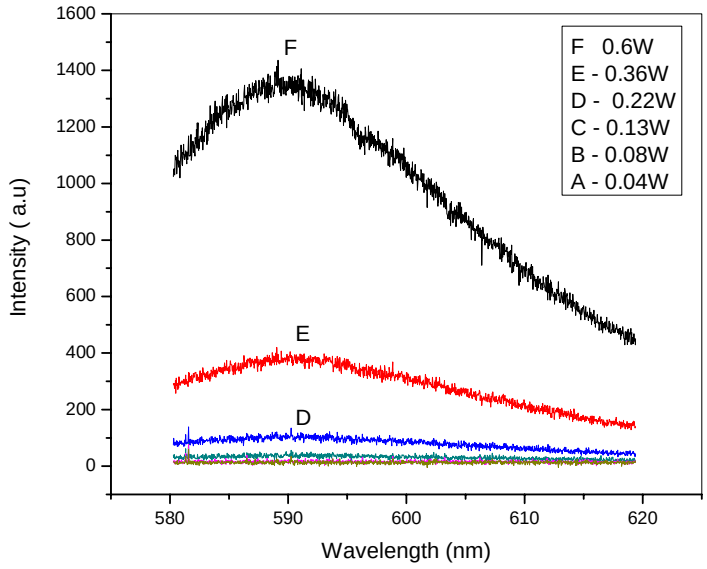

Fig.5.12. Emission spectrum of a 1cm long, 615μm diameter Rhodamine B doped hollow polymer optical fibre for excitation length 2mm

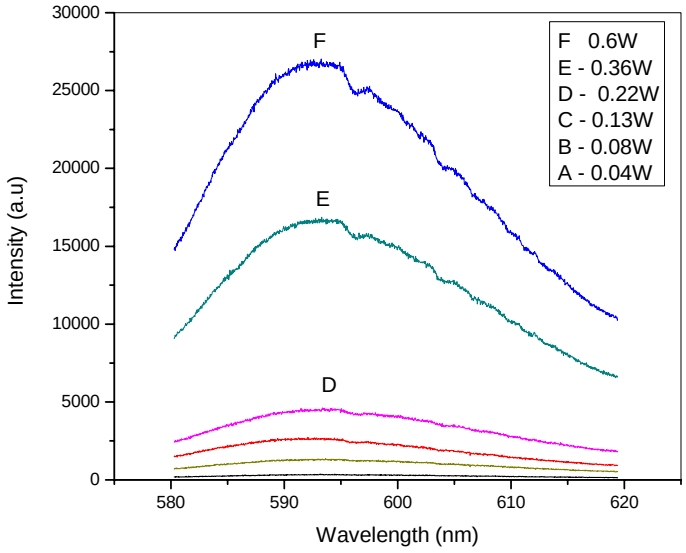

Fig.5.13. Emission spectrum of a 1cm long, 615µm diameter Rhodamine B doped hollow polymer optical fibre for excitation length 4mm

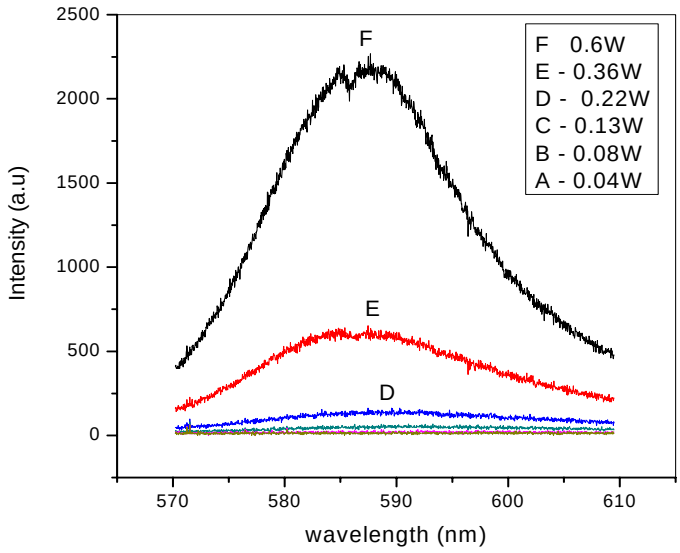

Fig.5.14. Emission spectrum of a 1cm long, 158 µm diameter Rhodamine B doped hollow polymer optical fibre for excitation length 2mm

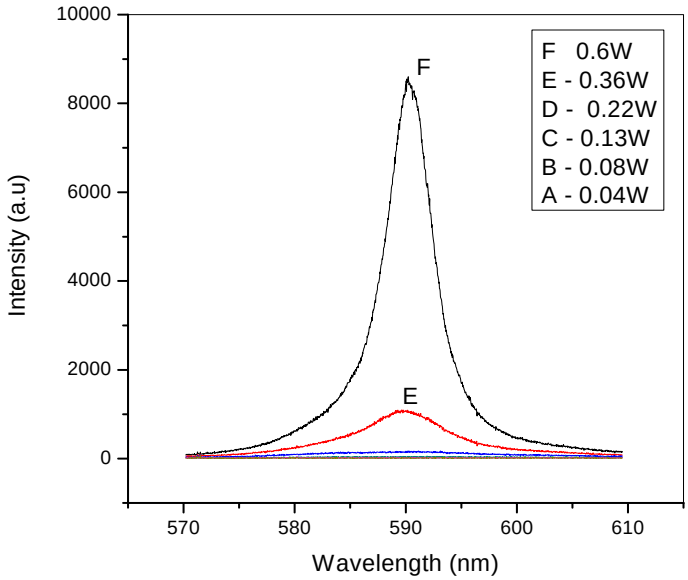

Fig.5.15. Emission spectrum of a 1cm long, 158 μm diameter Rhodamine B doped hollow polymer optical fibre for excitation length 4mm.

For the 158μm fibre as shown in figure 5.14, normal fluorescence was observed for 2mm long excitation. For 4mm excitation length, an ASE was observed at a pump power of 0.6W without any resolved mode structure as evident from figure 5.15. The absence of ASE in the case of 158μm fibre, is attributed to the fact that the width of the focused stripe of light from the cylindrical lens was much larger than the fibre diameter resulting in an inefficient pumping.

The pump power dependence of FWHM of the three fibres is presented in figure 5.16. Almost a linear variation of FWHM with pump power was observed for 615 μm fibre from 35nm to 32nm. In the case of 340μm fibre, FWHM varies from 26nm at the minimum pump power .049 W to 3.6 nm very rapidly and remains almost a constant till the highest pump power 0.6 W. For a 158 μm fibre,

the variation in FWHM is almost linear from 35nm to 9.2nm at a pump power of 0.36W, thereafter it reduces to 4.9nm at 0.6W.

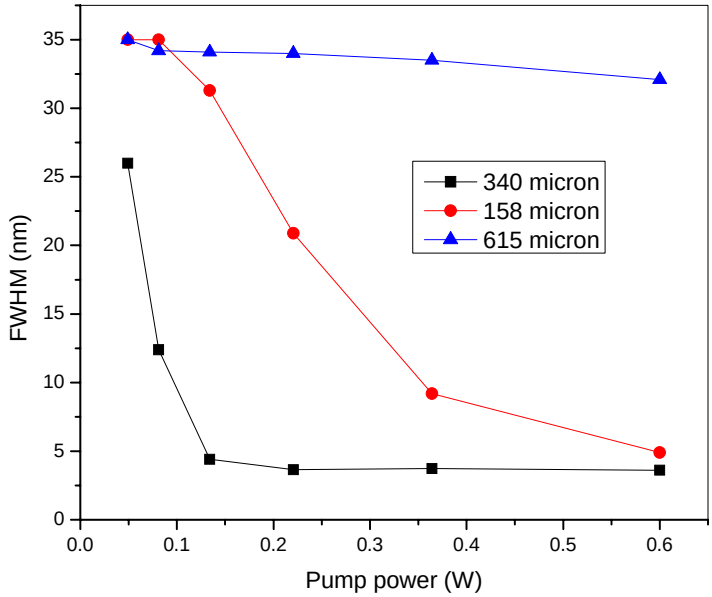

Fig. 5.16. The pump power dependence of FWHM of 340 μm diameter hollow fibre .

The dependence of emission characteristics of the fibre on the pumping scheme was studied by recording the emission using two more pumping methods viz; side illumination [21] and axial pumping [22] for the 340μm fibre. In the case of side illumination fluorescence, the pump laser was focused onto one side of the fibre in a transverse direction using a convex lens and the emission was collected from the other end of the fibre. This was done by just replacing the cylindrical lens by a convex lens in the experimental setup shown in figure 5.7. As seen in the figure 5.17, the optimum pump power was found to be 0.36 W for ASE in a 1 cm long fibre beyond which the intensity reduces considerably.

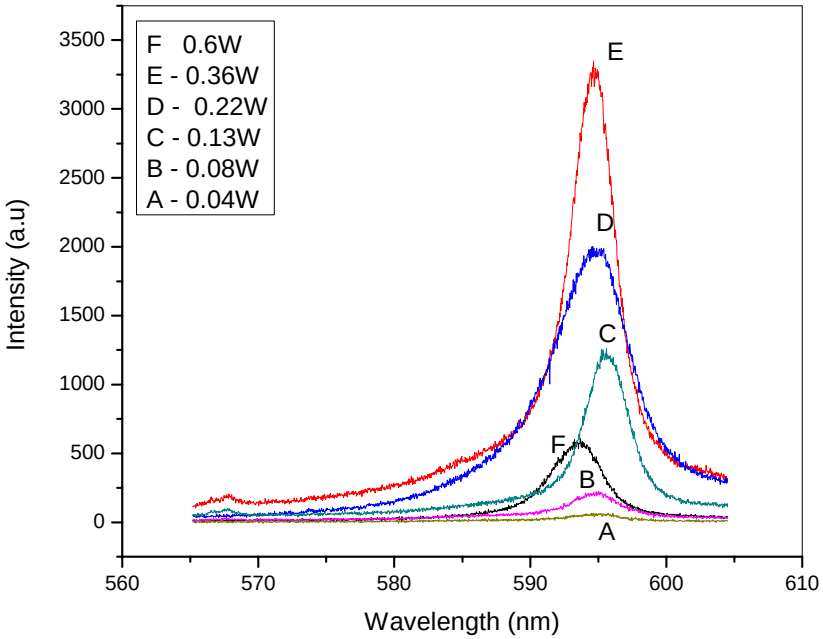

Fig.5.17. Side illumination fluorescence at 2mm away from a 1 cm long fibre end.

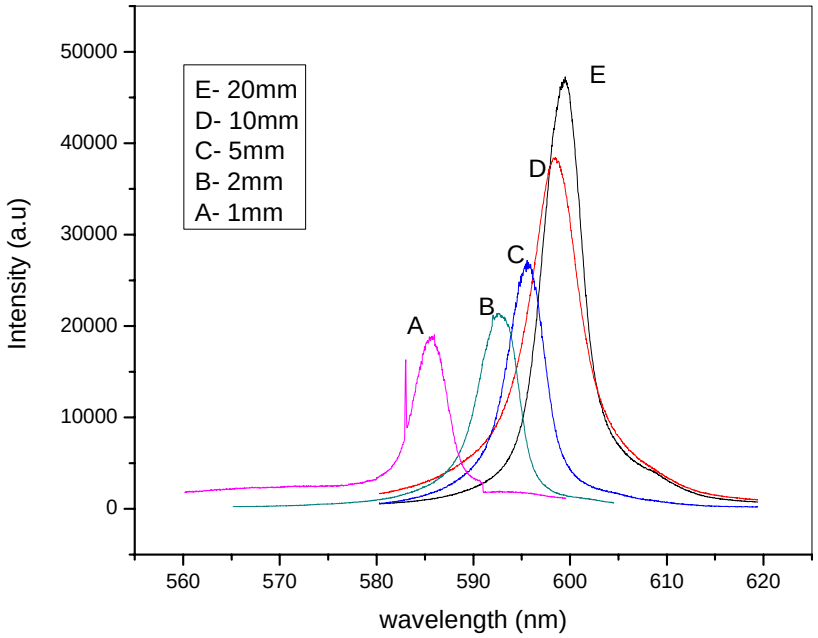

Fig.5.18. Dependence of ASE peak emission on the transmission length of fibre at 0.220W

It was also found that the peak of the ASE shifted continuously by changing the location of the point of illumination. Figure 5.18, shows the recorded ASE from one end of the fibre for excitation at different distances from the collection end for a fixed pump power 0.22 W. An exponential increase in the intensity was observed while changing the distance from 2mm to 20mm.which gives rise to a wavelength tunability of about 14nm.

Figure 5.19 depicts the experimental setup used for the axial pumping of the dye doped hollow fibre. In axial pumping scheme, the laser was directly focused into one end of the 1cm long fibre and fluorescence was collected from the other end. The recorded spectrum as seen in Figure 5.20 indicates that optimum fluorescence and ASE were observed at a pump power of 0.133 W beyond which, the emission intensity decreases considerably showing the degradation of the dye molecules.

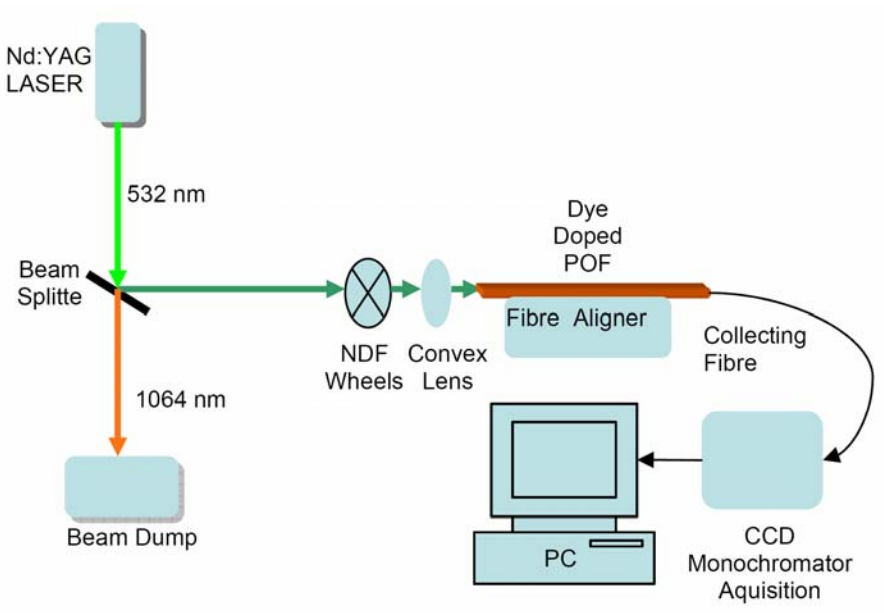

Fig. 5.19. Experimental setup for the axial pumping of the fibre

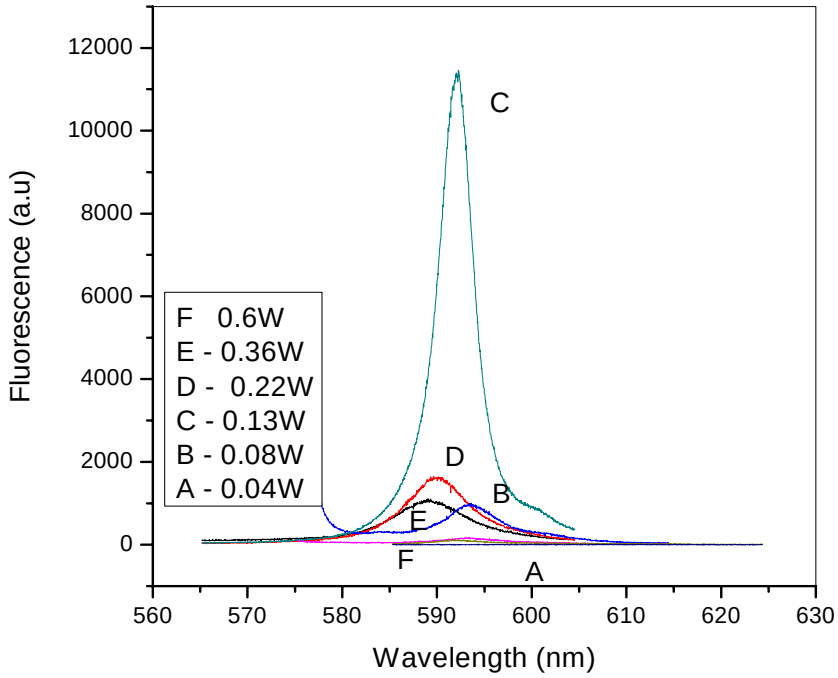

Fig.5.20. Fluorescence by Axial illumination of 1cm long hollow fibre

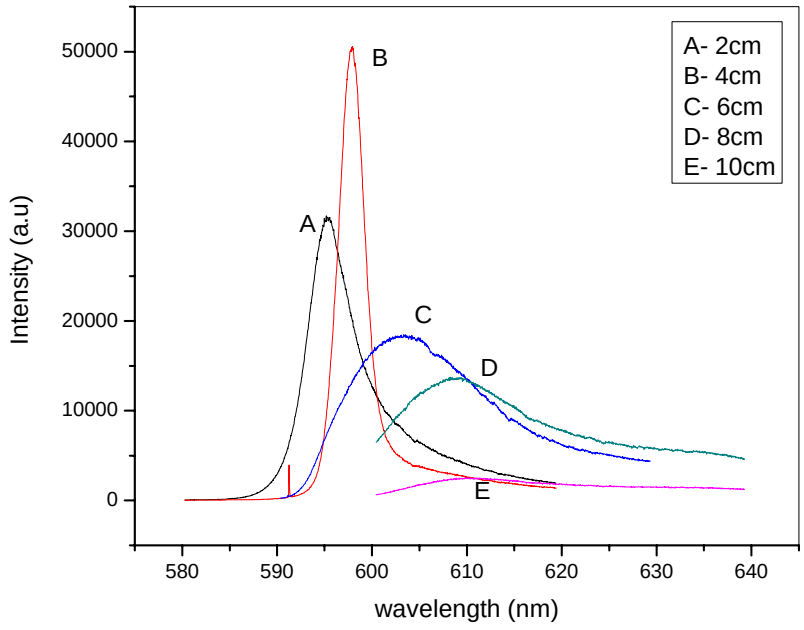

Fig. 5.21. Dependence of ASE peak emission on the transmission length of fibre at 0.220W

For axial pumping scheme, the dependence of fibre length on the emission was also studied by recording the spectrum for fibre of lengths 2cm, 4cm, 6cm, 8cm, and 10cm for a fixed pump power of 0.22W. As seen from figure 5.21, a 4cm long fibre gives optimum ASE for this pump power with an FWHM as small as 3.1 nm, beyond which ASE amplitude decreases. Again the peak wavelength of ASE was also found to be changing with length of the fibre from 595nm for a 2cm fibre to 609 nm for a 10cm fibre. Here light travels a longer distance and the emitted light is reabsorbed by the system resulting in a red shift.

5.5 Conclusions

Amplified spontaneous emission and multimode lasing from a free standing polymer micro ring cavity based on dye doped hollow polymer optical fibre have been observed and the corresponding threshold pump power was determined. Multimode laser emission was observed when 2mm of a 1cm long fibre was excited with a cylindrical lens. Peak of the ASE is found to have a strong dependence on the length of the fibre and pump power. A wavelength tunability of 14nm was obtained for side illumination fluorescence over a length of 2cms whereas for the direct axial illumination, it requires a fibre length of 10cm for achieving the same range of tunability. An FWHM as low as 3.1nm was observed for ASE in the case of axial pumping of a hollow fibre of length 4cm. The lasing threshold may be further reduced and the dye degradation can be prevented by using a smaller diameter fibre with an efficient pumping mechanism.

References

[1] Xiaomei Wang,R.A.Linke,G.Devlin, "*Lasing threshold behavior of microcavities: Observation by polarization and spectroscopic measurements*", Physical Review A,47,R-2488,1993.

[2] Gunnar Bjork, "*Spontaneous-emission coupling factor and mode characteristics of planar dielectric microcavity lasers*", Physical Review A,47,4451,1993.

[3] M.Kuwata.Gonokami, R.H.Jordan, A.Dodabalapur, H.E.Katz, M.L.Schilling, R.E.Slusherand S.Ozawa , "*Polymer microdisk and microring lasers*", Optics Letters,20,2093, 1995.

[4] G.D.Peng,Pak L.Chu,Zhengjun Xiong,Trevor W.Whitbread and Rod P.Chaplin, "*Dye-doped step-index polymer optical fiber for broadband optical amplification*", Journal of Light Wave Technology,14,2215, 1996.

[5] Mitsunori Saito and Kazuto Kitagawa, "*Axial and Radial Fluorescence of Dye-Doped Polymer Fiber*", Journal of Light Wave Technology,19,982, 2001.

[6] M.Rajesh, M.Sheeba, K.Geetha, C.P.G.Vallabhan, P.Radhakrishnan, and V.P.N.Nampoori, "*Fabrication and characterization of dye-doped polymer optical fiber as a light amplifier*",Applied Optics,46,1,2007.

[7] A.Tayaga, Y.Koike, T.Kinoshita, E.Nihei, T.Yamamoto and K.Sasaki, "*Polymer optical fibre amplifier*", Applied Physics Letters,63,883,1993.

[8] A.Tayaga, Y.Koike, E.Nihei,S.Teramoto,K.Fujii,T.Yamamoto and K.Sasaki "*Basic performance of an organic dye-doped polymer optical fiber amplifier* ",Applied Optics,34,988,1995.

[9] S.V.Frolov,M.Shkunov and Z.V.Vardeny, "*Ring microlasers from conducting polymers*",Physical Review B,56,8,1997.

[10] H.Becker,R.H.Friend andT.D.Wilkinson, "*Light emission from wavelength-tunable microcavities*", Appl.Phys.Lett.72,1266,1998.

[11] A.J.Campillo,J.D.Eversole and H.B.Lin, "*Cavity quantum electrodynamic enhancement of stimulated emission in microdroplets*", Phys.Rev. Lett.67, 437,1991.

[12] O.Svelto, Principles of Lasers (Plenum,New York,1989.

[13] Y.Yamamoto, R.Slusher, "*Optical processes in microcavities*",Physics Today 46,66,1993.

[14] J.C.Knight, H.S.T.Driver and G.N.Robertson, "*Morphology-dependent resonances in a cylindrical dye microlaser: mode assignments*," cavity Q

[15] H.P.Weber and R.Ulrich, "*A thin film ring laser*", Applied Physics Letters,19,38,1971.

[16] M.Heiblum and J.H.Harris,IEEE J., "*Analysis of curved optical waveguides by conformal transformation,*" Quantum Electron.QE-11,75,1975.

[17] T.Krauss,P.J.R.Laybourn,J.Roberts, "*CW operation of semiconductor ring lasers*", Electronics Letters,26,25,2095,1990.

[18] M.Kailasnath,T.S.Sreejaya,Rajeshkumar,V.P.N.Nampoori,C.P.G.Vallabhan, P.Radhakrishnan, "*Fluorescence characterization and gain studies on a dye-doped graded index polymer optical-fiber preform*", J.Opt.Las.Tech. 40, 687, 2008.

[19] Paulson.R.C,Levina.G,Vardeny.Z.V, "*Spectral analysis of polymer microring lasers*", Appl.Phys.Lett.76,3858,2000.

[20] S.V.Frolov, Z.V.Vardeny and K.Yoshino, "*Plastic microring lasers on fibers and wires*", Applied Physics Letters,72,1802, 1998.

[21] Kruhlak R.J,Kuzyk M.G, "*Side-illumination fluorescence spectroscopy. I. Principles*", J.Opt.Soc.Am.B,16,1749,1999.

[22] M.Saito and Kazuto Kitagawa, "*Axial and Radial Fluorescence of Dye-Doped Polymer Fiber*", Journal of Light Wave Technology, 19,982,2001.

[23] G.D.Peng, P.L.Chu, X.Lou and R.A. Chaplin, "*Fabrication and characterization of polymer optical fibre*", J. Elec. Electron. Eng. Australia, 15, 289, 1995.

[24] C.K.Sarkar "*Optoelectronics and Fiber Optics Communication*" 2001, New Age International, New Delhi.

[25] R.P. Khare, "*Fiber Optics and Optoelectronics*," 2004, Oxford University Press

[26] John M. Senior "*Optical Fiber Communications*" 2004, Prentice-Hall of India, New Delhi.

……ൠ…..

Chapter- 6

Fabrication and characterization of a liquid filled dye doped hollow polymer optical fibre

Contents

6.1 Introduction

The idea of transmitting light through hollow waveguides has become cutting-edge technology in the form of "Holey Fibres"[1-3]. Such fibres have a regular arrangement of air holes running along their length to act as the cladding, whereas the core is formed by the glitch in the centre of the regular pattern- either a solid region or an additional air hole. It is all really rather clever, with such fibre structures leading to a range of new and interesting properties with a variety of applications [4]. Because of its ability to confine light in hollow cores or with confinement characteristics not possible in conventional optical fibre, photonic crystal fibre (PCF) is now finding applications in optical communications, fibre lasers , nonlinear devices, high power transmission and highly sensitive gas (etc) sensors[5]. It has been shown that single-mode guidance in a relatively large core is possible [6], that non-linear processes can be enhanced by orders of magnitude [7,8], and that guidance in an air core can be achieved when the microstructure is arranged to create a photonic band gap [2].

Later, a new class of polymer optical fibres was also reported [9-13], in which the guiding of light is achieved by the introduction of a pattern of microscopic air holes that run down the entire length of the fibre. This eliminates the need for chemical modifications to the polymer material as is required for many conventional polymer optical fibres. Microstructured polymer optical fibres (MPOFs) offer new opportunities and can significantly enhance the functionality of polymer optical fibres (POFs). Stacking capillaries and drawing it in the form of a fibre is one of the methods of fabrication of polymer holey fibre. Polymer fibres generally are less expensive than silica fibres and often enable applications that would be economically impractical with silica. A range of different materials and fabrication methods can be used to make microctructerd polymer fibre. In addition to the capillary stacking technique, as is traditionally used for glass photonic crystal fibre, polymer preforms can be made using techniques such as extrusion, polymerization in a mould, drilling or injection moulding. With such techniques available, it becomes straight forward to obtain different cross sections in the prefrom, with holes of arbitrary shapes and sizes in any desired arrangement. This is a major advantage over silica-glass based PCF, where the hole structure is mostly restricted to hexagonal or square close packed structures due to commonly used capillary stacking technique.

Solid state dye lasers consisting of an organic dye dissolved in a solid matrix have been the subject of much interest since their demonstration nearly four decades ago [14,15]. Microstructured polymer optical fibre doped with Rhodamine 6G dye has been reported as a fibre laser [16,17]. Hollow optical fibre offers huge potential to the field of fibre-optic chemical and biochemical sensing. The characteristic micron-sized holes that run along the length of MOF can be filled with a fluid, thereby bringing the species to be quantified in contact with the mode field propagating

through the fibre over long lengths. Of particular importance is the ability of MOF to guide whilst being filled with low index materials such as aqueous solutions, which are important for biosensing, and gases. Sensing mechanisms can be based on the modulation of characteristics such as polarization, wavelength, intensity and phase [18]. This chapter deals with the fabrication of a Rhodamine 6G doped poly (methyl methacrylate) (PMMA) based hollow fibre and its fluorescence characterisation when an aqueous solution of the dye Sodium fluorescein filled in it by the technique of side illumination fluorescence [19].

6.2 Experimental

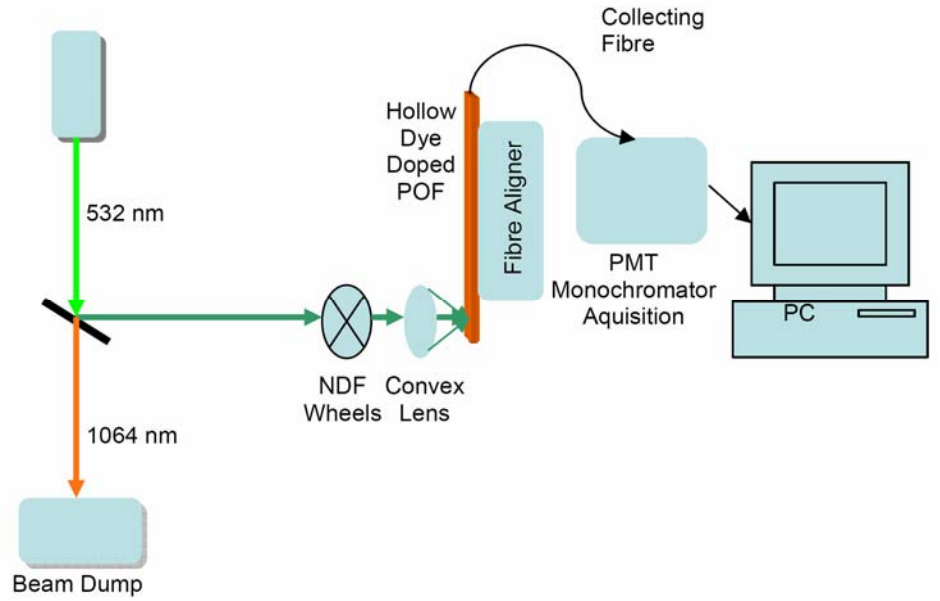

Fig 6.1. Experimental setup for recording the fluorescence from dye solution filled hollow fibre.

The undoped and dye doped hollow polymer optical fibres with outer diameter 450μm and inner diameter 200 μm were used for the present study. The pump beam was focused by a convex lens on the Rhodamine 6G doped

hollow fibre surface as shown in the figure 6.1. The fluorescence was collected using a collection fibre and given to a monochromator-PMT assembly. The Rhodamine 6G doped hollow fibre of length 10cm was filled with aqueous solution of Sodium fluorescein (FDS) (10^{-4} m/l) by making use of a syringe. The fibre was transversely pumped at 488 nm Argon ion laser (20mW) and 532 nm diode pumped slid state (DPSS) laser. The fluorescence spectra from the hollow fibre were recorded by changing the location of the point of excitation on the fibre. The experiment was repeated for a doped hollow fibre filled with an aqueous solution of dye, FDS, undoped hollow fibre filled with aqueous solution of Rhodamine B, undoped hollow fibre filled with aqueous solution of FDS and undoped hollow fibre filled with an aqueous solution of the dye mixture FDS: Rh.6G.

6.3 Results and discussion

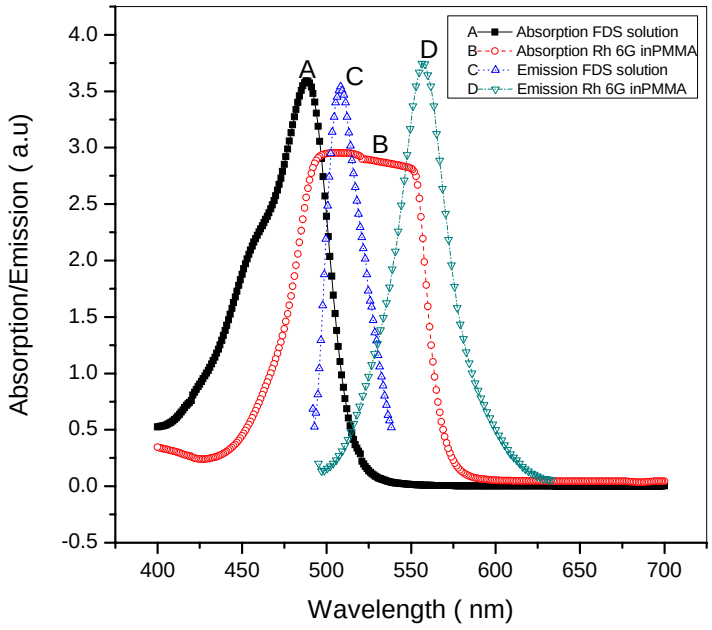

Fig. 6.2. Absorption/emission spectra of Sodium fluorescein in water and Rh 6G in PMMA.

Figure 6.2 shows the absorption spectra of FDS (10^{-4} m/l) in water and Rh 6G (10^{-5} m/l) in PMMA along with their emission. As seen in the spectrum, the absorption of the FDS dye solution extends from 425 nm to 525 nm with absorption maximum occurring around 488 nm. The absorption of Rh 6G doped polymer extends form 450 to 575nm. Therefore Ar ion laser emitting at 488 nm and a DPSS laser emitting at 532 nm were used as the excitation sources. As seen from the figure 6.3, at the excitation wavelength 488nm, there is considerable enhancement in the fluorescence intensity and a noticeable reduction in the FWHM with distance of propagation.

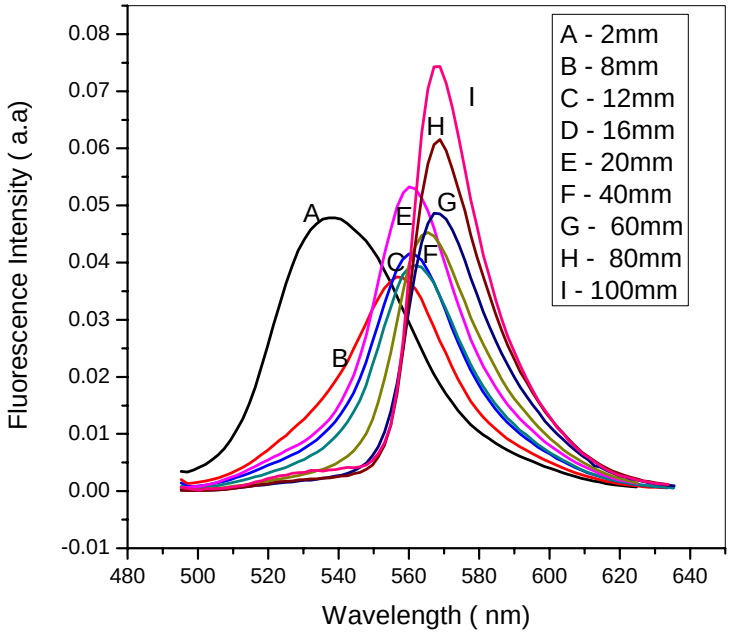

Fig. 6.3. Fluorescence emission from Rh 6G doped hollow fibre collected at different distances from the point of illumination at 488nm excitation

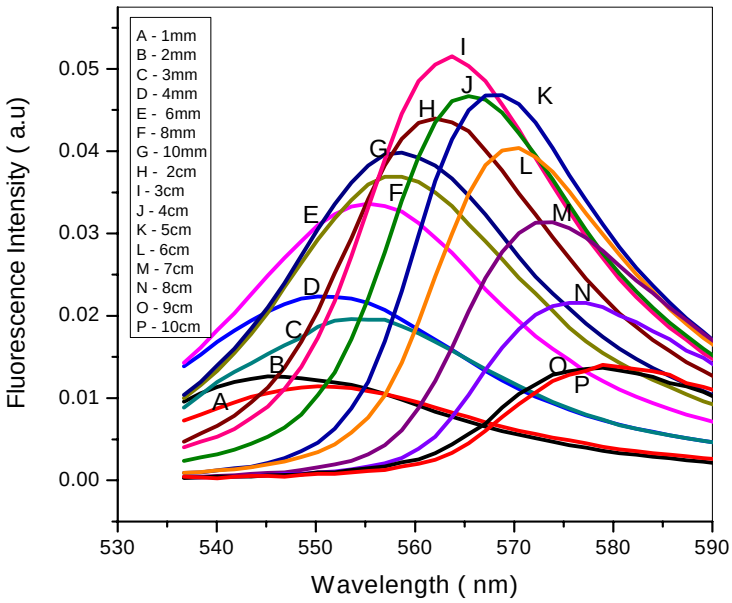

Fig.6.4. Fluorescence emission from Rh 6G doped hollow fibre collected at different distances from the point of illumination at 532 nm excitation.

A figure 6.4 depicts the fluorescence from the fibre for 532 nm excitation. An important difference noticed here is that the emission intensity becomes maximum at a fibre length of about 3cm above which, the fluorescence emission intensity decreases. This result suggests that there is an optimum fibre length for maximum gain with 532 nm excitation. As seen from the figure 6.3, for 488nm excitation this optimum length may be beyond the present 10cm length of the fibre.

In order to investigate the possibility of multi peak emission from the fibre, we filled the Rh 6G doped fibre with FDS solution and repeated the experiment. As depicted in figure 6.5, for fibre lengths up to 3mm, the emission peaks at about 510nm which is dominated by the contribution from the FDS solution. At a length of 4mm, a double peak was observed around 525nm and 565nm corresponding to the emission from dye solution as well as

fibre. Beyond this length, the fibre fluorescence is dominated and at a length of 4cm, emission intensity from the second peak becomes maximum. This result shows that, we can switch the emission wavelength by the appropriate choice of the length of the fibre containing FDS solution.

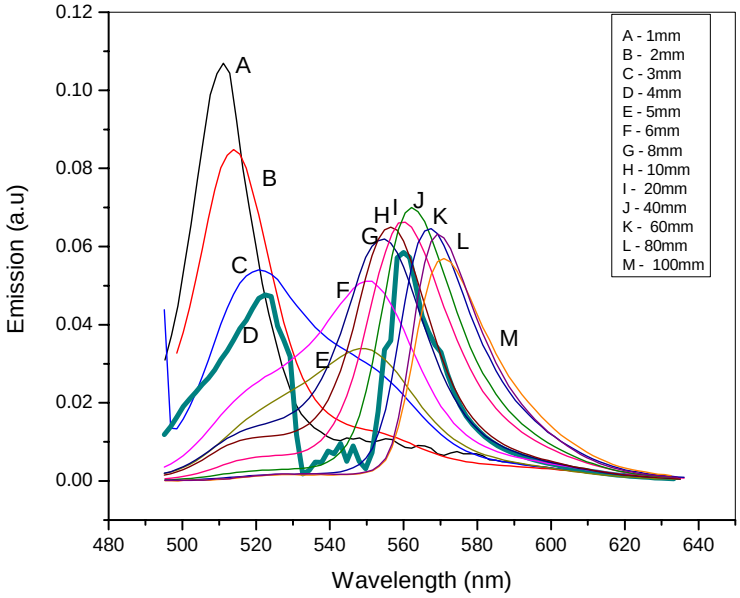

Fig.6.5. Fluorescence emission from the Sodium fluorescein solution filled Rh 6G doped hollow fibre located at different distances from the point of illumination

The fluorescence emission from the undoped hollow fibre was also investigated when it was filled with the aqueous solutions of the dyes. Figures 6.6 show the recorded fluorescence from the undoped hollow fibre filled with the dye solution of FDS for different propagation lengths when excited with 488nm. A considerable enhancement in the emission was noticed as the interaction length varied from 2mm to 5mm with a red shift of about 3nm. Beyond this length, the emission intensity reduces continuosly with a redshift of about 9nm.

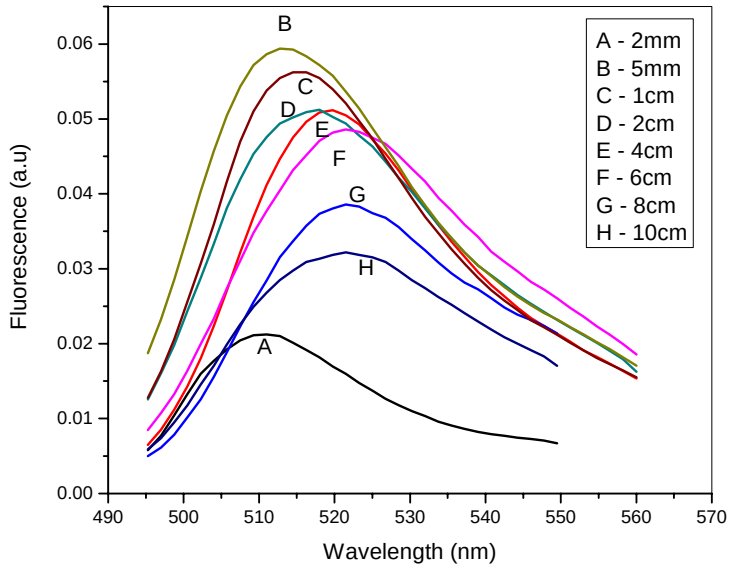

Fig. 6.6. Fluorescence emission from the Sodium fluorescein solution filled undoped hollow fibre with distance from the point of illumination with 488nm excitation.

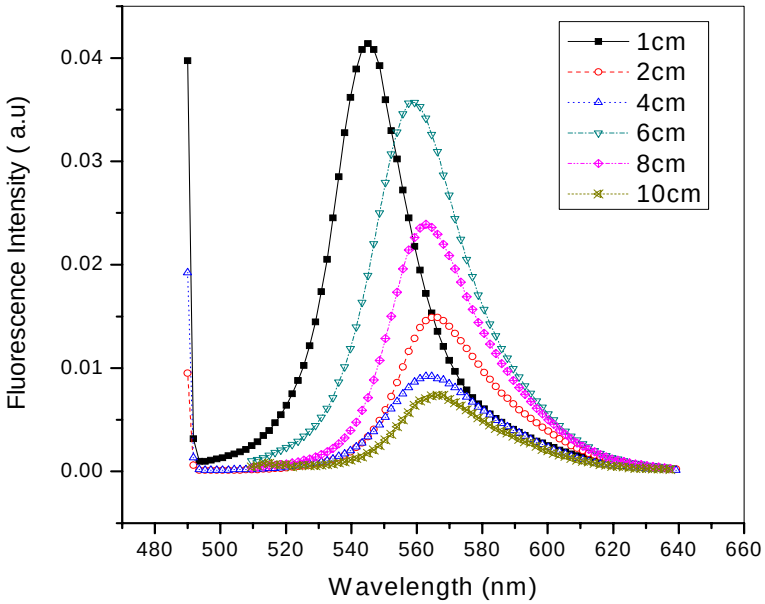

Fig. 6.7. Fluorescence emission from the Rh 6G solution filled undoped hollow fibre with distance from the point of illumination with 488nm excitation.

Figure 6.7 shows the recorded spectrum from an undoped hollow fibre filled with Rhodamine 6G solution at 488nm excitation. The emission intensity in this case decreased with interaction length with a redshift of about 20 nm. This result is attributed to the fact that 488nm is not an efficient wavelength of excitation for Rhodamine 6G whereas, it comes exactly at the absorption maximum of the FDS.

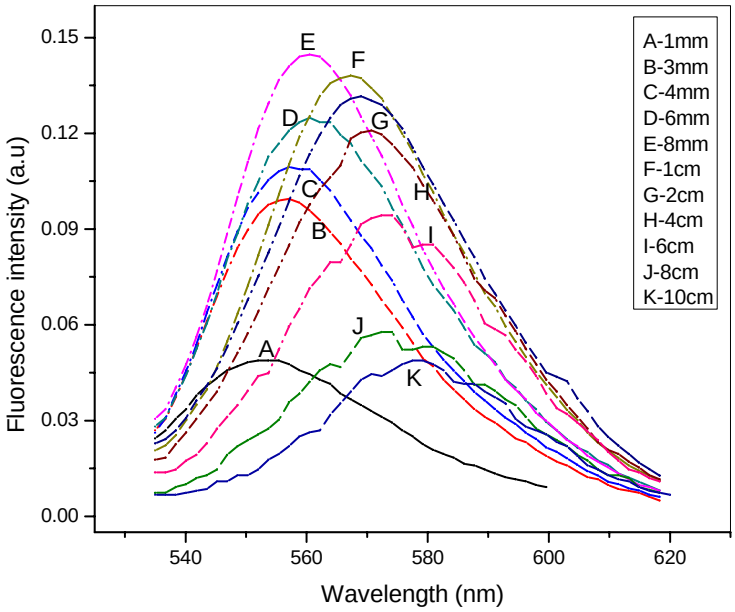

Fig.6.8. Fluorescence emission from the Rh 6G solution filled undoped hollow fibre with distance from the point of illumination with 532nm excitation.

Fluorescence recording of the Rh 6G solution filled undoped fibre was repeated with 532nm excitation. The recorded spectrum is shown in figure 6.8. An increase in intensity up to a length 8mm was noticed with a red shift of 7nm. Beyond this length, a decrease in intensity was observed with a continous redshift of 18nm. As the fluorescence light is guided through the dye solution filled fibre, the effective path length increases resulting in self-absorption and re-emission causing a red shift in the observed spectrum.

An equal-volume mixture of the FDS and Rh 6G dye solutions (10^{-4}m/l) was filled in to an undoped hollow fibre. Figure 6.9 shows the fluorescence obtained from this fibre at a 488nm excitation. It is clear that beyond a length of 1cm both the peaks corresponding to the dyes are distinct. Interestingly no prominent wavelength shifts were noticed even though there is considerable increase in the emission intensity up to 4cm length of the fibre. The light guidance is mainly through the undoped hollow fibre and no re-absorption of the emitted light happens in this case.

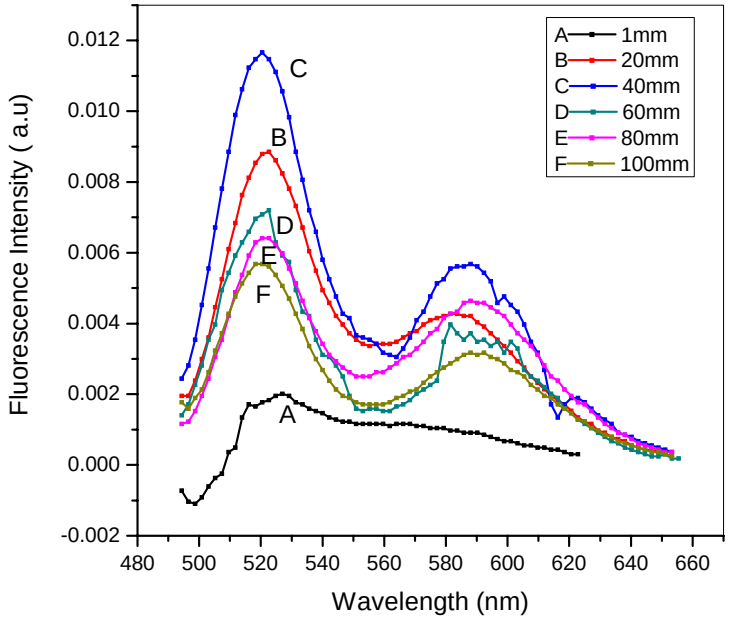

Fig. 6.9. Variation of fluorescence intensity from Rh 6G: Sodium Flurescein mixture solution filled undoped hollow fibre with distance from point of illumination at 488nm excitation

Figure 6.10 shows the tuning characteristics of the dye solution filled dye doped fibre. With 488nm excitation, the 10cm long Rhodamine 6G dye doped hollow fibre filled with FDS dye solution gives rise to a tunability of about 60 nm as compared with the 31 nm for the doped hollow fibre with out FDS dye filling.

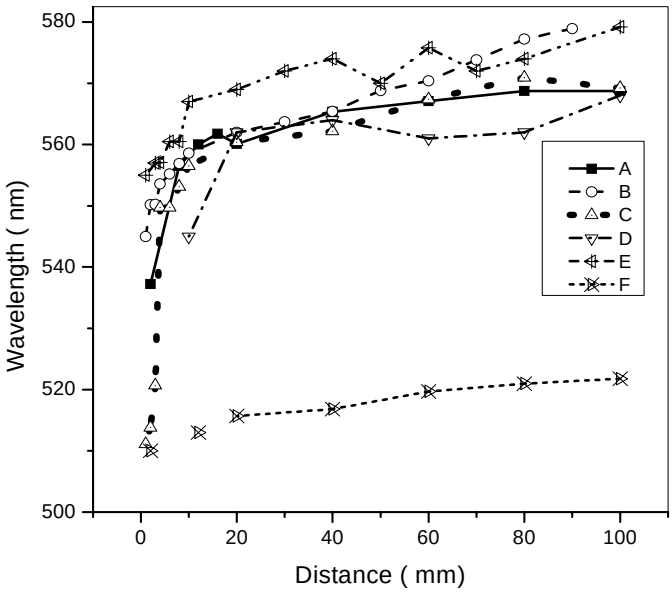

Fig.6.10. Tuning characteristics of 10 cm long fibre, A- Rh 6G doped hollow fibre at 488nm excitation, B- Rh 6G doped hollow fibre at 532nm excitation, C- FDS solution filled Rh 6G dopednhollow fibre at 488nm excitation, D- Rh6G solution filled undoped hollow fibre at 488nm excitation, E- Rh6G solution filled undoped hollow fibre at 532nm excitation, F- FDS solution filled undoped hollow fibre at 488nm excitation

Almost a smooth variation of emission wavelength was observed with a double peak appearing for an excitation at a distance 4mm from the collection end of the fibre. With out the solution, the Rh 6G doped hollow fibre gives a tunability of 34nm when excited with 532nm. Rh 6G solution filled in an undoped hollow fibre gives rise to a tunability of about 23nm for both 488 and 532 nm excitation. The shortest tunability range of 12nm was noticed for the FDS solution filled undoped hollow fibre,

6.4 Conclusions

Any increase in the interaction length of the medium is equivalent to the increase in concentration of the dye molecules, which results in an enhanced gain.

The light transmission capability of the hollow fibre is more than that of the solution filled in it. The value of gain reaches a maximum and beyond a certain length, it was found to decrease. In a dye solution filled dye doped hollow fibre, the emission wavelength can be selected by appropriate choice of the fibre length. Another important observation is that, multi peak emissions are possible by using a dye mixture filled undoped hollow fibre. Maximum tunability can be obtained by using a Rh 6G doped hollow fibre filled with FDS solution. There is a red shift for the propagating light with increase in the propagation distance. The result from the present study on the liquid fibre can be extended to different solvents for the development of a high gain optical medium and tunable optical amplifiers operating in the visible region.

References

[1] Bjarklev, J. Broeng, and A. S. Bjarklev, "*Photonic crystal fibres*" ,Kluwer Academic Publishers, Boston, MA, 2003.

[2] R.F. Cregan, B.J. Mangan, J.C. Knight, T.A. Birks, P.St.J. Russell, P.J. Roberts, D.C. Allan, "*Single mode Photonic band gap guidance of light in air,*" Science 285,1537,1999.

[3] T.M. Monro, W. Belardi, K. Furusawa, J.C. Baggett, N.G.R. Broderick, D.J. Richardson, "*Sensing with microstructured optical fibres*", Meas. Sci. Technol. 12 ,854,2001.

[4] Kyunghwan Oh; Choi, S.; Yongmin Jung; Lee, J.W. "*Novel hollow optical fibres and their applications in photonic devices for optical communications*"Journal of Lightwave Technology, 23, 2, 524, 2005.

[5] http://en.wikipedia.org/wiki/Photonic-crystal_fibre

[6] J.C. Knight, T.A. Birks, R.F. Cregan, P.St.J. Russell, J.-P. de Sandro, "*Large mode area photonic crystal fibre,*" Electron. Lett. 34 ,1347,1999.

[7] T.M. Monro, K.M. Kiang, J.H. Lee, K. Frampton, Z. Yuso, R. Moore, J. Tucknott, D.W. Hewak, H.N. Rutt, D.J. Richardson, "*High nonlinearity extruded single-mode holey optical fibres*", in: Optical Fibre Communications Conference, 2002, PD-FA1.

[8] F. Benabid, J.C. Knight, G. Antonopoulos, P.St.J. Russell, "*Stimulated Raman scattering in hydrogen-filled hollow-core photonic crystal fibre*", Science 298,375,2002.

[9] M.A. van Eijkelenborg, M.C.J. Large, A. Argyros, J. Zagari, S. Manos, N.A. Issa, I. Bassett, S. Fleming, R.C. McPhedran, C.M. de Sterke, N.A.P. Nicorovici, "*Microstructured polymer optical fibre*", Opt. Express 9 ,7, 319, 2001.

[10] Argyros, I.M. Bassett, M.A. van Eijkelenborg, M.C.J. Large, J. Zagari, N.A.P. Nicorovici, R.C. McPhedran, C.M. de Sterke, "*Ring structures in microstructured polymer optical fibres*", Opt. Express 9 ,13,813,2001.

[11] M.C.J. Large, M.A. van Eijkelenborg, A. Argyros, J. Zagari, S. Manos, N.A. Issa, I. Bassett, S. Fleming, R.C. McPhedran, C.M. de Sterke, N.A.P.Nicorovici, "*Microstructured polymer optical fibres: a new approach to POFs*", in: POF 2001 Conference, Amsterdam, The Netherlands, September, 2001, post deadline paper.

[12] M.C.J. Large, M.A. van Eijkelenborg, A. Argyros, J. Zagari, S. Manos, N.A. Issa, I. Bassett, S. Fleming, R.C. McPhedran, C.M. de Sterke, N.A.P. Nicorovici, "*Microstructured polymer optical fibres: progress and promise*", in: Proceedings of SPIE, Vol. 4616, San Jose, CA, January, 2002, paper 33.

[13] M.C.J. Large, M.A. van Eijkelenborg, A. Argyros, J. Zagari, S. Manos, N.A. Issa, I. Bassett, S. Fleming, R.C. McPhedran, C.M. de Sterke, N.A.P. Nicorovici, "*Single-mode microstructured polymer optical fibre*", in: Optical Fibre Communication Conference (OFC '2002), March, 2002, paper ThS.

[14] Akihiro Thayaga, Shigehiro teramoto, Eisuke Nihei, Keisuke Sasaki and Yasuhiro Koike "*High power and high gain organmic dye doped polymer optical fibre amplifiers:novel techniques for preparation and spectral investigation*". Appl Opt 36, 3, 572-578 (1997)

[15] AkihiroThayaga, S.Teramoto, T.Yamamoto, K.Fujii, E.Nihei, Y.Koike and K.Sasaki "*Theoretical anmd experimental investigation of Rhodamine B doped polymer optical fibre amplifiers*" IEEE journal of Quantum Electron 32, 2215,1995.

[16] Alexander Argyros, Martijn A. van Eijkelenborg, Stuart D. Jackson, and Richard P. Mildren , "*Microstructured polymer fibre laser*" , Optics Letters, Vol. 29, Issue 16, pp. 1882-1884 doi:10.1364/OL.29.001882

[17] Kang Li; Xinghua Yang; Lili Wang; Wei Zhao, "*Dye-doped Microstructured Polymer Optical Fibre Laser with High Numerical Aperture Air-clad, Lasers and Electro-Optics*," 2007.CLEO2007. Conference on Volume , Issue , 6-11 May 2007 Page(s):1 – 2

[18] F. M. Cox, A. Argyros, M. C. J. Large, "*Liquid-filled hollow core microstructured polymer optical fibre*", OPTICS EXPRESS,14,9, 4135,2006.

[19] R.Kruhlak and M.Kuzik "*Side illumination fluorescence Spectroscopy*" J Opt Soc Am B**,**16, 1749,1999.

[20] Akihiro Tayaga, Yasuhiro Koike, Eisuke Nihei, Shigehiro Teramoto, Kazuhito Fujii, "*Tsuyoshi Yamamoto and Keisuke Sasaki Applied Optics,*" 34, 988,1995.

[21] M.G.Kuzyk, U.C.Paek and C.W.Dirk Appl. Phys.Lett, 59, 902,1991.

[22] G.D.Peng, P.L.Chu, X.Lou and R.A. Chaplin, J. Elec.Electron. Eng. Australia, 15, 289 ,1995.

[23] S. Huntington, J. Katsifolis, B.C. Gibson, J. Canning, K. Lyytikainen, J. Zagari, L.W. Cahill, J.D. Love, "*Retaining and Characterising nanostructure within tapered air-silica structured optical fibres*", Opt. Express 11,2,98.2003.

[24] J. DiGiovanni, R.S. Windeler, "*Article comprising an air-clad optical fibre*", US Patent 5,907,652; G02B 006/20 (1998 filed 1997); based on previous patent: E.A.J. Marcatili, "*Air clad optical fibre waveguide,*" US patent 3,712,705 ,1973.

[25] M. Aslund, J. Canning, "*Air-clad fibres for astronomical instrumentation: focal-ratio degradation*", Exp. Astronomy, 24, 1-7, 2009.

[26] J. Canning, "*Fresnel Optics Inside Optical Fibres,*" in Photonics Research Developments, Chapter 5, Nova Science Publishers, United States, (2008) and refs therein

[27] J. Canning, E. Buckley, K. Lyytikainen, T. Ryan, "*Wavelength Dependent Leakage in a Fresnel-Based Air-Silica Structured Optical Fibre*", Opt. Comm. 205 (1-3), 95,2002.

[28] P. St. J. Russell, "*Photonic crystal fibres," Science* 299, 358,2003. (Review article.)

[29] P. St. J. Russell, "*Photonic crystal fibres*", *J. Lightwave. Technol.*, 24 (12), 4729, 2006. (Review article.)

[30] F. Zolla, G. Renversez, A. Nicolet, B. Kuhlmey, S. Guenneau, D. Felbacq, "*Foundations of Photonic Crystal Fibres*" (Imperial College Press, London, 2005). ISBN 1-86094-507-4.

[31] Burak Temelkuran, Shandon D. Hart, Gilles Benoit, John D. Joannopoulos, and Yoel Fink, "*Wavelength-scalable hollow optical fibres with large photonic bandgaps for CO2 laser transmission*", *Nature* 420, 650,2002.

[32] J. C. Knight, J. Broeng, T. A. Birks and P. St. J. Russell, "*Photonic band gap guidance in optical fibres*," Science 282, 1476,1998.

[33] J. C. Knight, T. A. Birks, P. St. J. Russell and D. M. Atkin, "*All-silica single-mode fibre with photonic crystal cladding*," *Opt. Lett.* 21, 1547-1549 (1996). Erratum, *ibid* 22, 484,1997.

[34] R. F. Cregan, B. J. Mangan, J. C. Knight, T. A. Birks, P. St.J. Russell, P. J. Roberts, and D. C. Allan, "*Single-mode photonic band gap guidance of light in air*," Science, 285, no. 5433, 1537, Sep. 1999.

[35] P. J. Roberts, F. Couny, H. Sabert, B. J. Mangan, D. P. Williams, L. Farr, M. W. Mason, A. Tomlinson, T. A. Birks, J. C. Knight, and P. St.J. Russell, "*Ultimate low loss of hollow-core photonic crystal fibres*," Opt. Express, vol. 13, no. 1, pp. 236–244, 2005.

[36] P. Yeh, A. Yariv, and E. Marom, "*Theory of Bragg fibre*," J. Opt. Soc. Am. 68, 1196,1978.

[37] Martijn A. van Eijkelenborg, Maryanne C. J. Large, Alexander Argyros, Joseph Zagari, Steven Manos, Nader A. Issa, Ian Bassett, Simon Fleming, Ross C. McPhedran, C. Martijn de Sterke and Nicolae A.P. Nicorovici, "*Microstructured polymer optical fibre*", Optics Express Vol. 9, No. 7, 319, 2001.

[38] J. M. Dudley, G. Genty, S. Coen, "*Supercontinuum Generation in Photonic Crystal Fibre*," Reviews of Modern Physics 78, 1135,2006..

……ଌ…..

Chapter- 7

Light amplification in a dye doped Graded index polymer optical fibre

Contents

7.1 Introduction

As a key element for the development of all optical subscriber systems, studies on graded index (GI) polymer optical fibre (POF) are of great interest. The bandwidth of the GI POF is about 400 times larger than that of any conventional step index (SI) POF's, which will cover the band widths of any attractive high speed multimedia inside the customer premises [1]. Laser dyes are highly efficient media either for laser source with narrow pulse width and wide tunable range or for optical amplifier with high gain, high power conversion and broad spectral width. Polymers like PMMA have higher efficiency, better beam quality and superior homogeneity[2]. Doping an organic dye into polymer matrix provides an opportunity to produce active elements for solid state amplifiers and lasers[3]. In solid state dye gain medium with geometry of an optical fibre, the pump power can be used in a most efficient way because it is well confined in the core area and propagates diffraction free. Therefore, it is

expected that the pump power requirement can be substantially relaxed because of possible long interaction length and small core cross section. The reduced pump power is significant in practical applications, and especially in optimising the lifetime of the solid state gain media [4].

Light amplification and spectral narrowing are studied in various systems both in liquid and solid forms, where the spectral line width is reduced to a value less than10nm [5]. Spectral narrowing in most of the systems is explained in terms of amplified spontaneous emission (ASE), where the spontaneously emitted light is amplified by the gain medium as it propagates along the path of the maximum optical gain[6] . The excitation of dye lasers through energy transfer processes provides one of the means of extending the lasing wavelength region. The probability of such an energy transfer is large if the emission spectrum of the donor strongly overlaps with the absorption spectrum of the acceptor. The extended tunability of laser emission from the Rh 6G: Rh B dye mixture system from a step index (SI) polymer optical fibre has been reported [7]. This chapter details the ASE and lasing from an axially pumped graded index (GI) poly (methyl methacrylate) (PMMA) optical fibre doped with a mixture of Rh 6G and Rh B dyes. The effect of pump power and fibre length on the laser emission was also investigated.

7.2 Experimental

The dye doped graded index polymer optical fibre preforms were prepared by the well-known interfacial gel polymerization technique [8]. To obtain, any particular refractive index profile along the radial direction of a fibre core, a preform with the desired profile can be employed. The refractive index profiles of the GI rods were measured by the method explained in section 1.4.4 [9]. Various optical fibres were heat drawn from

step index and graded index preforms of known refractive index profiles (from Chapter 4) at 180^{o}C. For the present study, six fibre samples of approximately equal diameter and 10^{-4}m/l dye concentration were prepared viz; Rh 6G doped SI(470μm), Rh 6G doped GI(465μm), Rh B doped SI(464μm), Rh B doped GI(461μm), Rh 6G:RhB mixture doped SI (462 μm) and Rh 6G:RhB mixture doped GI (453 μm). The effect of length of the dye doped fibre on ASE and laser emission is studied using different lengths of the fibre, namely 2,4,6,8 and 10cm.

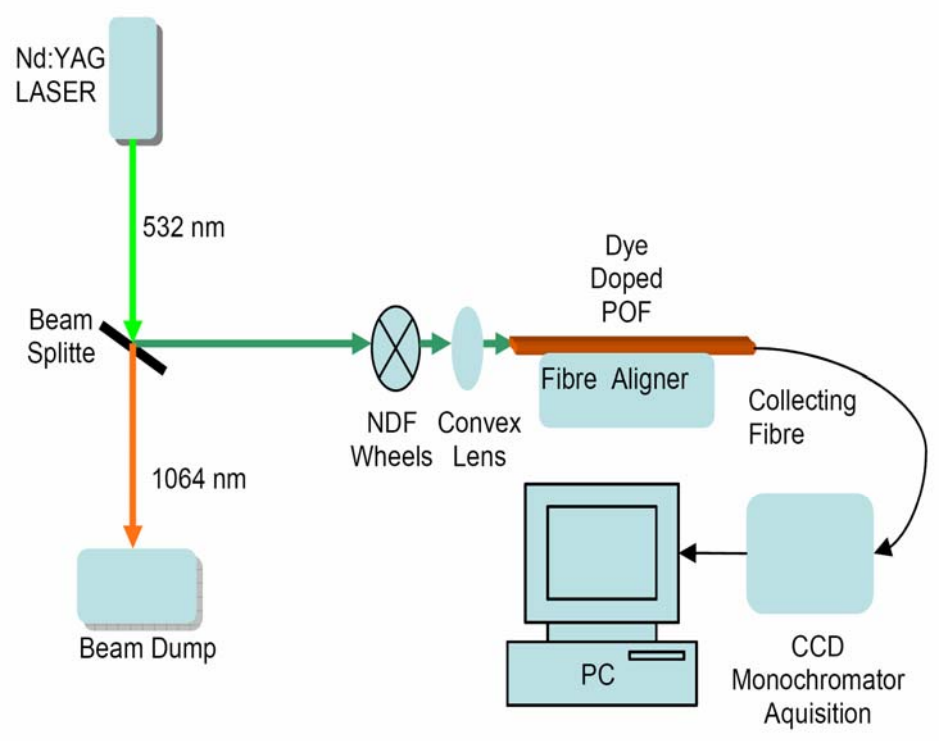

Fig.7.1. Experimental setup for the axial pumping of the fibre

A schematic diagram of the experimental setup for the ASE and laser emission studies from the dye doped step index /graded index fibre is shown in figure 7.1. The dye doped fibre is mounted on an optical fibre aligner. The fibre is axially pumped using 10ns pulses from a frequency doubled Nd:YAG laser (532nm, 10Hz). The pump energy is varied using a calibrated neutral density filter and the beam was focused at the tip of the fibre using a microscope objective.The emission is collected from the other end of the dye doped fibre using a collecting optical fibre coupled to a monochromator-CCD system (Acton Spectrapro) having a resolution of 0.03 nm.

7.3 Results and discussion

Figures 7.2a and 7.2b shows the recorded fluorescence emission spectra from a Rh 6G doped step index fibre and graded index fibres when excited using the 532nm Nd:YAG laser at various average pump powers ranging from 0.049 to 0.6W. There is a noticeable enhancement in the ASE and corresponding reduction in the FWHM for the GI fibres in comparison with SI fibre. In the case of Rh.6G doped fibre of length 2cm, FWHM varies from 41nm at 0.049W to 10nm at 0.6W of pump power. Figure 7.2b shows that for Rh 6G doped GI fibre, the threshold pump power for the onset of ASE is reduced to a value of 0.364W from 0.6W applicable to the step index fibre. Minimum FWHM achieved for the GI fibre was 5nm at 0.6W of pump power. As seen in figure 7.3, the effect of spectral narrowing and a reduction in the threshold pump power is more predominant for the Rh.B doped fibre where ASE begins at a still lower pump power of 0.22W.The FWHM for the SI fibre in this case varies from 33 to 11.2nm and from 26 to 3.6 nm for the GI fibre.

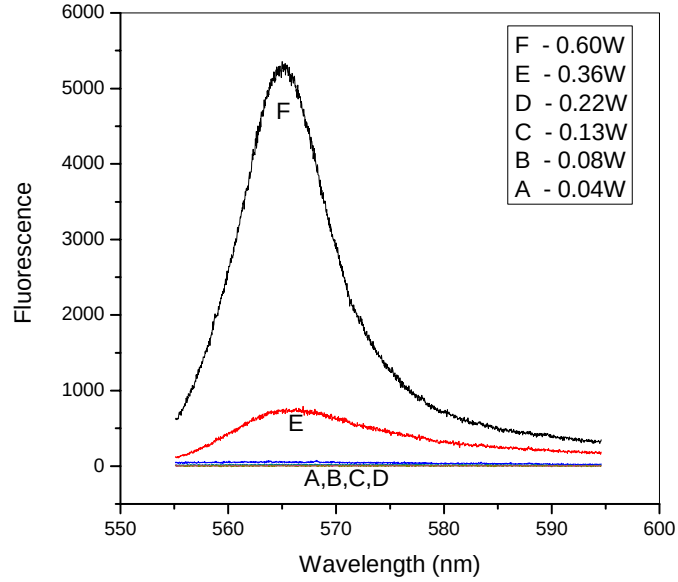

(a)

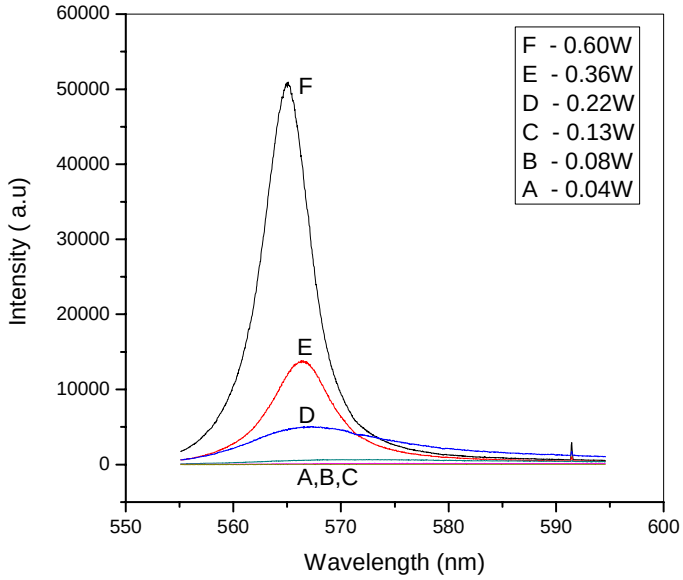

(b)

Fig. 7.2a and 7.2b show the typical fluorescence emission spectra from a 2cm long Rh 6G doped step index fibre and graded index fibre for different pump powers

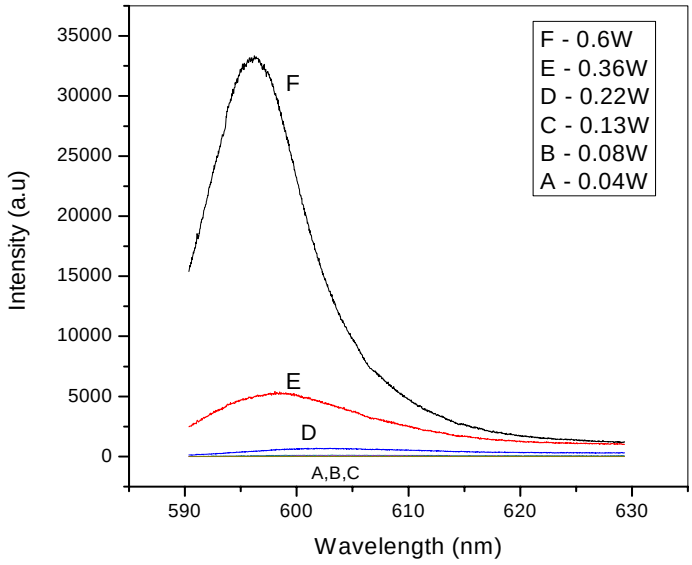

(a)

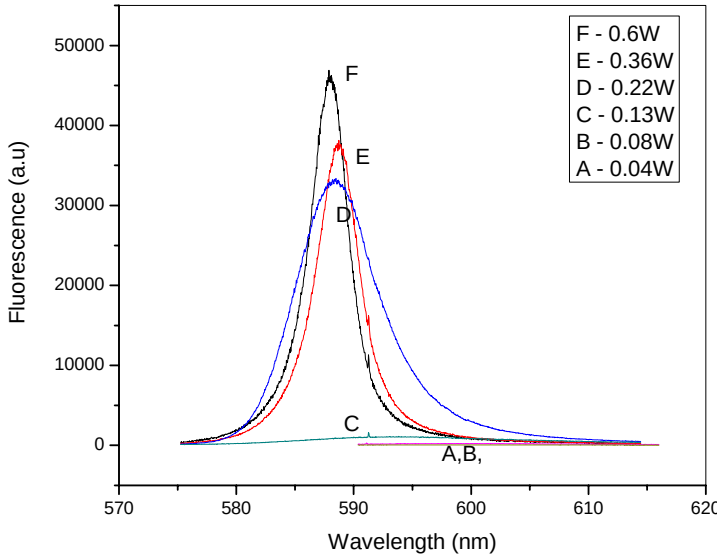

(b)

Fig.7.3a and 7.3b ASE spectra from a 2cm long Rh B doped step index fibre and graded index fibre for different pump powers

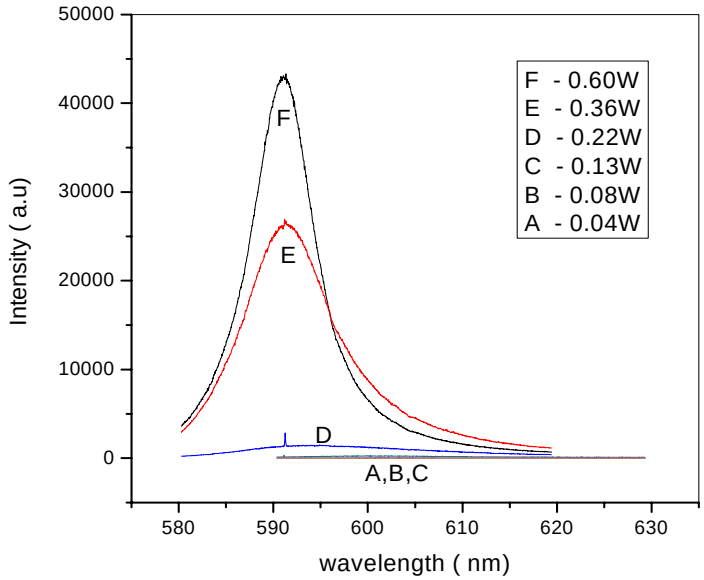

(a)

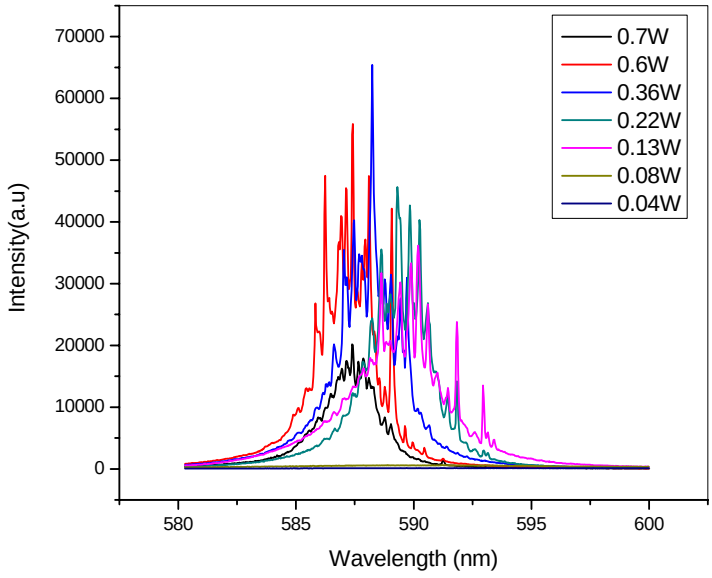

(b)

Fig 7.4a and 7.4b. ASE spectra from a 2cm long Rh6G:Rh B mixture doped step index and graded index fibre for different pump powers.

Figure 7.4a shows the emission characteristics of 2cm long Rh 6G:Rh.B mixture doped SI fibre. Unlike the other fibres, the onset of ASE in this case starts at lower pump power for SI fibre and the FWHM varies from 25.6 to 7.8nm.Some of the light emitted by the fibre is guided along the length of the fibre. This guided spontaneous emission can be amplified by stimulated emission before being emitted from the edge of the fibre. Light wavelengths at the peak of the gain spectrum will be amplified more than other light, leading to a spectrally narrowed emission [10]. In the case of dye mixture doped GI fibre (figure 7.4b), with the same input conditions, normal fluorescence was observed upto a pump power of 0.08W. As the pump power is increased further to 0.13W, a multi mode emission is observed without any sign of ASE. At still high pump powers, more and more modes in the blue region of the spectrum were found to be excited and well resolved. As the pump power is increased beyond 0.6 W, a decrease in the lasing intensity was observed with mode structure disappearing. The peak wavelengths observed were found to have a separation of 0.135nm or its multiples. This observation is in close agreement with the value calculated by considering the optical feedback from the cylindrical surface of the fibre with diameter 453μm. In a dye doped graded index fibre, the effective area of cross section is less and the dye density is larger at the interacting region. Light concentrated along the axis results in an enhanced excitation rate and corresponding gain. This leads to enhanced line narrowing and the appearance of mode structure in the spectrum. Spectra observed for different pump powers shown in the figure 4b are separated and given as figures 7.5-7.10. As the pump power increased, more and more modes in the blue side of the spectrum get excited.

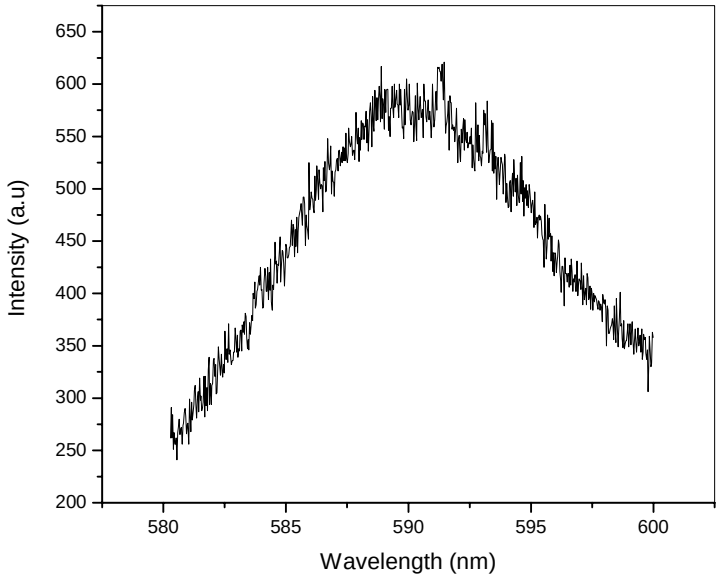

Fig. 7.5. Fluorescence from 2cm GI fibre doped with dye mixture at a pump power 0.04 W

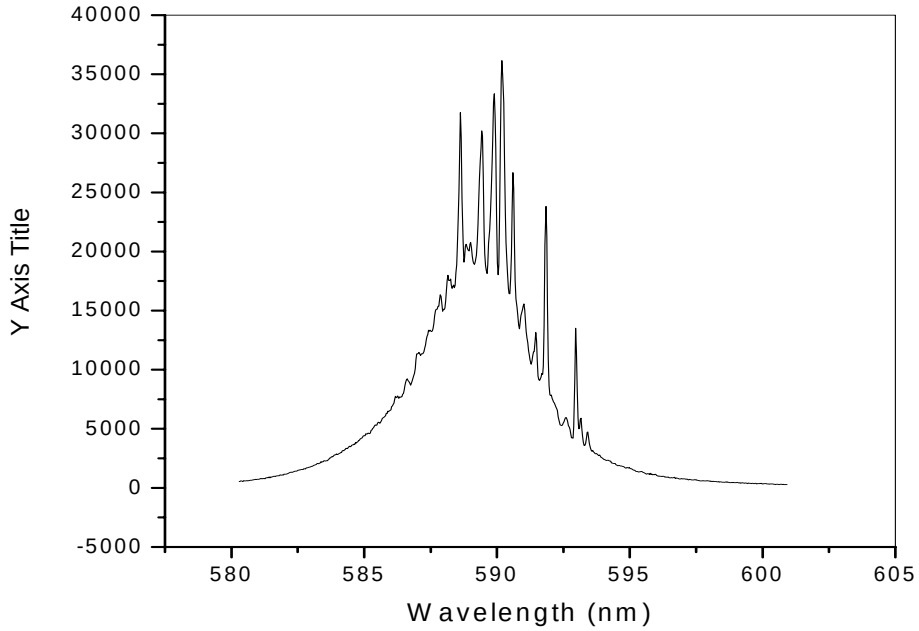

Fig. 7.6. Multimode emission from 2cm GI fibre doped with dye mixture at a pump power 0.08 W

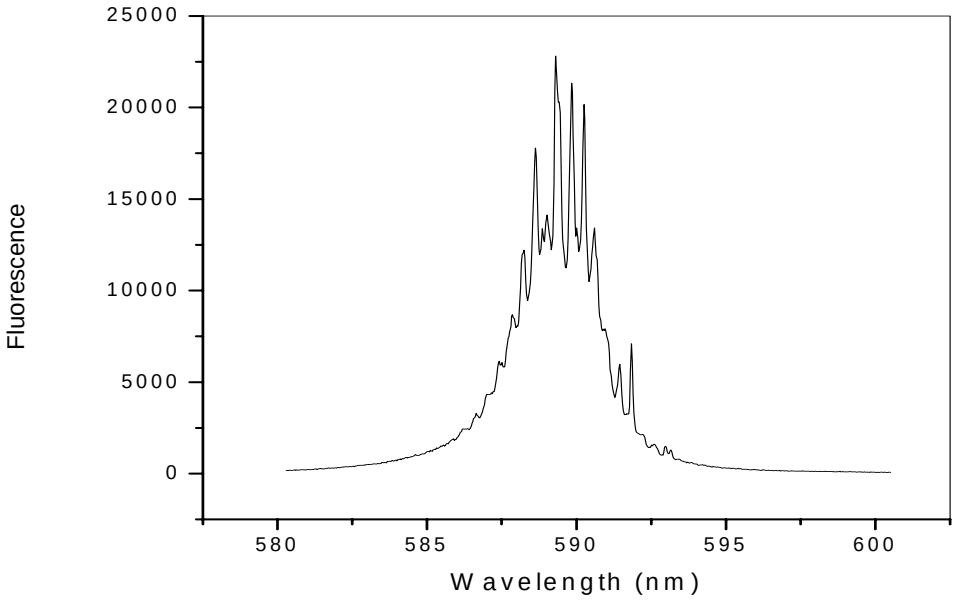

Fig. 7.7. Multimode emission from 2cm GI fibre doped with dye mixture at a pump power 0.13 W

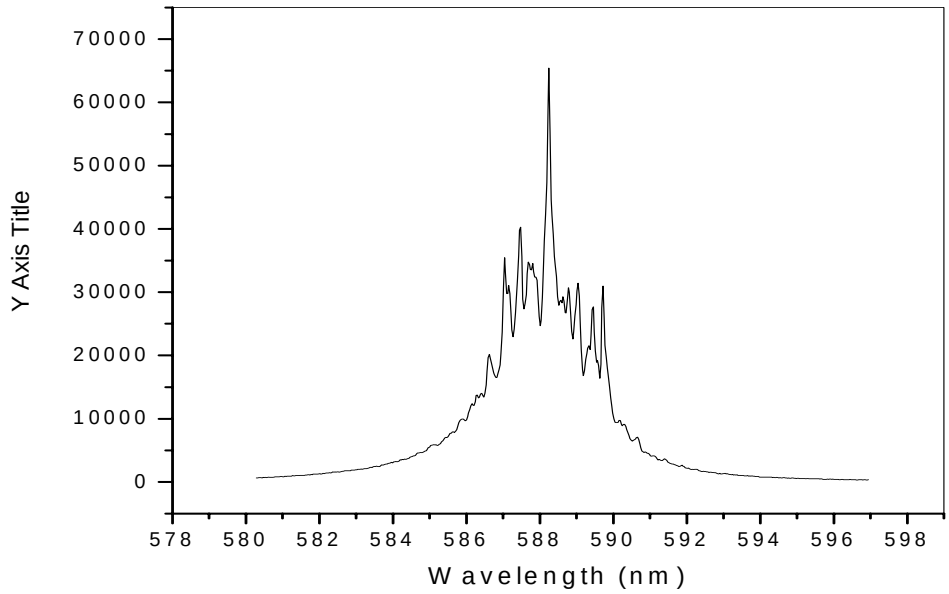

Fig.7.8. Multimode emission from 2cm GI fibre doped with dye mixture at a pump power 0.36 W

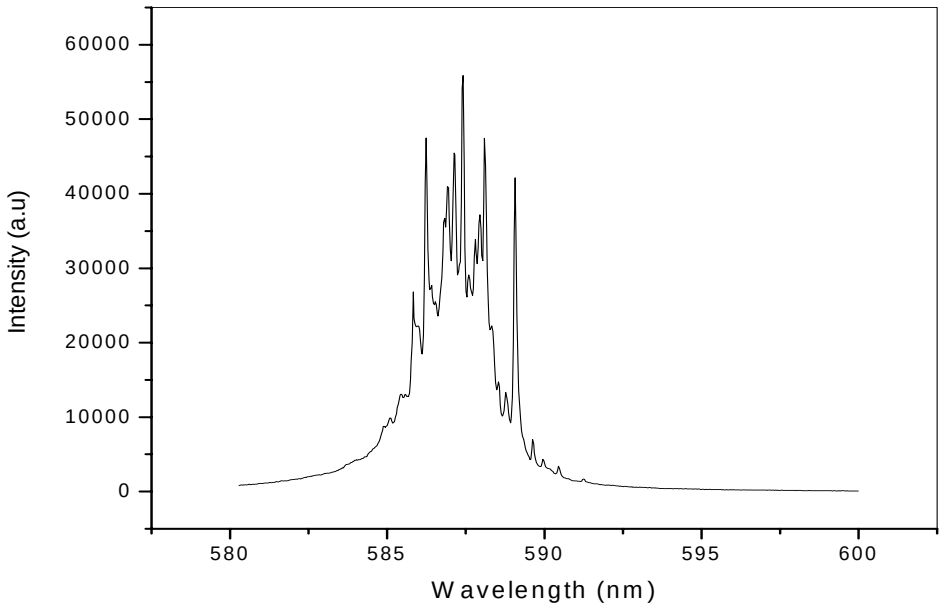

Fig.7.9. Multimode emission from 2cm GI fibre doped with dye mixture at a pump power 0.6 W

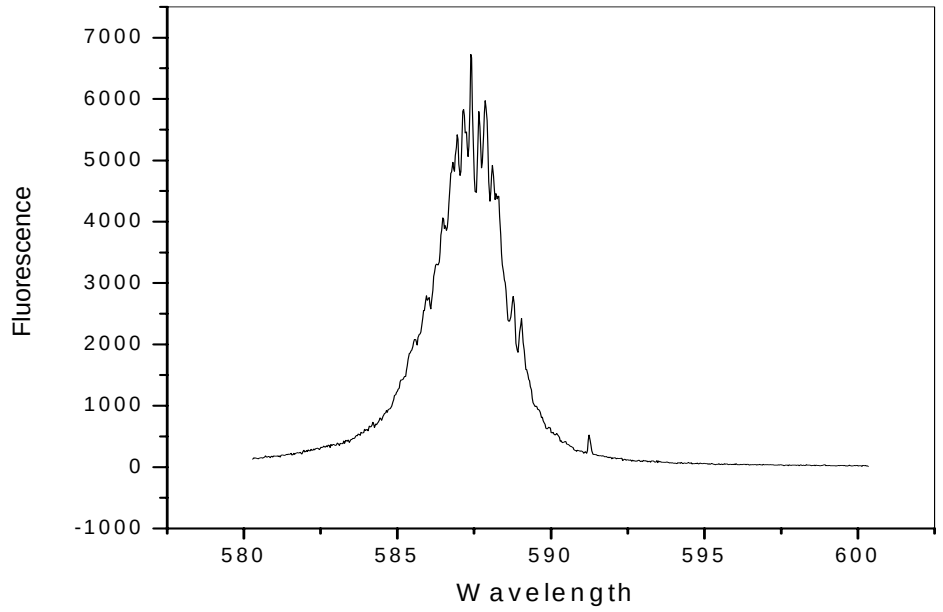

Fig.7.10. Multimode emission from 2cm GI fibre doped with dye mixture at a pump power 0.7 W.

The effect of self absorption is minimized in a dye mixture doped system where the donor emission is absorbed by acceptor and is uniformly distributed throughout the entire length of the fibre. If the fibre is doped with single dye, the emission occurs at one end of the fibre and the emitted light amplitude will exponentially decrease along the length of the fibre. But in a dye mixture doped system, the emission and absorption happens in a larger volume giving rise to a larger effective physical dimension of the emitting region. This explains the enhanced gain and appearance of mode structure in the dye mixture doped polymer fibre.

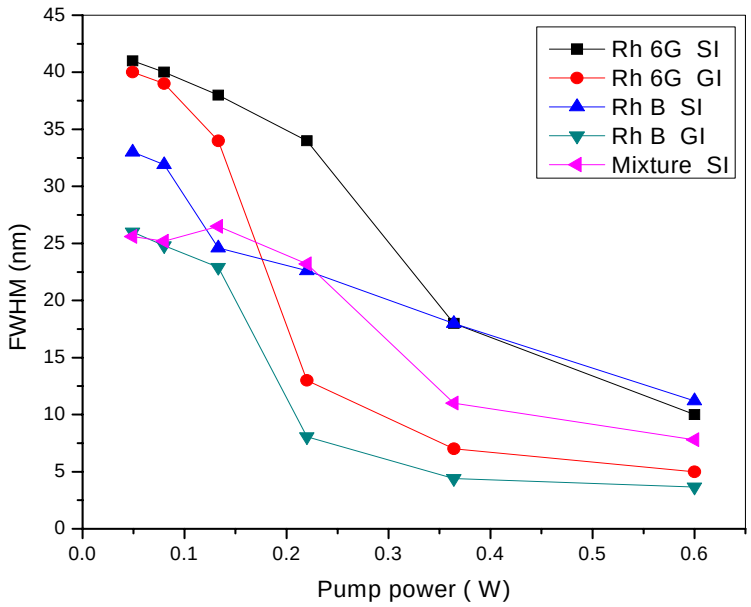

Fig. 7.11. Variataion of FWHM for SI and GI fibres (fibre length 2cm).

Results shown in figure 7.11 exhibits the enhanced reduction in FWHM in the GI fibre compared to the SI fibre. In the case of Rhodamine 6G GI fibre,the FWHM varied from a value of 40nm at 0.04W to 5nm at 0.6W compared to 41nm to 10nm at the corresponding power levels for SI fibre. In the case of Rh.B doped graded index fibre,FWHM reduced from a value of

28nm to 3.6nm whereas for the SI fibre the reduction was from 33nm to 11nm. In the case of dye mixture doped SI fibre, FWHM varied from 25nm to 7.8nm. This result again shows the effect of graded index structure of the fibre on the FWHM and amplified spontaneous emission. In the presence of effective energy transfer, the gain of the dye mixture system is enhanced by a factor,

$$(K_F + K_R)\sigma_e^A \frac{F_D}{1-F_D} \frac{N_A}{K_F N_A + K_D} \alpha_D N_A$$

as explained by equation (1.11) in chapter 1.

As seen from the figures 7.12 and 7.13, the effect of spectral narrowing is exhibited by longer fibres also. A 4cm long dye mixture doped GI fibre shows enhanced spectral narrowing compared to the dye mixture doped SI fibre of the same length. This behavior was confirmed by recording the spectrum of all the 6 samples at various lengths viz, 2cm,4cm,6cm,8cm and 10cm.In all the cases, the FWHM was found to be smaller for GI fibres.

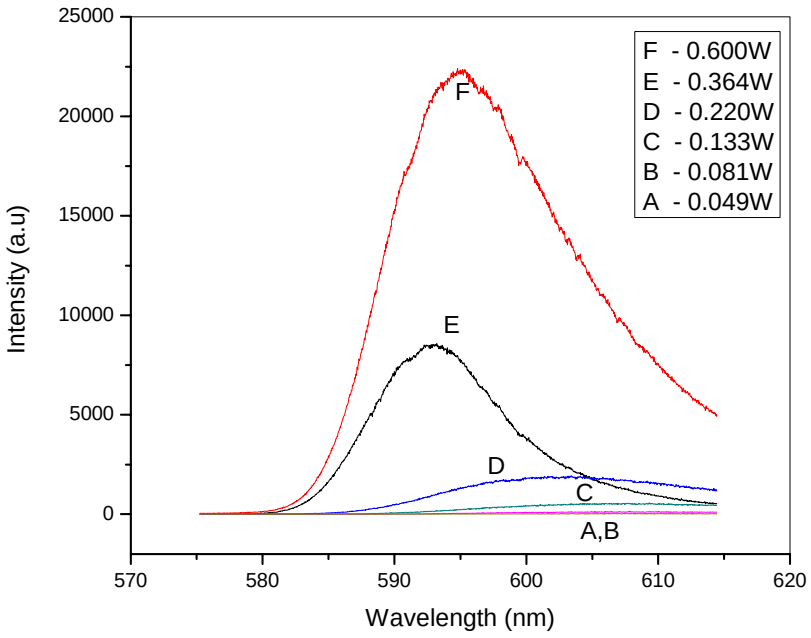

Fig.7.12. ASE from a 4cm long dye mixture doped SI fibre

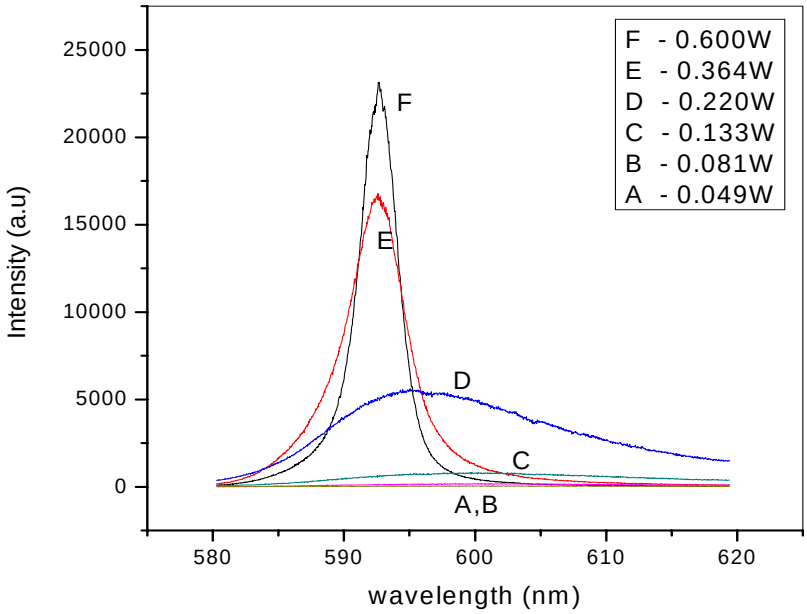

Fig.7.13. ASE from a 4cm long dye mixture doped GI fibre

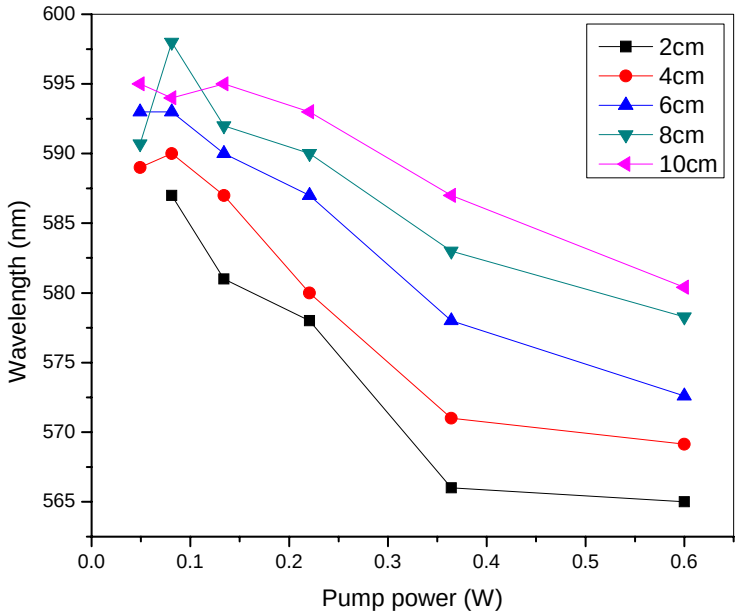

Fig.7. 14 (a)

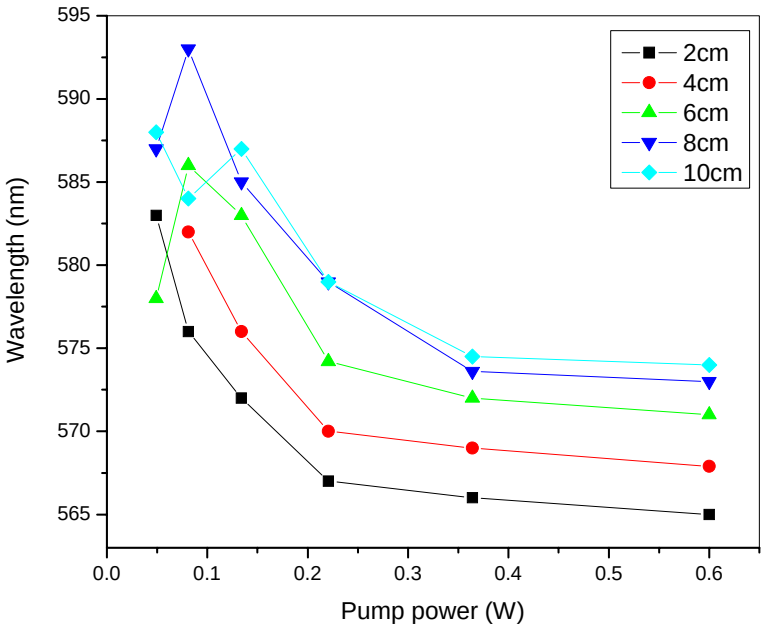

Fig.7. 14 (b)

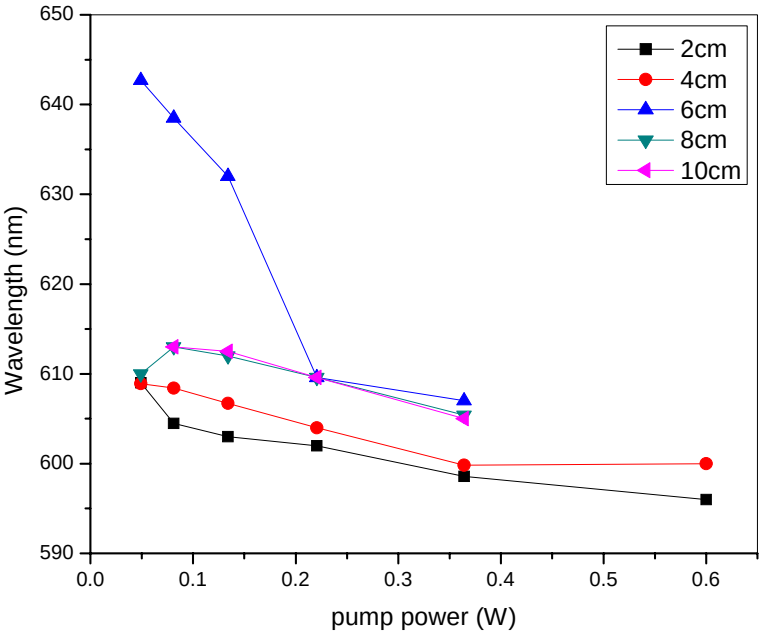

Fig.7. 14 (c)

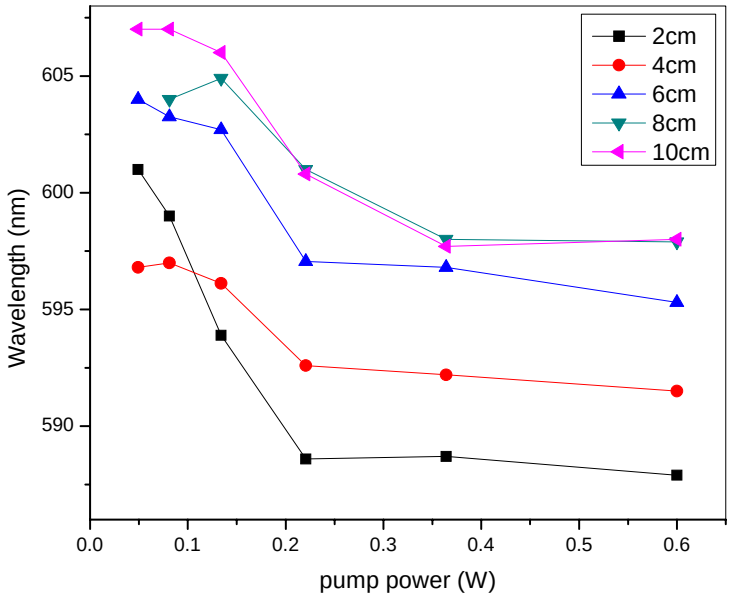

Fig.7. 14 (d)

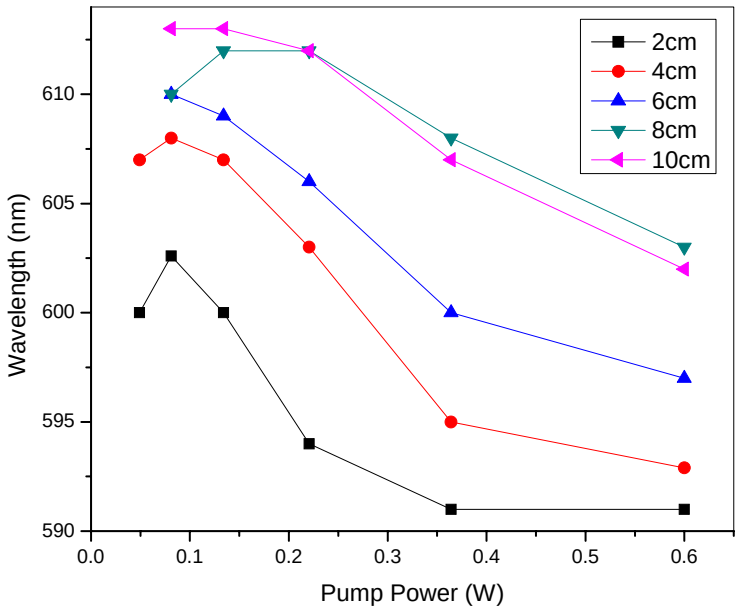

Fig.7. 14 (e)

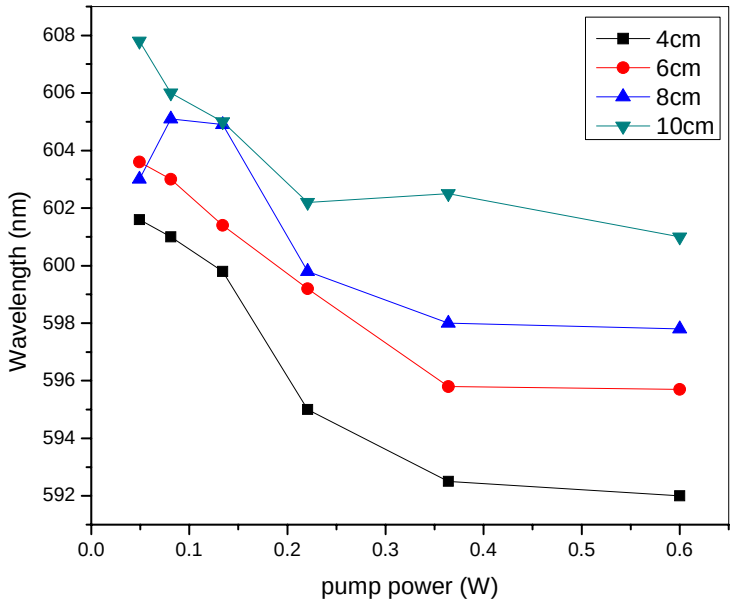

Fig.7. 14 (f)

Fig.7. 14 (a) to (f) shows the variation of peak emission wavelength with pump power for fibres of length 2,4,6,8and 10cm fibre for (a) Rh 6G SI, (b) Rh 6G GI,(c) Rh B SI,(d) Rh B GI, (e) Rh6G:RhB mixture SI and (f) Rh6G:RhB mixture GI fibres

There is a strong dependence of the peak emission wavelength on pump power. At all the fibre lengths, the peak emission wavelength is blue shifted with an increase in pump power. As seen from figure 7.14, maximum blue shift in the emission peak was observed for a fibre length of 2cm. At the minimum pump power, the peak emission from a Rh 6G doped SI fibre is at 584nm. At the highest pump power of 0.6W, this is blue shifted by 19nm to 565nm. A similar blue shift of 18nm was observed for Rh 6G doped GI fibres of length 2cm. In the case of 2cm long RhB doped SI and GI fibres the emission was blue shifted by about 14nm to 596nm and 588nm respectively. The 2cm long dye mixture doped SI fibre shows a blue shift of about 9nm whereas for the 2cm long GI fibre , the modes structure appears. The blue shift in the emission

peak of the dye mixture system can be explained in terms of the existence of additional band in the spectrum corresponding to deexcitation from a higher vibronic level. As the pump power is increased, the radiative transition probability gets enhanced at shorter wavelength side of the spectrum by energy transfer from mode at low energy side to high energy side creating an apparent shift in the spectrum towards the blue side.

In a single dye system, an increase in the concentration leads to reabsorption of the emitted light and reduction in the quantum efficiency. The shift in the peak emission wavelength will be towards the redside of the spectrum. In a dye mixture system the due to the overlap between the donor emission and acceptor absorption, the quantum efficiency of the acceptor gets enhanced. The emission from the acceptor in this case is arising from two factors: (1) direct excitation of the acceptor and (2) energy transfer from the donor. In the mixture, the populations of the upper laser level in the Rh 6G and Rh B molecules are given by the rate equataions:

$$\dot{N}_{u,6G} = \alpha_{6G} I_p N_{o,6G} - I_p N_{u,6G} \sigma_{6G} - N_{u,6G} A_{sp.6G} \quad \text{.....(7.1)}$$

$$\dot{N}_{u,B} = \alpha_B I_p N_{o,B} + E_{6G,B} I_p N_{o,B} - I_p N_{u,B} \sigma_B - N_{u,B} A_{sp.B} \quad \text{.....(7.2)}$$

where α is the absorption coefficient and I_p is the pump power. At low pump powers the spontaneous emission term A_{sp} dominates and normal fluorescence is observed. As the pump power increases the stimulated emission cross section term σ takes over and a faster depletion of the upper laser level occurs. The second term in equation 7.2 is the energy transfer term which contributes additional number of upper level atoms in Rh B molecules in the mixture giving rise to laser emission of Rh B at the peak wavelength. Here $E_{6G,B} = KN_{u,6G}$ where K is the energy transfer rate constant. The striking change in the operation of graded index

fibre around the lasing threshold can be explained by considering the many 'photon modes' into which the light may be emitted[11].Below threshold, there may be ~10^6 to 10^{10} spectral and spatial modes in to which light may be emitted. That is it may be emitted into a wide range of different spatial directions and wavelengths. In comparison with a dye doped step index fibre, a graded index fibre, which has a smaller core diameter, effectively reduces the number of modes by confining the gain medium as well as maximum field into a small region near the core centre. As the pump excitation power increases, the probability of finding a photon in any one or some of these modes at a given time rises and lasing occurs.

7.4 Conclusions

Multimode laser emission was observed from graded index dye mixture doped polymer optical fibre. Mixing of two dyes considerably reduces the threshold for lasing. In comparison with dye doped step index fibres, graded index fibres show enhanced line narrowing and amplified spontaneous emission. The emission peak wavelengths coincide with the modes corresponding to the feedback from the outer diameter of the fibre. Confinement of the gain medium (dye) into a small region inside the fibre core, leads to a non uniform distribution of optical power among different modes in the spectrum for different pump powers. The laser emission is dominated by the RhB emission wavelengths due to the effective energy transfer mechanism from Rh 6G to Rh B. The laser emission is found to be broad band in nature. As the pump power increased, more and more modes in the blue side of the spectrum get excited.

Reference

[1] Y.Koike, T.Ishigure, and E.Nihei, "*High-bandwidth graded-index polymer optical fibre,*" IEEE J.Lightwave. Technol., 13,1475 ,1995.

[2] K.Geetha, M.Rajesh, V.P.N.Nampoori, C.P.G.Vallabhan and P. Radhakrishnan, "*Laser emission from transversely pumped dye-doped free-standing polymer film*", J.Opt.A:Pure Appl.Opt.8,189,2006.

[3] Akihiro Tayaga, , Shigehiro Teramoto, Eisuke Nihei, Keisuke Sasaki and Yasuhiro Koike, "*High-power and high-gain organic dye-doped polymer optical fibre amplifiers: novel techniques for preparation and spectral investigation*", Applied Optics, 36, 572 ,1997.

[4] G.D.Peng,Pak L.Chu,Zhengjun Xiong,Trevor W.Whitbread and Rod P.Chaplin, "*Dye-doped step-index polymer optical fibre for broadband optical amplification*", Journal of Light Wave Technology,14,2215, 1996.

[5] RittyJ.Nedumpara,K.Geetha,V.J.Dann,C.P.G.Vallabhan,V.P.N.Nampoori and P.Radhakrishanan,"*Light amplification in dye doped polymer films*", J.Opt.A:Pure Appl.Opt.9,174, 2007.

[6] Walter K. "*Solid State Laser Engineering*" (Berlin Springer) pp 182-5

[7] M.Sheeba,,K.J.Thomas,M.Raresh, V.P.N.Nampoori, C.P.G.Vallabhan and P. Radhakrishnan, "*Multimode laser emission from dye doped polymer optical fibre*", Applied Optics,46,33,2007.

[8] Koike Y,Ishigure.T, Nihei E., "*High-bandwidth graded-index polymer optical fibre,*" J.Light Technol ,13:1475,1995.

[9] M.Kailasnath,Sreejaya,Rajesh Kumar,,P. Radhakrishnan, V.P.N.Nampoori, C.P.G.Vallabhan, "*Fluorescence characterization and gain studies on a dye-doped graded index polymer optical-fibre preform*", J.Opt.Las.Tech. 40 ,687,2008.

[10] I.D.W.Samuel, G.A.Turnbull. "*Organic semiconductor lasers*", Chem.Rev., 107,1272,2007.

[11] Siegman,A.E. "*Lasers*", University Science Books,Sausalito,CA,1986.

[12] P.Halley, "*Fibre Optic Systems,*" Wiley, NewYork,1987.

[13] R.Olshansky and D.B Keck, "*Pulse broadening in graded-index optical fibres*", Appl.Opt.15,483, 1976.

[14] D.Gloge and E.A.J.Marcatili, "*Bell System Tech.J.*" 52,1563 ,1973.

[15] T.Ishigure,E.Nihei, and Y.Koike, "*Optimum refractive-index profile of the graded-index polymer optical fibre, toward gigabit data links*", Appl. Opt.35,2048,1996.

[16] T.Ishigure,M.Satoh,O.Takanashi,E.Nihei,T.nyu,S.Yamazaki and Y.Koike, J. Lightwave Technol. "*Formation of the Refractive Index Profile in the Graded Index Polymer Optical Fibre for Gigabit Data Transmission*", 15,2095 ,1997.

[17] Y.Koike,E.Nihei, *U.S.Patent* 5,382,488,1995.

[18] Y.Koike *US Patent* 5,541,247,1996.

[19] C.K.Sarkar "*Optoelectronics and Fibre Optics Communication*" 2001, New Age International, New Delhi.

[20] John M. Senior "*Optical Fibre Communications*" 2004, Prentice-Hall of India, New Delhi.

[21] Y.Koike,Y.Takezawa and Y.Ohtsuka, "*New interfacial-gel copolymerization technique for steric GRIN polymer optical waveguides and lens arrays*", Appl.Opt.27,486 ,1988.

[22] Y.Koike, N.Tanio, E.Nihei and Y.Ohtsuka, "*Gradient-index polymer materials and their optical devices*", Polym.Eng. Sci. 29,1200 ,1989.

[23] Y.Koike, "*High-bandwidth graded-index* polymer *optical fibre*" Polymer 32,1737 ,1991.

[24] Y.Koike and E.Nihei, *U.S.Patent* 5,253,323, 1993.

[25] T.Ishigure,E.Nihei, and Y.Koike, "*Graded-index polymer optical fibre for high-speed data communication*", Appl.Opt.33,4261,1994.

[26] Y.Koike, T.Ishigure and E.Nihei, J.Lightwave Technol. "*High-bandwidth graded-index polymer optical fibre,*"13, 1475 ,1995.

[27] T.Ishigure,A.Horibe,E.Nihei and Y.Koike, "*High-bandwidth, high-numerical aperture graded-index polymer optical fibre*" J.Lightwave Technol.13, 1686, 1995.

……ൠ…..

Chapter- **8**
Summary and Conclusions

Dye mixture doped polymer rods were fabricated and their fluorescence emission characteristics were studied. The variation in the lifetime of the donor molecules in the presence of acceptor was also studied. Acceptor concentration dependence of the energy transfer, the blue shift in the donor molecules and the variations in the donor lifetime clearly show that the radiative energy transfer process is having a major contribution in the present ETDL system. The mechanism of energy transfer and peak emission wavelength depends on the excitation wavelength and acceptor concentration. Many of the fabricated rods emit at two peak wavelengths simultaneously when excited with 445nm, 465nm and 488nm.

Using the interfacial gel polymerization technique, dye doped graded index polymer rods were fabricated and their refractive index profiles were measured. Maximum doping level of the dye was found to be along the axis of the rods. Dye doped polymer rods with an inner hole were also fabricated. A compact polymer optical fibre drawing machine was fabricated and optical fibers with different refractive index profiles were heat drawn. Undoped SI and GI fibres exhibited minimum attenuation at wavelength 532 and 632nm. Multimode laser emission was observed from a polymer ring microcavity based on a dye doped hollow polymer optical fibre. The threshold pump power and the optimum fibre diameter to observe a multi mode emission are determined.

A dye solution filled dye doped polymer hollow optical fibre, offers a widely tunable fluorescence emission when excited with 488nm Argon ion laser. Here the emission wavelength can be selected by the appropriate choice of the fibre length. The simultaneous emission from the doped hollow fibre and the filled solution occurs only for a certain specific length of the fibre,

With axial pumping, multimode laser emission was observed from a dye mixture doped graded index fibre. With 532nm excitation, mixture of two dyes rhodamine 6G and rhodamine B considerably reduces the threshold for lasing due to the effective energy transfer mechanism. In comparison with dye doped step index fibres, dye doped graded index fibres show enhanced line narrowing and amplified spontaneous emission.

Since organic dyes possess a number of outstanding qualities including high value of optical nonlinear coefficients and high quantum efficiencies, the dye doped polymer optical fibres can be used to construct a good variety of devices and systems ranging from tunable lasers and amplifiers to nonlinear optical devices such as switches and modulators. When such fibres are doped with a mixture of dyes, the devices can operate in a wider range of wavelengths. The high value of losses of the fabricated optical fibres may be reduced by optimizing or changing the present materials and methods. Lasing threshold for the microring cavity based on dye doped hollow optical fibre may be further reduced by using a smaller dimension fibre with a better pumping mechanism. Optically important nanomaterials and rare earths can also be doped in to the polymer optical fibres. Since the graded index dye doped fibres exhibit ASE and laser emission at comparatively lower threshold pump powers, the effect of using other high molecular weight dopants like benzyl benzoate and benzyl butyl phthalate to form the refractive index gradient in the core region may also be studied. Both long period and Bragg gratings can be written in the fabricated dye doped polymer optical fibres. Since micro structured optical fibre or photonic crystal fibre offers huge potential in the field chemical and biochemical sensing, the method of fabrication of the hollow optical fibres can be extended for the fabrication of micro structured fibres.

……ൠ…..